Acoustic measurements and the Individual Subjective evaluation for sound fields

Sakai, Hiroyuki

(Degree)
博士（学術）

(Date of Degree)
2001-03-09

(Date of Publication)
2008-12-11

(Resource Type)
doctoral thesis

(Report Number)
乙2503

(URL)
https://hdl.handle.net/20.500.14094/D2002503

THESIS FOR THE DEGREE OF
DOCTOR OF PHILOSOPHY

ACOUSTIC MEASUREMENTS AND THE INDIVIDUAL SUBJECTIVE EVALUATION FOR SOUND FIELDS

（音場の物理計測と個人の心理評価）

HIROYUKI SAKAI

JANUARY 2001

GRADUATE SCHOOL OF SCIENCE AND TECHNOLOGY
KOBE UNIVERSITY

PREFACE

This dissertation is submitted, for the Doctor of Philosophy degree, to Graduate School of Science and Technology, Kobe University, Japan.

This dissertation attempts to describe acoustical measurements and individual subjective evaluations for sound fields based on a model of auditory-brain system and subjective preference theory. In acoustical measurement part, measurement results for historical opera houses and for outdoor sound fields in forests are discussed by analyzing temporal and spatial factors in preference theory. In subjective evaluation part, intra-individual changes of preference are especially focused on as well as its individual differences. Also, a preference test inside an opera house is discussed.

I assume responsibility for any errors, which may occur in the pages, which follow.

Hiroyuki Sakai

ACKNOWLEDGMENTS

I take this opportunity to express my thanks to the many people who have helped me, in various ways, to attain my objective of preparing this dissertation. I would like to express my gratitude for the considerable guidance and encouragement received from Professor Yoichi Ando, Kobe University, whose contribution to this research has been substantial. I also wish to express appreciation to Professor Takaji Matsushima and Professor Shinichi Murakami, Kobe University.

I would like to express my thanks to Dr. Shin-ichi Sato, Kobe University for his many supports and strengthening interaction. Especially, the data in chapter 4 was assisted by his efforts. Also I would like to express my thanks to Professor Roberto Pompoli and Dr. Nicola Prodi, University of Ferrara, Italy, for strong collaboration on my research for opera house acoustics. It is pleasure to acknowledge the hospitality and encouragement of the members of Ando Laboratory, Graduate School of Science and Technology, Kobe University. I also wish to express the thanks for the subjects who participated in the investigations.

Hiroyuki Sakai

CONTENTS

CHAPTER I: INTRODUCTION

1.1 General Introduction

Considering the fact that natural environments exist before the advent of human being, it is almost clear that human psychology has been greatly affected from nature. In order to evaluate a sound field, it is essential to take account of both physical and psychological aspects, and know to the relationship between them. This study describes acoustical measurements and individual subjective evaluations for sound fields. And the study is based on a model of human auditory-brain system and subjective preference theory in a sound field (Ando, 1998).

Subjective preference, which is said as primitive and overall psychological response, is evaluated by psychological experiments in a sound field simulation room and in an existing opera house in changing physical factors independently. Also a theory of individual subjective preference is summarized.

As applications of the study, a concert hall with a number of columns and proposed system for environmental noise are introduced.

1.2 Previous Studies of Acoustical Measurement for Sound Fields

1.2.1 Acoustical Measurement in a Concert Hall and an Opera House

In order to evaluate quality of a sound field in a concert hall or an opera house, acoustical measurements obtaining binaural impulse responses between a sound source and a listener are usually conducted. It represents a relationship between a signal generated at a sound source as an (impulse) and signals at the ears of a listener through space or walls, assuming a room as a linear system. Thus, all acoustical information should be included in binaural impulse responses. Impulse responses are obtained by the correlation method, which is expressed by the crosscorrelation between the input signal and the output signal of a linear system. Alrutz (1981) proposed a fast method, using a pseudo-random binary signal (maximum length sequence signal, MLS signal) (Davies, 1966; Borish and Angell, 1983) to take acoustical measurements in a room.

Since the introduction of a formula to quantify reverberation time by Sabine (1900), a great number of acoustic parameter to evaluate a room. As reverberation time

belongs to temporal-monaural factors (Ando, 1985), it is inadequate to represent the quality of a sound field in a room. That is to say, Ando (1985) proposed the introduction of binaural effects (binaural-spatial factors). As described in following subsection, all physical factors are extracted from binaural impulse responses at the ears of a listener. For an acoustical measurement in a concert hall, omni-directional sound source (for example, dodecahedron loudspeaker) is generally used on a stage. As a receiver, tiny condenser microphones at left and right ear entrances of a person are used.

For opera houses, acoustical conditions among musicians are especially important not only for an interchange among instrumental players in the orchestra pit but also for an interchange between a singer on the stage and each player in the pit. Thus, in a typical opera house, a special attention has to be paid for designing sound fields on the stage and in the orchestra pit. If such acoustical characteristics of sound fields for musicians are known, more appropriate design procedure can be given to opera theaters. There are some systematic measurement surveys for opera houses to obtain physical factors (Barron, 1993; Beranek, 1996; Hidaka and Beranek, 2000). These surveys are conducted to characterize theaters mainly for audience area. However, studies dealing with a relationship between a singer on the stage and players in the pit are few (O'Keefe, 1998).

1.2.2 Physical Factors to be Evaluated

All physical factors to be evaluated are extracted from binaural impulse responses at the left and right ears, h_{jl} and h_{jr} (Osaki and Ando, 1983). The index j indicates the sampled elements of MLS with time interval σ (j = 0, 1, 2, ..., L - 1). These physical factors should be orthogonal each other in order to evaluate subjective preference in a sound field. From binaural impulse responses, following four orthogonal factors (LL, Δt_1, T_{sub}, and IACC) and additional factors (A, τ_{IACC}, and W_{IACC}) are extracted (Ando, 1983).

(1) LL (listening level)

The LL at a listener's position is obtained relative to sound pressure of the reference position. The LL at each ear is given by the autocorrelation function $\Phi_{ll,rr}(\tau)$ at $\tau = 0$ of the impulse responses $h_{jl,r}$

$$\Phi_{ll,rr}(0) = \sum_{j=0}^{L-1} h_{jl,r}^2 . \tag{1.1}$$

The relative LL in decibell scale is defined by

$$\mathrm{LL} = 10\log_{10}\frac{\sqrt{\Phi_{ll}(0)\Phi_{rr}(0)}}{\Phi^{(ref)}(0)} \quad \text{if } h_{jl,r} \neq 0, \tag{1.2}$$

where

$$\Phi^{(ref)}(0) = \sqrt{\Phi_{ll}^{(ref)}(0)\Phi_{rr}^{(ref)}(0)}\,. \tag{1.3}$$

Here, $\Phi^{(ref)}(0)$ is the geometrical mean of the autocorrelation functions of binaural-impulse responses at $\tau = 0$ at the reference position as indicated by Eqn. (1.3). Reference position is usually 1-m apart from a sound source.

(2) Δt_1 (initial time delay gap between the direct sound and the first reflection)

The Δt_1 is defined as an initial time delay gap between the direct sound and the first reflection with the first maximum amplitude. The Δt_1 is determined by crosscorrelation between the direct sound component and its impulse response. In a concert hall, Δt_1 generally appear as a reflection with the maximum amplitude.

(3) T_{sub} (subsequent reverberation time)

The value of T_{sub} is defined by the time interval for 60-dB attenuation for the regression line of initial decay of reverberation curve. The decay curve is obtained by squaring and integrating the impulse responses (Schroeder, 1965). The T_{sub} is obtained by fitting the regression line of the curves for the initial 15-dB decay after the arrival of the direct sound.

(4) IACC

The normalized interaural cross-correlation function is given by

$$\phi_{lr}(j\sigma) = \frac{\Phi_{lr}(j\sigma)}{\sqrt{\Phi_{ll}(0)\Phi_{rr}(0)}}, \tag{1.4}$$

where the values of $\Phi_{ll}(0)$ and $\Phi_{rr}(0)$ represent the autocorrelation functions at $\tau = 0$ of impulse responses at both ears. The denominator means the geometrical mean of the sound energies arriving at the two ears. The $\Phi_{lr}(j\sigma)$ is the crosscorrelation function of impulse responses at both ears. The magnitude of interaural crosscorrelation function is defined by

$$\mathrm{IACC} = \left|\phi_{l,r}(\tau)\right|_{\max}, \quad |\tau| \leq 1 \text{ [ms]}. \tag{1.5}$$

This is a significant factor in determining the degree of subjective diffuseness as well as subjective preference in the sound field (Ando, 1983). It represents the degree of similarity in incident sound waves between both ears. The definitions of IACC as representative factors of interaural crosscorrelation function are shown in Figure 1.1 as well as τ_{IACC}, and W_{IACC}.

In addition, following related factors are also analyzed.

(5) A value (total amplitude of reflections)

The value of total amplitude of reflections A is calculated from $h_{jl,r}$ as the energy ratio between the direct sound and early-plus-subsequent reverberation by

$$A = \sqrt{\sum_{\varepsilon+1}^{L} h_j^2 \Big/ \sum_{1}^{\varepsilon} h_j^2} \tag{1.6}$$

where ε is the short delay time for the duration of direct sound.

(6) τ_{IACC} (interaural time delay)

The definitions of τ_{IACC} and W_{IACC} as representative factors of interaural crosscorrelation function are shown in Figure 1.1 as well as IACC. The τ_{IACC} is determined as interaural delay time, at which the IACC is determined. This factor corresponds to the horizontal sound localization and the balance of the sound field. When τ_{IACC} is zero, the frontal-sound-source image and a well-balanced-sound field may usually be perceived.

(7) W_{IACC} (width of the normalized interaural crosscorrelation function)

The W_{IACC} is defined by the interval of delay time at a value 10% below the orthogonalized IACC as shown in the figure. W_{IACC} is a significant factor related to the apparent source width (ASW). It is worth noting that apparent source width (ASW) can be evaluated using IACC and W_{IACC} (Sato and Ando, 1999; Ando et al., 1999).

In order to represent quality of a sound source or a sound field, following factors are extracted from exact binaural signals. From autocorrelation function ACF at each ear, four factors are extracted; (1) $\Phi(0)$, (2) τ_e, (3) τ_1 and (4) ϕ_1. The first factor is the autocorrelation function at $\tau = 0$ represented as the sound energies arriving at both ears $\Phi_{ll,rr}(0)$.

$$\Phi_{ll,rr}(0) = \frac{1}{2T}\int_0^{2T} p(t)dt, \tag{1.7}$$

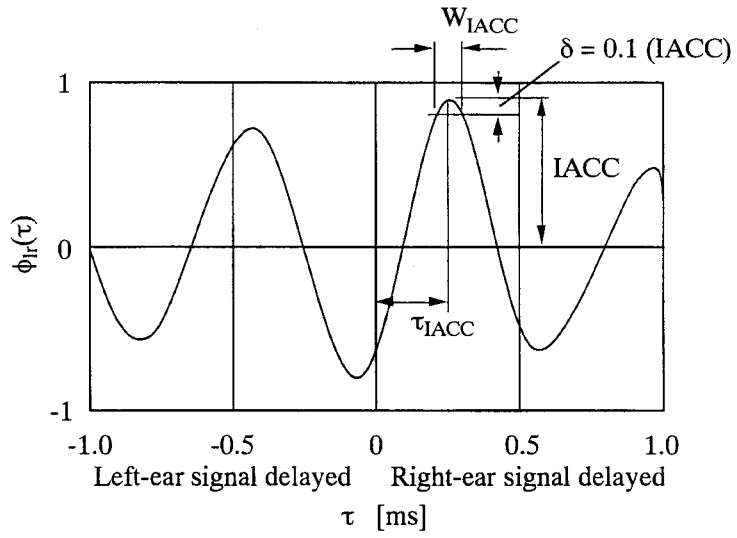

Figure 1.1 Definitions of IACC, τ_{IACC}, and W_{IACC} as representative factors of interaural crosscorrelation function.

where $p(t)$ is a sound signal at the ear, and $2T$ is integration interval. They correspond to equivalent sound pressure level. The second factor is the effective duration of ACF, τ_e. This factor is defined by the ten-percentile delay representing a kind of repetitive feature or reverberation within the source signal itself. The τ_e is obtained practically from the decay rate in the range from 0 dB to –5 dB of normalized ACF as shown in Figure 1.2(a). The third and fourth factors are the amplitude and the delay time of the first dominant peak of normalized ACF, represented respectively as ϕ_1 and τ_1 as shown in Figure 1.2(b). As can be easily understood, the factors ϕ_2, ϕ_3, ... and τ_2, τ_3, ... are closely related to ϕ_1 and τ_1.

From interaural crosscorrelation function (IACF) between the ears, following four factors are extracted; (5) LL, (6) IACC, (7) τ_{IACC}, and (8) W_{IACC}. The physical factors are extracted as fine structures of IACF. Although LL is not extracted from IACF, this factor LL is implied as a binaural factor. This factor is a denominator of the normalized IACF. The second factor is IACC, which is the maximum value of the normalized IACF for the time delay, within ±1 ms as defined in Eqn. (1.5). The third and fourth factors are interaural time delay, τ_{IACC}, and width of the IACF, W_{IACC}, which are also already described in Figure 1.1.

These functions are calculated in at every certain interval (integration intervals, $2T$) as running function. The starting time of each integration interval is delayed for a short time. The time is called the running step. In the case of sound source for music, the length of the integration interval may be decided within psychological present with its duration between 2 and 5 s, which a person feels the duration of time of what is considered to be

"now" (Freisse, 1982). However, it is probably better to use a shorter integration interval, say 0.5 s, for environmental noise for instance as described in Section 6.3.

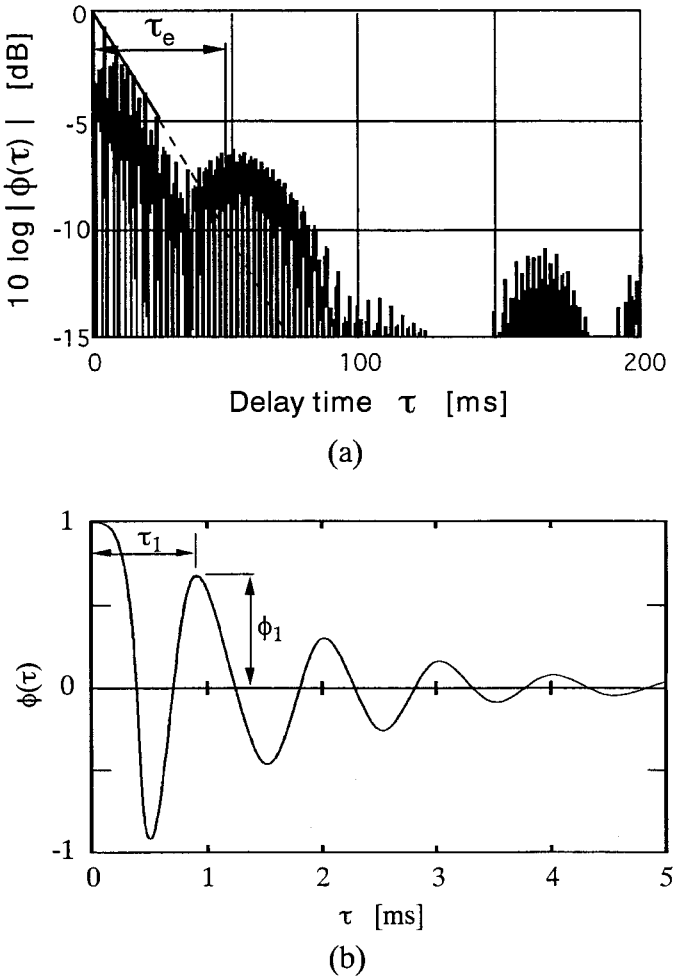

Figure 1.2 Definitions of independent factors extracted from the normalized autocorrelation function (ACF). (a): τ_e obtained practically from the decay rate in the range from 0 dB to –5 dB of normalized ACF; (b): ϕ_1 and τ_1 as fine structures of normalized ACF.

1.2.3 Acoustical Measurements in Forest

A number of acoustical measurements in outdoor fields involved a forest have been carried out (for example: Eyring, 1946; Embleton, 1963; Price et al., 1988). Most of them are related to the sound propagation in terms of sound pressure level (SPL) and its frequency characteristics. In a recent study, the reverberation time and the SPL attenuation as a function of the distance in a forest were reported (Huisman and Attenborough, 1991). In designing sound fields, however, both temporal and spatial factors must be simultaneously satisfied to achieve a total preference maximum.

1.3 Previous Studies of Subjective Evaluation for Sound Fields

1.3.1 Subjective Preference Theory

Since the numbers of orthogonal factors, which are included in the sound signals at both ears, are limited, the scale value of any one-dimensional subjective responses may be expressed by:

$$S = g(x_1, x_2, ..., x_l). \tag{1.8}$$

In this study, the linear scale value of preference based on the law of comparative judgment (Thurstone, 1927) is described. It has been verified by a series of experiments that four objective factors act independently of the scale value; changing two of four factors simultaneously. Results indicate that the units of scale values are almost constant, so that we may add scale values to obtain the total scale value (Ando, 1983),

$$\begin{aligned} S &= g(x_1) + g(x_2) + g(x_3) + g(x_4) \\ &= S_1 + S_2 + S_3 + S_4 \end{aligned} \tag{1.9}$$

where S_i (i = 1, 2, 3, 4) is the scale value obtained relative to each objective parameter. This equation indicates a four-dimensional continuity.

The dependence of the scale values on each objective parameter is also discussed by Ando (1983). From the nature of the scale value, it is convenient to put a zero value at the most preferred conditions. These results of the scale value of subjective preference obtained from the different test series, using different music programs, yield the following a common formula:

$$S_i \approx -\alpha_i |x_i|^{3/2}, \quad i = 1, 2, 3, 4 \tag{1.10}$$

where the values of α_i are weighting coefficients. If α_i is close to zero, then a lesser contribution of the factor x_i on subjective preference is signified.

The factor x_1 is given by the sound pressure level difference, measured by the A-weighted network, so that

$$x_1 = 20\log P - 20\log[P]_p \tag{1.11}$$

P and $[P]_p$ being the sound pressure at a specific seat and the most preferred sound

pressure that may be assumed at a particular seat position in the room under investigation;

$$x_2 = \log (\Delta t_1 / [\Delta t_1]_p) \tag{1.12}$$

$$x_3 = \log (T_{sub} / [T_{sub}]_p) \tag{1.13}$$

$$x_4 = \text{IACC} \tag{1.14}$$

Thus, the scale values of preference have been formulated approximately in terms of the 3/2 power of the normalized objective parameters, expressed in the logarithm for the parameters, x_1, x_2 and x_3. The spatial binaural parameter x_4 is expressed in terms of the 3/2 power of its real values, indicating a greater contribution than those of the temporal parameters are. Thus, the scale values are not greatly changed in the neighborhood of the most preferred conditions, but decrease rapidly outside of the ranges. Since the experiments were conducted to find the optimal conditions, this theory holds in the ranges of preferred condition tested for the four factors.

1.3.2 Calculation of Individual Difference

Similar to the manner described in previous subsection for a number of subjects, the scale values of subjective preference for each listener is also approximately expressed as Eqn. (1.10) (Ando and Singh, 1996). Therefore, the individual preference may be characterized by the coefficients α_i, i = 1, 2, 3, 4 along with positive and negative values of every x_i, and the most preferred values $[LL]_p$, $[\Delta t_1]_p$ and $[T_{sub}]_p$. Obviously, the preferred LLs greatly differ for each subject. The most remarkable facts are that all of individuals preferred the low value of IACC without any exception and without regard for any music motifs. Great individual differences are also obtained for Δt_1 and T_{sub} among the individuals. These most preferred conditions are well related to the effective duration of the ACF of source signal for each individual.

Ando and Singh (1996) developed a simple method of calculating individual scale values from a single observation for a set of stimuli. The procedure for calculating scale values of preference is outlined in Table 1.1. The scores for each presented pair are obtained by giving scores of +1 and 0 corresponding to positive and negative judgments, respectively. For example, the score of the pair (66 dBA, 72 dBA) listed in Table 1.1 is zero. This result shows that the subject prefer the sound field with 72 dBA to the sound field with 66 dBA. The ideal preference score comparing sound fields with same stimuli is

0.5 as "a tie" (Glenn and David 1960) and, thus, the scores of diagonal set in the table are 0.5. The values of T_i represent the total score. The scale value of subjective preference for sound field i can be obtained by assuming a normal distribution of preference judgment as following equation:

$$S_i \approx \frac{\sqrt{2\pi}(2T_i - N)}{2N}, \tag{1.15}$$

where N indicates the number of sound fields (= 5). This approximate equation is derived from Case-V of Thurstone's law of comparative judgment (Thurstone, 1927) and holds the linear domain of a normal ogive ($0.05 < P < 0.95$, P: probability judged). Each subject's most preferred value is obtained at the peak of the preference curves. The formula used for fitting scale values of preference is given by Eqn. (1.10). The individual α value can be obtained from the average of preference score T_i in Table 1.1 for all series of tests and all subjects.

Table 1.1 An example of procedure for calculating scale values of preference.

LL [dBA]	Sound field (LL [dBA])					T_i	S_i
	66	72	78	84	90		
66	0.5	0	0	1	1	2.5	0.00
72	0	0.5	1	1	1	3.5	0.50
78	1	0	0.5	1	1	3.5	0.50
84	1	0	0	0.5	1	2.5	0.00
90	0	0	0	0	0.5	0.5	-1.00

1.3.3 Subjective Responses for Musician

In order to support musicians on the stage by the stage reflections, there are some subjective experiments in a laboratory. Marshall et al. (1978) evaluated ease of ensemble among instrument players in changing delay time and amplitude of initial reflections in order to investigate the effect of stage size. Gade (1989a) proposed a factor ST (Support) value in changing temporal factors (initial reflections or reverberation) for instrument players through psychological experiments in a sound field simulation room. And, subjective experiments for musicians in an existing hall were also conducted by use of the factor (Gade, 1989b). Preferred delay time or direction of a single reflection for alto-recorder soloists or cellists were performed by Nakayama (1984), Nakayama et al. (1988),

and Sato et al. (2000). These papers describe the relationship between the delay time of the reflection and the effective duration τ_e of a sound source itself. Marshall and Meyer (1984) investigated the directivity of singings and the auditory impression in singing in a laboratory in terms of temporal factors. Recent studies in changing a single reflection in singing for solo singers indicate the preferred acoustical condition with the relationship between the delay time of the reflection and the τ_e of a sound source (Noson et al, 2000). These all papers discuss for sound fields in a concert hall. However, they may be adopted for sound fields in opera houses.

For the acoustics in the orchestra pit, there are some difficulties for players in the pit to hear or contact each other due to the standing wave between the pit floor and overhanged ceiling, and temporal masking effect (Meyer, 1998; Blair, 1998). However, the research of the relationship between a singer on the stage and players in the pit are not found in the present stage.

In the field of concert hall acoustics, theory of subjective preference in a sound field has been adopted to evaluate the preference for musicians as well as for listeners. This theory may be applied for the case of opera house, because the theory deals the relationship between the psychological responses from musicians (and also listeners) and orthogonal physical factors extracted from signals arriving at each ear.

1.4 Model of Auditory-Brain System

1.4.1 Model

A model of the auditory-brain system are shown in Figure 1.3 (Ando 1998). In this figure, a sound source $p(t)$ is located at r_0 in a three-dimensional space and a listener is sitting at r which is defined by the location of the center of the head, $h_{l,r}(r \mid r_0, t)$ being the impulse responses between r_0 and the left and right ear-canal entrances. The impulse responses of the external ear canal and the bone chain are $e_{l,r}(t)$ and $c_{l,r}(t)$, respectively. The velocities of the basilar membrane are expressed by $V_{l,r}(x, \omega)$, x being the position along the membrane. The action potentials from the hair cells are conducted and transmitted to the cochlear nuclei, the superior olivary complex including the medial superior olive, the lateral superior olive and the trapezoid body, and to the higher level of two cerebral hemispheres. According to the tuning of a single fiber (Katsuki et. al. 1958; Kiang, 1965), the input power density spectrum of the cochlea $I(x')$ can be roughly mapped at a certain nerve position x'. Neural activities include sufficient information to attain the ACF at a higher level, probably near the lateral lemniscus as indicated by $\Phi_{ll,rr}(\sigma)$. The interaural crosscorrelation mechanism may exist at the inferior colliculus. The output signal of the interaural crosscorrelation mechanism including the IACC and the loci of maxima may be

dominantly connected to the right hemisphere. Also, the listening level may be processed in the right hemisphere. Effects of the initial time delay gap between the direct sound and the single reflection Δt_1 included in the autocorrelation function may activate the left hemisphere. The specialization of the human cerebral hemisphere may relate to the highly independent contribution between the spatial and temporal criteria on subjective attributes.

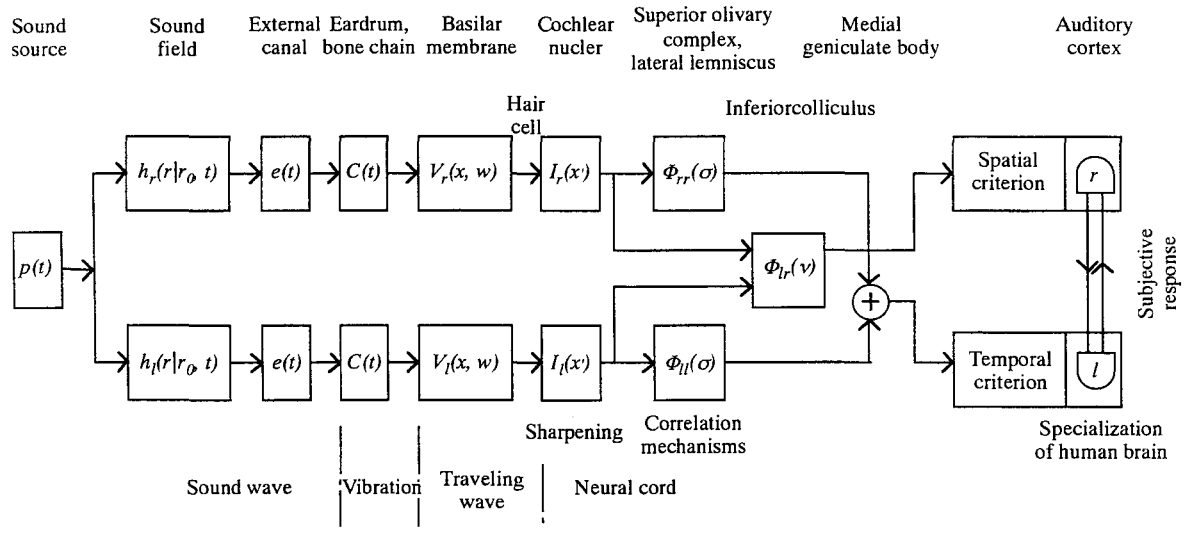

Figure 1.3 A model of human auditory-brain system

1.4.2 Subjective Attributes for Sound Field

It may be convenient to apply the auditory-brain model to evaluate subjective attributes in a sound field. For example, a sound may be perceived as noisy in a given situation even though its SPL is quite low. A good example is the beep of a mobile phone in an otherwise quiet train. Thus, loudness is related to not only LL, but also to τ_e, which is one of the ACF factors (Merthayasa at al, 1997; Sato et al., 2001). Moreover, the phenomenon that the fundamental pitch of a complex tone can be perceived by a person is well known as the "phenomenon of missing fundamental." In this phenomenon, the pitch of harmonic components without a fundamental frequency is perceived as being the same as the pitch of a pure tone of the fundamental frequency. While this fundamental pitch cannot be predicted by frequency analysis of the signal, it can be predicted by temporal analysis even when the complex tone consists of random phase components (Inoue et al., 2001). With binaural measurement, spatial information including subjective diffuseness and directional information can be obtained from the IACF factors. Consequently, the use of ACF and

IACF analysis to subjectively evaluate noise is quite reasonable. The ACF and IACF factors can also be used to identify a noise source as timbre by using multi-dimensional analysis. Recently, the use of four primitive sensations, including duration sensation, was proposed (Saifuddin et al., 2001). Duration sensation comparing pure tone and noise varies with τ_e. In addition, a short-time moving (running) ACF and IACF can be used to evaluate time-variant noise. In addition to the effects for subjective attributes, floor impact noise (Jeon, 2001) and transmission loss between rooms (Soeta et al., 2001) can be well described by ACF and IACF factors.

1.5 Aim of this Study

In this study, acoustical measurement and individual subjective evaluations for a sound field are discussed. For acoustical measurement, the orthogonal factors obtained from binaural impulse responses are discussed. Procedure of acoustical measurements and its results are described in historical opera houses and outdoor sound fields including general forest and bamboo forest. For measurements in opera houses, sound fields for musicians on the stage and in the orchestra pit are especially focused on as well as a sound field for listeners in a box. For measurements in outdoor fields, multiple scattering effects from tranks of trees are mainly discussed. For individual subjective evaluations, intra-individual changes of subjective preference are discussed as well as its individual difference. Subjective preference tests were conducted at sound field simulation room and existing opera house. Theory of subjective preference for individual is summarized. As applications, a concert hall with a number of columns and proposed measurement system for environmental noise are introduced.

CHAPTER II. ACOUSTIC MEASUREMENT FOR SOUND FIELDS

2.1 Introduction of Chapter II

Acoustical measurement procedure, which has been used for a concert hall, is applied to historical opera houses and outdoor sound fields including general forest and bamboo forest. As historical opera houses usually have specific equipment as orchestra pit, boxes, balcony seats, stage house with huge volume, interior decorations, sound fields in opera houses is necessary to distinguish from that in concert halls. Most remarkable differences between sound field in an opera house and that in a concert hall is performances. Namely, a singer sings on the stage and orchestra plays instruments in a pit in the case of an opera house. In accordance with these facts, sound fields on the stage and in orchestra pit are especially focused here. Also, sound fields for listeners in box seats are investigated as a specific sound field for listeners in an opera house. As measurements in outdoor sound fields, sound fields in a general forest and a bamboo forest are investigated. Sound fields in forests may include multiple scattering effects from trunks of trees as columns. Excellent sound fields are obtained from acoustical measurements, although acoustical environment in a forest has experientially been felt to be fine. An application for a concert hall using the effect of columns is introduced in Chapter 6.

2.2 Acoustical Measurement in Historical Opera Houses

2.2.1 Acoustical Measurement for a Singer on the Stage

In order to clarify sound fields for a singer on the stage in relation to performers in the orchestra pit, acoustical measurements were conducted in a typical historical opera house, the "Teatro Comunale" in Ferrara, Italy. Based on the subjective preference theory, orthogonal factors and related factors in a sound field are analyzed and are used to evaluate the sound fields. The present investigation provides useful knowledge for a singer on the stage for the sound emitted by sources in the orchestra pit.

The plan of the theater is illustrated in Figure 2.1(a). The hall shape of the plan is elliptical (truncated). Number of the seats is 800 (2/3 in the five tiers of boxes). Volume of the hall part without stage house is 5000 m^3.Volume of the stage house is 8500 m^3. Width and height of the proscenuim are 13.5 m and 11.0 m, respectively. Maximum depth and

width of the stage are 20.0 m and 23.5 m, respectively. Mean height of stage house is 18.0 m. The stage floor is moderately sloped. The section of the pit is illustrated in Figure 2.1(b). The pit depth, which is the height from the pit floor to the underside of the stage, is 1.95 m. The depth of the pit from the pit rail to the rear wall in the pit is 5.17 m and the widths of the pit are 14.9 m for frontal area near the pit rail, and 13.2 m near overhanged rear wall. The pit rail is made of a hard wooden board and is installed between the stall and the orchestra pit. Its height is 2.08 m from the pit floor. The top of the pit rail is in line with the stage. The surface of orchestra pit is 67 m^2.

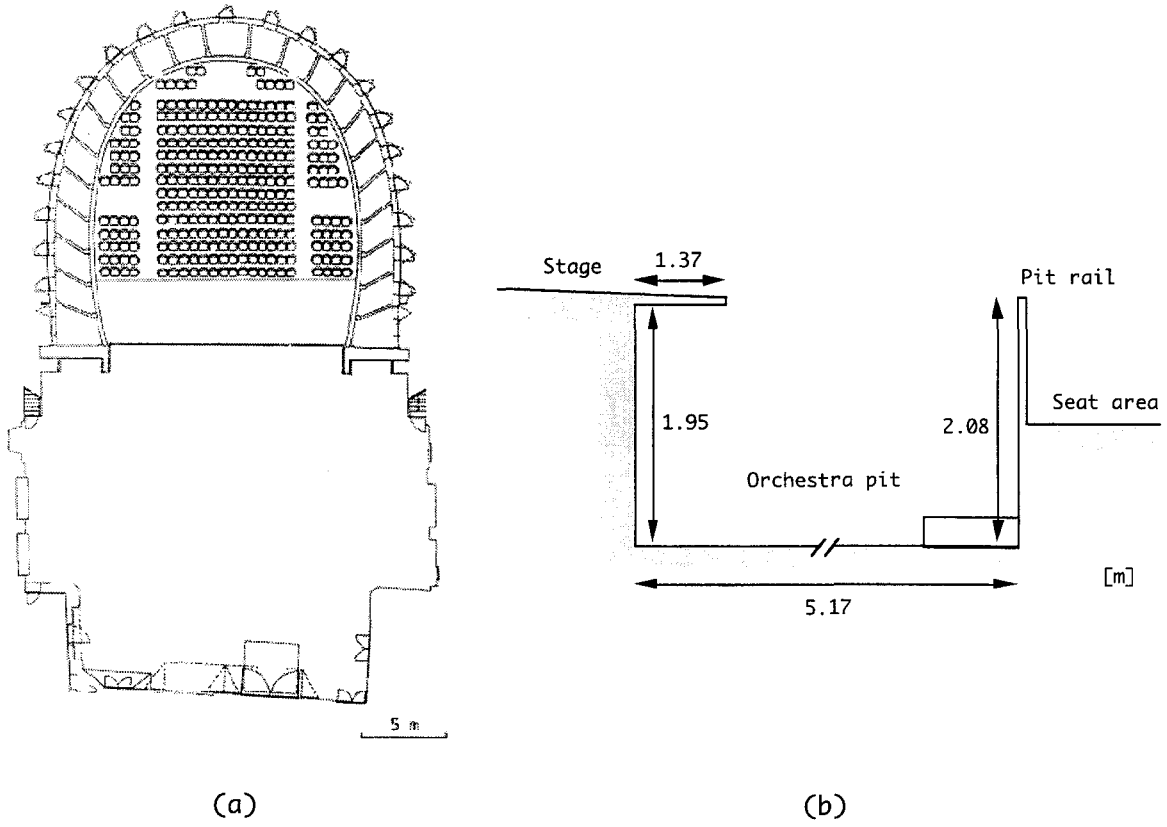

Figure 2.1 "Teatro Comunale" in Ferrara, Italy. (a): Plan of the theater; (b): Sections of the orchestra pit.

Procedure

The employed measurement system and the diagram are shown in Figure 2.2. During the measurements, the stage was completely empty and in the pit, chairs and music stands of players were removed. Measurements were conducted in the unoccupied hall. The test signal consisted in the MLS sequence with its duration 2.97 s (sampling frequency: 44.1 kHz), which was averaged eight times to improve the S/N ratio. The MLS signal was

radiated from an omni-directional dodecahedron loudspeaker in the pit. As a receiver, a human head with two tiny condenser microphones at each ear entrance was used.

Locations of sound sources and receivers were determined according to the possible locations of a singer on the stage and players in the pit, as shown in Figure 2.3. Two locations of the sound source S1 and S2 in the pit, and fifteen locations of the receiver (M01-M15) on the stage were selected. The S1 and S2 were selected as typical locations for the first violin player and for an overhanged musician by the upstage wall, respectively. The sound source S1 was located at 2 m from the pit rail and 1 m away from the centerline. The source S2 in the deep pit was located at 1.5 m from a lateral wall and 1.0 m from the rear wall in the pit. The height of the sources was 1.2 m considering sitting performers in the pit. Fifteen receivers were distributed with its grid 2.5-m on the stage as shown in the figure. The height of the human receiver (the location of the ears) was 1.5 m from the stage floor. The receiver was always faced frontal direction toward to the stall during the measurements. Reference measurements were conducted at a distance of 1 m for both sources. Note that the locations of the source S1 and the receivers were 1 m away from the centerline axis not to affect the results of IACC because of a symmetrical shape of the theater (Okano et al., 1998).

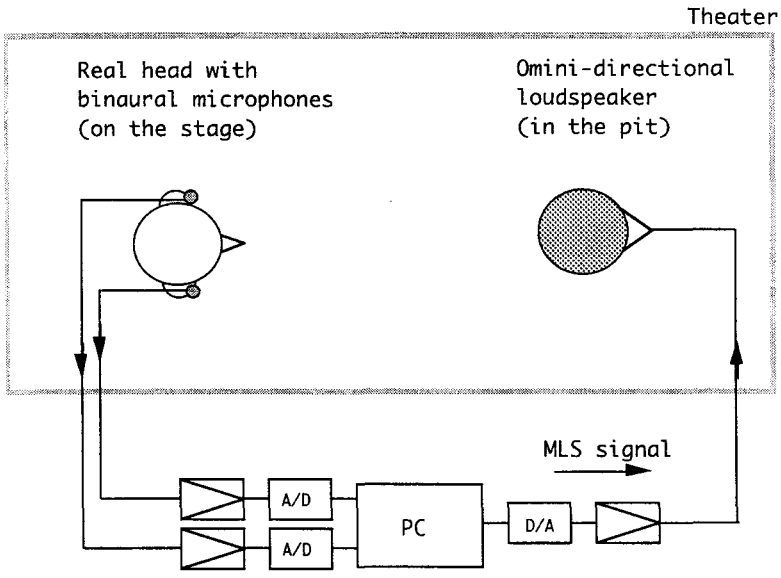

Figure 2.2 Acoustical measurement system and the diagram.

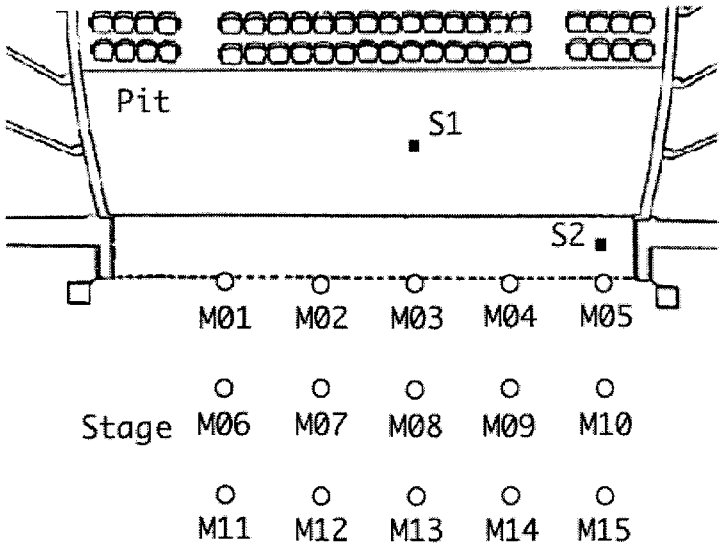

Figure 2.3 The locations of sound sources (S1 and S2) and receivers (M01-M15).

Results and discussions

Figure 2.4(a-d) shows binaural impulse responses as typical examples of the measurements. When the sound source is located at S1, although the largest amplitude in the impulse responses appears as a direct sound for the receivers in the front row (M01-M05) as shown in Figure 2.4(a, b), it appears in the initial reflections for the receivers in the second and third rows (M06-M10 and M11-M15) as shown in Figure 2.4(c). This phenomenon is deeply connected to the sight line between a sound source and each receiver. As there is no obstacle between S1 and receivers in the front row, the direct sound has the maximum amplitude. The amplitudes of impulse response at right channel for M01 exposed to S1 was larger than at left channel, although those of receiver M03 had well-balanced responses. Figure 2.4(c) shows a typical example of impulse responses (M13 for S1) for which the amplitude of the first reflection is larger than the direct sound. On the other hand, as shown in Figure 2.4(d), the amplitude of direct sound is always smaller than that of the initial reflections at all receivers' locations for S2. This is due to the overhanged stage, which weakens the direct sound by the diffraction from the stage edge. Such a phenomenon in relation to impulse responses is one of the significant characteristics for sound field between a singer and the musicians in the pit.

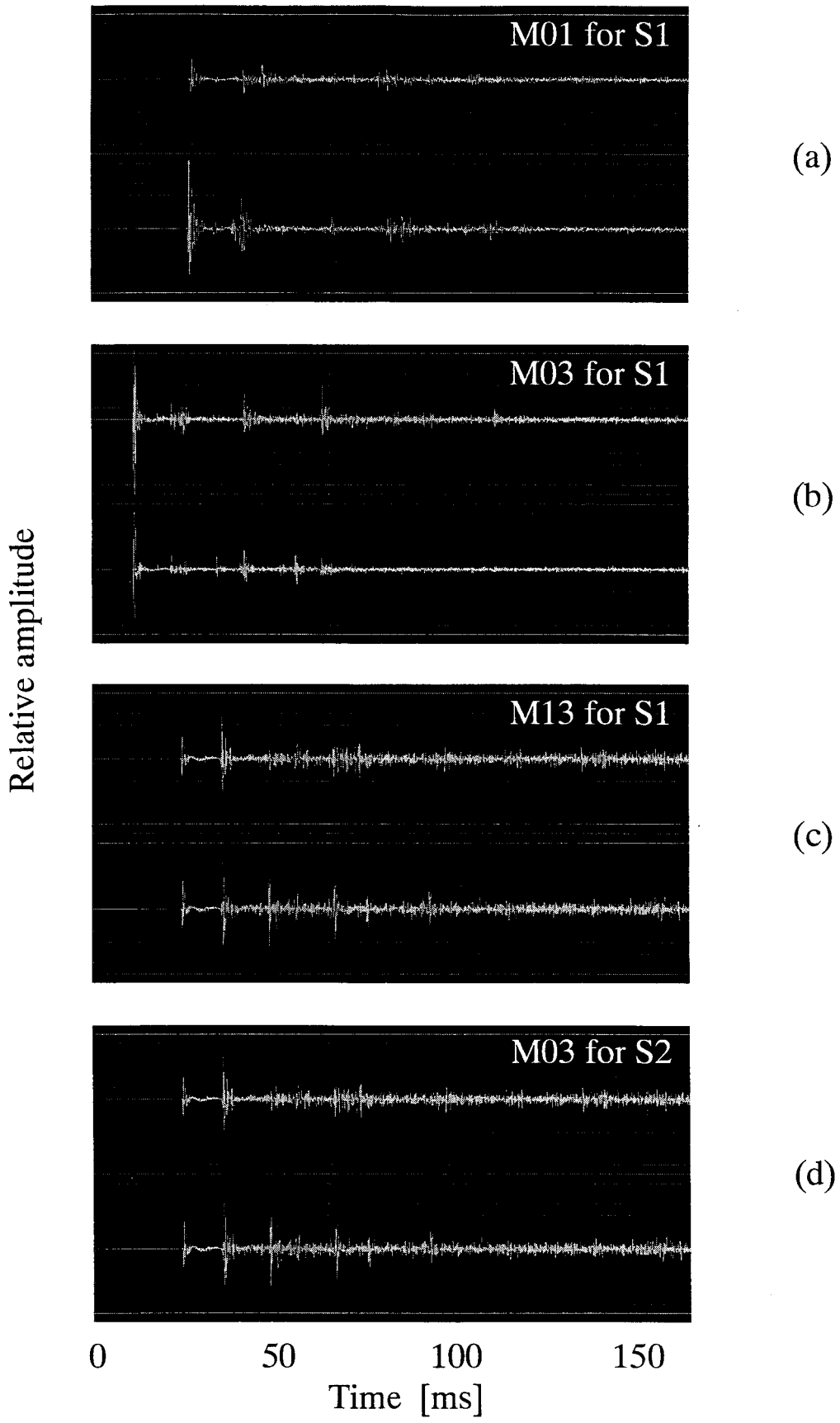

Figure 2.4 Binaural impulse responses as typical examples of the measurements. Initial 150 ms part is shown. (a): M01 for S1; (b): M03 for S1; (c): M13 for S1; and (d): M03 for S2.

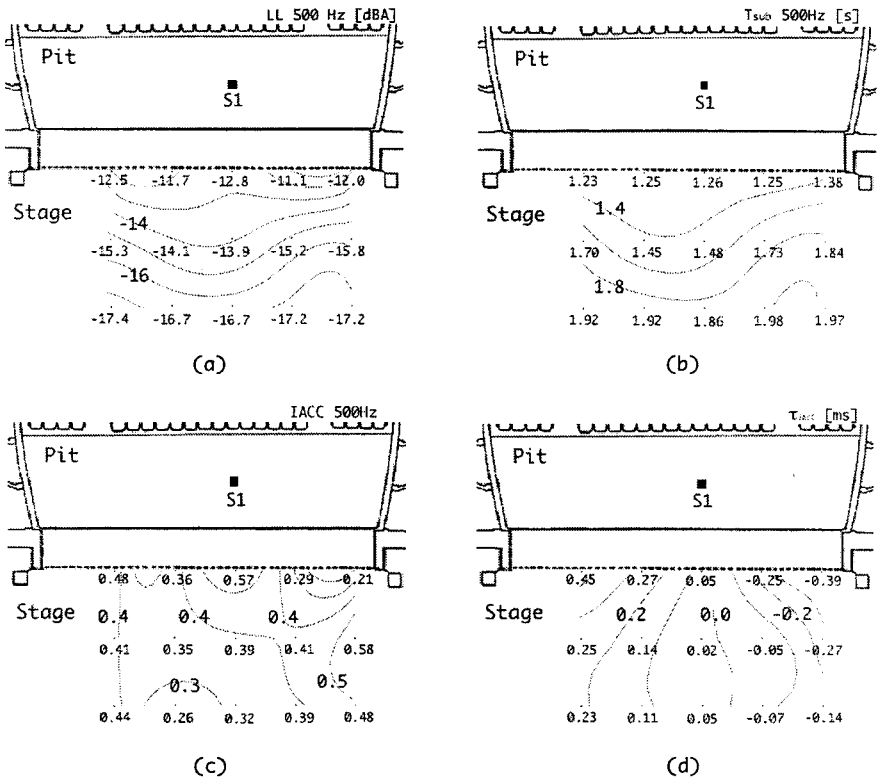

Figure 2.5 Contour lines of measurement result for S1. (a): *LL* (500 Hz); (b): T_{sub} (500 Hz); (c) IACC (500 Hz) and; (d): τ_{IACC}.

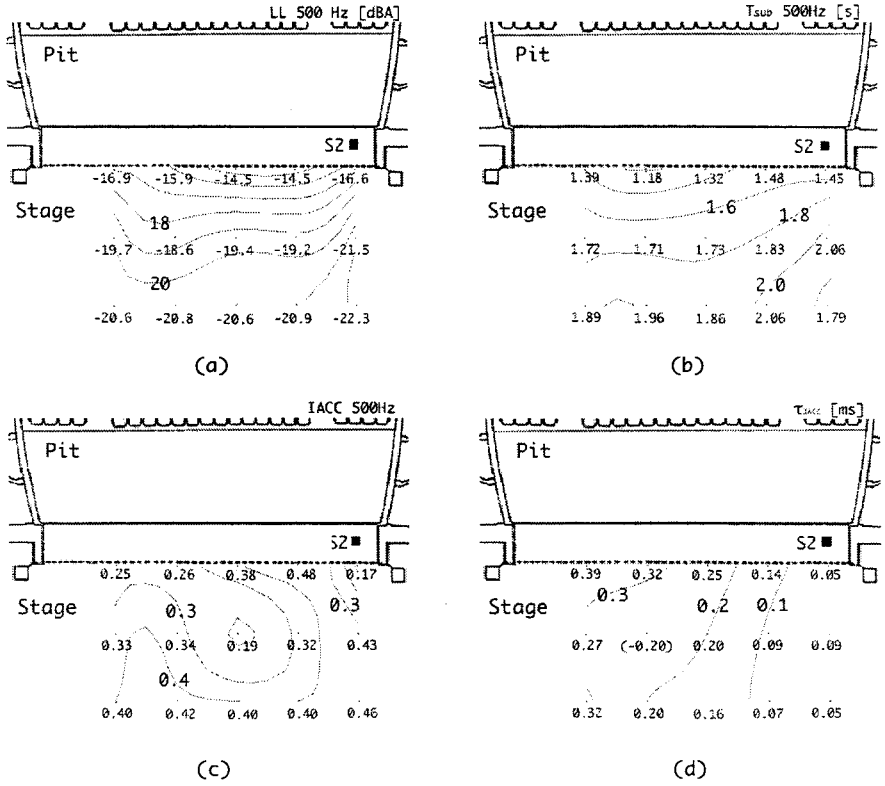

Figure 2.6 Contour lines of measurement result for S2. (a): *LL* (500 Hz); (b): T_{sub} (500 Hz); (c) IACC (500 Hz) and; (d): τ_{IACC}.

Figure 2.5(a) and Figure 2.6(a) shows the contour lines of *LL* (500 Hz) for S1 and S2, respectively. The range of each contour line is 1 dB. The *LL* orderly decreases from the front row to third row for both sources. The difference of averaged *LL* (500 Hz) between S1 and S2 was 4.8 dB. Figure 2.7 shows the results of *LL* as a function of 1/1 octave band center frequency for both sources. As the *LL* orderly decrease from the front row to third row, values of *LL* among each row are averaged in the figure. Empty and filled plots indicate the results for S1 and S2 respectively. The average *LL* values among all receivers of S1 at allpass band are 9.2 dB larger than that of S2. This difference happens mainly by strong sound attenuation due to the screening of direct sound path by the overhang. Values of *LL* orderly decrease at all frequency ranges from S1 to S2. Concerning to alteration at frequency response, the shape is similar between rows among each source, but different between the two sources. For S1, *LL* at lower frequency (125 and 250 Hz) is smaller than other higher frequency ranges. At 1 kHz, attenuation larger than the other frequency range (6.6 dB) was observed between the first and second row. For S2, *LL* at lower (125 and 250 Hz) and higher (2 and 4 kHz) frequency ranges were decreased comparing to those for S1. The attenuation of higher frequency is due to the diffraction by overhanged stage edge. For example, difference of *LL* at 125 Hz and 4 kHz between S1 and S2 is 6.7 dB and 10.4 dB respectively, whereas those at 500 Hz are 4.2 dB. Thus, for both sources, variances of *LL* for the back-and-forth axis were much remarkable at frontal area on the stage.

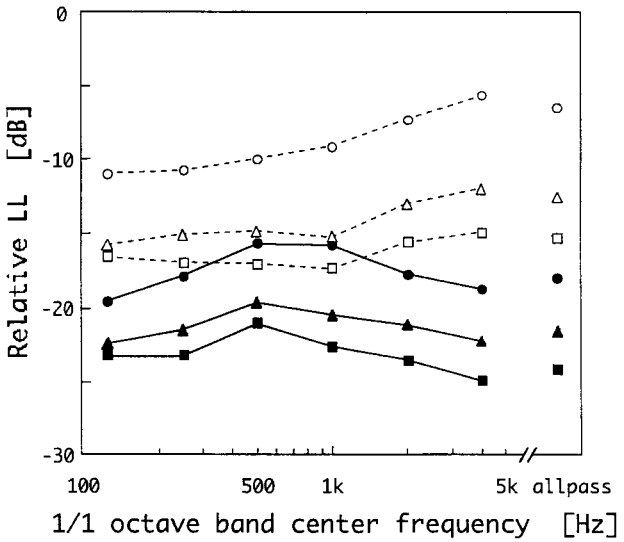

Figure 2.7. Results of relative *LL* as a function of frequency. Each plot indicates the average value of *LL* at each row. Right side plots without lines are the results for allpass band. ○: front row (M01-M05) for S1; △: middle row (M06-M10) for S1; □: rear row (M11-M15) for S1; ●: front row for S2; ▲: middle row for S2; and ■: rear row for S2.

Figure 2.8(a, b) shows the results of *LL* at 500 Hz as a function of distance from S1 and S2 respectively. The *LL* for S1 decreased almost linearly. However, the *LL* for S2 decreased with more scattered values. Generally much lower values are measured for equal distances. This is because sound transmission path is screened by the overhang, and particularly occurred at the near locations to S2 for each row (M05, M10, and M15). For example, though the *LL* at M03 (500 Hz) was –14.5 dB, it was –16.6 dB at M05, where is closer to S1 than M03. The same tendency can be seen at each row as shown in Figure 2.8(b). Variances of *LL* for the side direction were small for both sources.

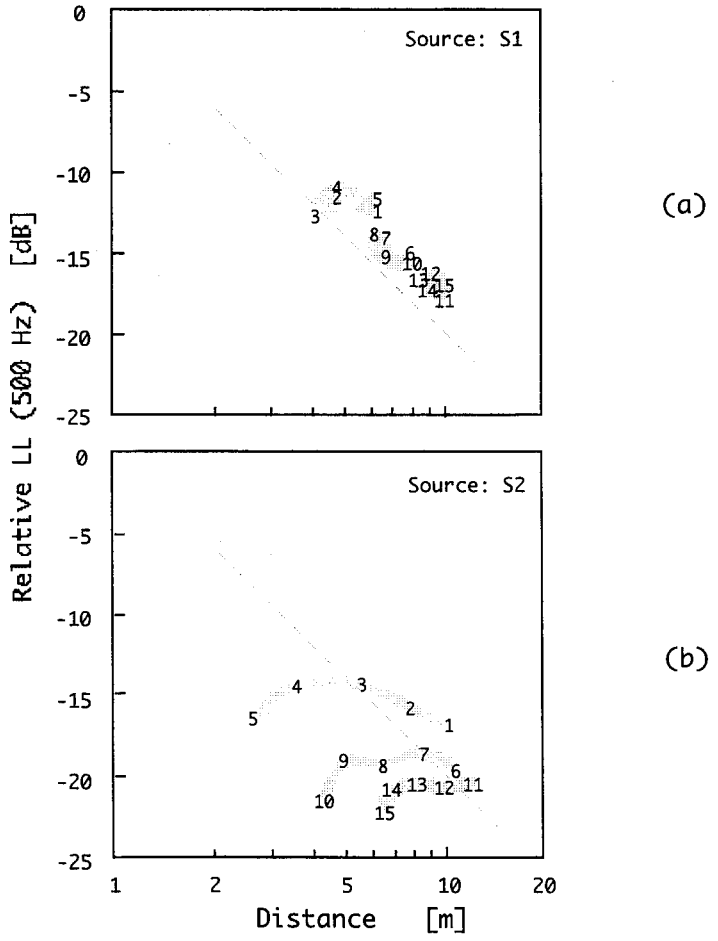

Figure 2.8 Results of *LL* at 500 Hz as a function of distance. (a): S1; and (b): S2. Dotted line represents the inverse square low. The numbers (1-15) are correspond to the receivers (M01-M15).

The value of Δt_1 is defined as a delay time of the first reflection. Generally, the first reflection is outstanding in a concert hall. However, in a sound field including the stage and the orchestra pit, this does not happen because of both at the stage overhang and the stage house. For this reason, Δt_1 is defined as a delay time of the reflection with maximum amplitude here. As the different Δt_1 were obtained at both ears even for some receivers, both left and right Δt_1 values were calculated separately. The contour lines of Δt_1 are not illustrated in this paper, because the reflective surface of the Δt_1 dramatically varies at different receiver's locations as shown in Table 2.1. At audience area in concert halls, Δt_1 orderly varies, because the first reflection arrives from the large lateral walls. In other words, in an opera house, it is important to know the reflective surface providing the Δt_1 in order to adjust Δt_1. Table 2.1 shows the results of left and right Δt_1 at each receiver for S1 and S2.

For S1, note that sound paths of the direct sound of second and third rows were disturbed by stage overhang. For S1, Δt_1 around 10-11 ms, which may be reflections from the pit rail behind the source, were dominant, especially at third row. They provide the frontal reflection for receivers. That around 25-30 ms may be reflections from the proscenium arch. Relatively large Δt_1 (52 ms) was obtained for left channel at M03. This may be a reflection from the ceiling or lateral wall of the hall. On the other hand, quite small Δt_1 (3 ms) was obtained for right channel at M05. This is the reflection from the proscenium arch next to the M05. In the second row, a reflection with maximum amplitude is difficult to determine due to complicated initial reflections arriving at receivers. This means that a reflection with the maximum amplitude does not arrive from a same reflective surface inside the theater.

For S2, Δt_1 values around 20 ms were reflections from the pit rail, those around 40 ms are reflections from the proscenium arch, and the others may be reflections from walls inside the hall. Although values of Δt_1 at M06 (left) and M07 (left) can be considered to be reflections from the proscenium arch, many initial reflections arrived at each receiver of second row. It means that reflections with similar amplitude (due to multiple reflections in the pit) arrive around 20 ms at such locations as well as other receivers' location in the first and second rows. The Δt_1 at M15 (left) (70 ms), which may be from a wall inside the hall, has the longest sound path among the receivers.

Table 2.1. Results of Δt_1 for each receiver locations. The results for both source locations in the pit, S1 and S2 are shown. Range means the difference between the maximum and minimum value.

	Δt_1 [ms] for S1		Δt_1 [ms] for S2	
Receiver	Left	Right	Left	Right
M01	10	10	19	18
M02	25	10	22	23
M03	52	30	23	23
M04	13	14	24	24
M05	11	3	25	24
M06	47	9	46	21
M07	45	11	40	23
M08	11	53	24	23
M09	11	19	22	25
M10	10	28	22	27
M11	10	10	43	20
M12	11	11	24	25
M13	11	11	50	52
M14	11	11	54	50
M15	10	10	70	51
Range	42.4	50.0	50.9	33.9

Table 2.2 represents the results of A value, which is defined as total amplitude of reflections for the direct sound, for S1 and S2. For S1, mean values of A were 4.4 and 3.7 at left and right ear, respectively. For S2, larger A values were observed (55.1 at left ear and 31.8 at right eat) because of the stage overhang on the direct sound path. A value at left eat was larger than that at right, because the right ear is closer to the sound source than the left ear for both sources.

Figure 2.5(b) and Figure 2.6(b) show the contour lines of T_{sub} (500 Hz) for S1 and S2 respectively. Figure 2.9 shows the results of T_{sub} as a function of frequency for S1 and S2, respectively. Each plot is averaged among each row for both sources. Values of T_{sub} are larger as the raw is rear for both sources. For S1, the values of T_{sub} are almost constant between 1.2 and 1.3 s in the first row. In the second row, the T_{sub} at middle locations (M06 and M07) were relatively small around 1.5 s comparing with lateral locations (M05, M08, and M09) as 1.7–1.8 s due to the large volume of the stage house. In the third row, they are almost constant between 1.9 and 2.0 s again. The variation in the second row may reflect the complicated structures of initial reflections of impulse responses as described above. For S2, the values of T_{sub} were almost constant among each row, as the sound source is overhanged by the stage. The T_{sub} values were between 1.3 and 1.4 s, between 1.7 and 1.8 s,

and between 1.9 and 2.0 s for first, second and third row, respectively. Comparing between the values of T_{sub} for S1 and S2, T_{sub} at same receiver location is almost same at each center frequency as shown in Figure 2.9. When switching between S1 and S2, the values at T_{sub} are not significantly changed for a given receive position.

Table 2.2. Results of A value for each receiver locations. The results for both source locations in the pit, S1 and S2 are shown. Range means the difference between the maximum and minimum value. SD represents standard deviation.

	A value for S1		A value for S2	
Receiver	Left	Right	Left	Right
M01	2.9	1.0	55.6	26.6
M02	3.2	1.4	52.7	24.3
M03	1.0	1.1	53.4	28.2
M04	1.0	2.4	47.6	22.8
M05	0.7	1.3	37.1	24.5
M06	9.1	4.3	63.0	32.9
M07	7.6	3.5	66.2	31.6
M08	3.8	4.3	45.4	18.6
M09	2.9	5.6	60.2	38.9
M10	2.1	3.8	55.6	43.8
M11	10.2	6.4	55.3	33.0
M12	8.6	6.4	55.8	28.6
M13	5.9	5.3	54.5	32.4
M14	3.0	4.1	57.5	38.1
M15	3.6	5.2	66.2	53.3
Average	4.4	3.7	55.1	31.8
SD	3.1	1.9	7.7	8.9

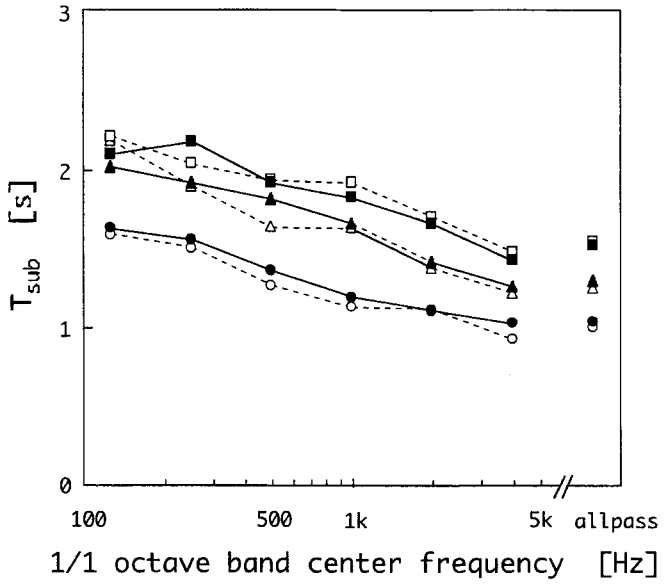

Figure 2.9 Results of T_{sub} as a function of frequency. Each plot indicates the average value of T_{sub} at each row. Right side plots without lines are the results for allpass band. ○: front row (M01-M05) for S1; △: middle row (M06-M10) for S1; □: rear row (M11-M15) for S1; ●: front row for S2; ▲: middle row for S2; and ■: rear row for S2.

Figure 2.5(c) and Figure 2.6(c) show the contour lines of IACC (500 Hz) for S1 and S2, respectively. For S1, the value of IACC at M03 has a large value as 0.57, because the source existed in front of the receivers in the symmetrical theater. However, when moving to the sides, the IACC become small below 0.3 at M04 and M05. For S2, the IACC was much lower than that for S1. Region above 0.4 clearly increased for S1. Figure 2.10 shows the results of IACC as a function of frequency for each row of S1 and S2. The values of IACC were larger above 1 kHz at front row for both S1 and S2. The values of IACC in second and third rows above 1 kHz are near 0.2 or less. For S2, IACC at 1 kHz (0.45) and 2 kHz (0.35) at the first row were larger than other receivers' locations. Maximum difference as 0.3 appeared at 1 kHz between first and second row for S2. Such an increase of IACC above 1 kHz is unpredictable phenomenon in the present stage.

Figure 2.11(a-d) shows examples of interaural crosscorrelation functions at 500 Hz. For S1, as shown in Figure 2.11(a), the value of τ_{IACC} (500 Hz) was 0.59 ms at M01. Positive value means that the sound source is located at the right side for the frontal direction of the receiver. Figure 2.11(b, c) clearly shows the sound source at M03 (τ_{IACC} = 0.07 ms) and M13 (-0.02 ms) is located at frontal direction of the receiver. Figure 2.5(d) and Figure 2.6(d) shows the contour lines of τ_{IACC} for S1 and S2 respectively. For both sources, the τ_{IACC} varies in accordance with the direction of each source at all locations as expected. In this figure, the τ_{IACC} at M07 with a minor peak as 0.25 ms is indicated in the

brackets.

Values of W_{IACC} were almost constant at all receivers. Average value of W_{IACC} among M01-M15 was 0.04 for both sources. Their standard deviations are 0.007 and 0.004 for S1 and S2, respectively. W_{IACC} extracted from impulse responses are not so significant because the frequency characteristic of the source (MLS signal) is flat.

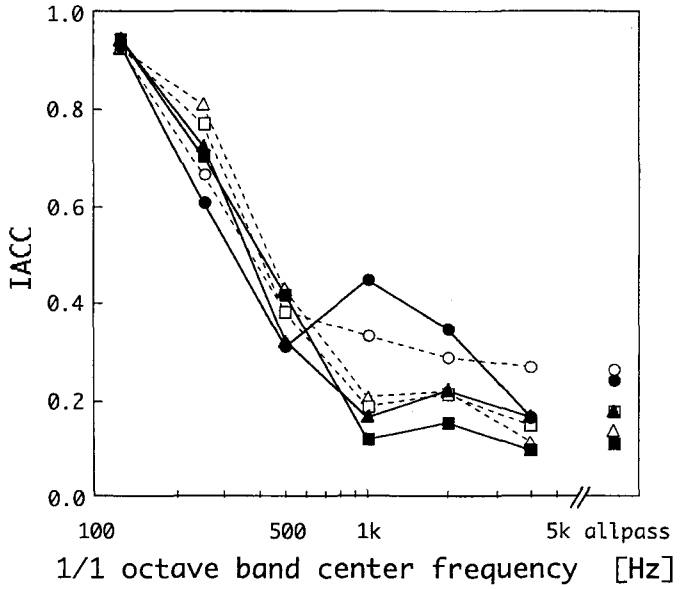

Figure 2.10 Results of IACC as a function of frequency. Each plot indicates the average value of IACC at each row. Right side plots without lines are the results for allpass band. ○: front row (M01-M05) for S1; △: middle row (M06-M10) for S1; □: rear row (M11-M15) for S1; ●: front row for S2; ▲: middle row for S2; and ■: rear row for S2.

The results of *LL* show, variance of *LL* for the back-and-forth direction was much remarkable at frontal area on the stage regardless of the source location than that for the side direction. As the difference of *LL* between the first and second row (2.5 m) was about 5 dB, a singer on the stage can adjust the preferred sound field by the back-and-forth movement. On the other hand, the movement of a side direction gives minor effect for *LL* for a singer. For T_{sub}, variance of T_{sub} for the back-and-forth direction was much remarkable between the first and second rows regardless of the source location than that for the side direction. Average values of T_{sub} for first and second row were 1.27 and 1.64 s for S1, and 1.36 and 1.81 s for S2. Thus, a singer on the stage can also adjust the sound field by moving for the back-and-forth direction.

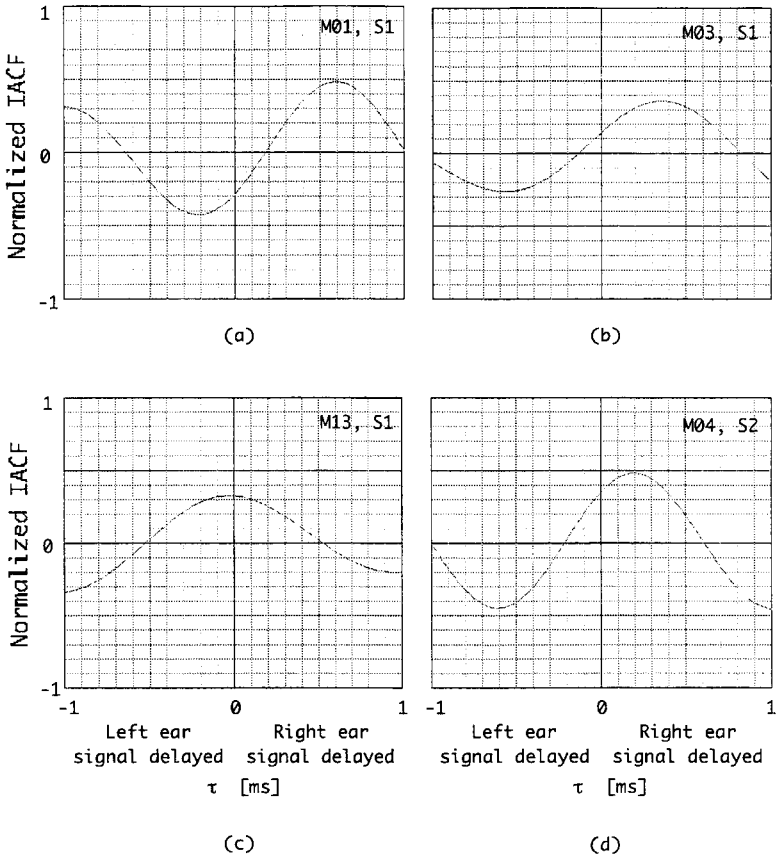

Figure 2.11 Examples of interaural crosscorrelation functions. (a): M01 for S1; (b): M03 for S1; (c): M13 for S1; and (d): M04 for S2.

Attenuation of *LL* at lower frequency range was observed for S2 under the stage overhang. As lower frequency instruments are mainly played under the stage overhang, this low frequency attenuation is a conflict in terms of the location of musicians in the pit. In terms of a sound field for a singer on the stage, this result suggests to move the lower frequency instruments to frontal area in the pit in order to suppress the low frequency attenuation.

As shown in Figure 2.8, *LL* variation among each row for S2 was small for the distance between the source and each receiver. Initial reflection components mainly from the pit rail may be much effective for the receivers than the obstructed direct sound.

Figure 2.12 shows the relationship between left and right Δt_1 for both sources. Week significant difference was observed for S2 was (R^2 = 0.57), although the difference was not significant for S1. This may be caused by the Δt_1 for S2, which mainly arrived from the pit rail. It is considered that different Δt_1 at both ear were observed for S1, as the Δt_1 for S1 arrived from different reflective surface (the pit rail, proscenium arch, etc.).

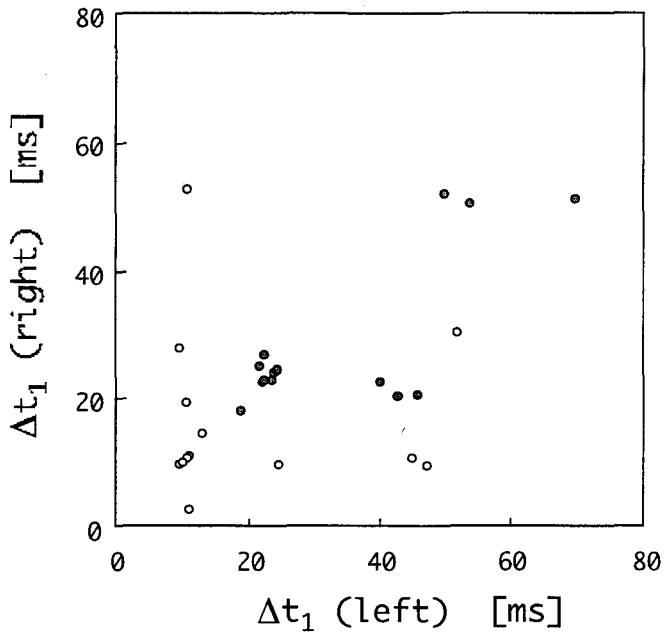

Figure 2.12. Relationship between left and right Δt_1. ○: Δt_1 for S1 (R^2 = 0.57); and ●: Δt_1 for S2 ($R^2 < 0.01$).

Figure 2.13 shows the relationship between left and right Δt_1 at each receiver for S1 and S2, and the ratio of amplitude of Δt_1 to that of the direct sound. Vertical axis is the amplitude of the Δt_1 relative to that of the direct sound. Generally, a plot above unity represents the interference of the sight line between the source and a receiver. For S1, vertical values are always less than 3 for all receivers, although the sight line was interfered. On the other hand, the values for all receivers were above 8.8, because the direct sound was completely interfered by the stage overhang. Also this figure well represents the dominance of Δt_1 for each source, namely around 10 ms and 20 ms were dominant for S1 and S2 respectively. This figure is useful to determine the reflective surface for each receiver, too

A singer prefers a first reflection of a singer's own voice and ensemble not from upward direction but from frontal and lateral reflections [12, 13]. Considering this fact, in terms of Δt_1, it may be better for a singer to shift singing location from the middle on the stage like M03 or M08. On the other hand, in terms of acoustical design, it is necessary to adjust the degree of the upper part of the proscenium arch not to provide upward reflection toward a singer on the stage. As the lack of psychological response data for a singer in relation to the orchestra, it is necessary to conduct psychological experiments for a singer in changing acoustical conditions playing orchestra in future.

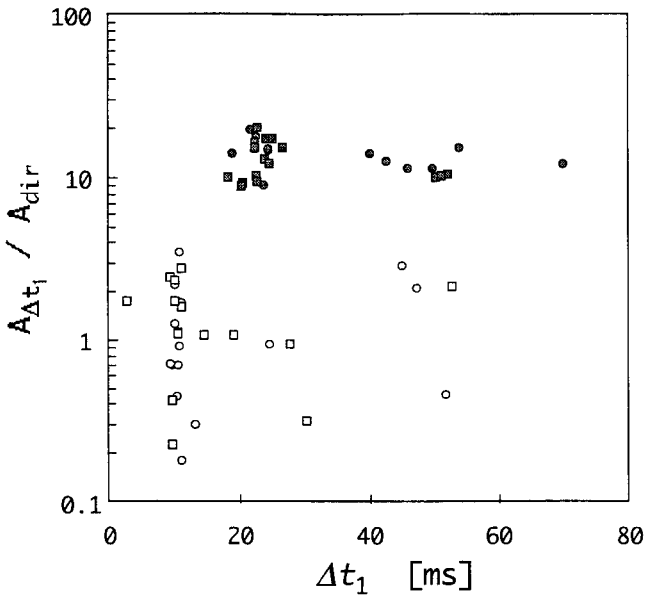

Figure 2.13. Relationship between left and right Δt_1 at each receiver for S1 and S2, and the ratio of amplitude of Δt_1 to that of the direct sound. ○: left Δt_1 for S1; □: right Δt_1 for S1; ●: left Δt_1 for S2; and ■: right Δt_1 for S2.

A large value IACC, which a sound source or a strong reflection arriving from the frontal direction of a receiver can provide, is preferred for a singer [11]. Thus, it is better for a singer to perform on the middle of the frontal stage as well as Δt_1, in terms of IACC. A large value of IACC was obtained even when the source located at S2 overhanged (0.48 at M04 for 500 Hz). However, it must be noted that there is a risk to get an upward reflection at such a central-front area as described above.

There is an area with small IACC below 0.3 at 500 Hz. This occurred because a receiver always faces to frontal direction toward to the stall. If a receiver face the direction of the source, IACC may increase more or less. In performance, a skilled singer can adjusts to obtained a better sound field unconsciously.

In relation to τ_{IACC} in Figure 2.5(d) and Figure 2.6(d), clear peak of interaural crosscorrelation function can be seen even for S2 under the stage, as well as S1. This suggests that a singer on the stage can localize the direction of the source even for the source under the stage.

Remarks

The present investigation provides useful knowledge for a singer on the stage for the sound emitted by sources in the orchestra pit in a typical historical opera house. Conclusions are obtained as following.

As each physical factor greatly varies on the stage for the sources in the orchestra pit, a singer can adjust to the preferred sound field by moving the location on the stage. For *LL* and T_{sub}, the variance of these factors are remarkable for the back-and forth direction in the frontal area on the stage. On the other hand, the variance is not so significant for the side direction.

In terms of IACC, it can be suggested for a singer to perform in the middle-front on the stage where has a strong reflection from the frontal direction. On the frontal-center location on the stage, however, an un-preferred upward reflection for a singer from the proscenium arch should be avoided.

From the results of τ_{IACC}, a singer on the stage can localize the direction of the source even for the source under the stage.

These results suggest the necessity of the psychological experiments for a singer in relation to the orchestra music in the orchestra pit in a laboratory regarding to the complicated initial reflections inside an opera house.

Also these data gives valuable and information in designing a stage and an orchestra pit inside opera houses. In order to improve the sound field on the stage, it is proposed that the location of musician playing lower frequency part should move to the closer to a conductor in order to avoid the attenuation at low frequency range under the stage. And the significance in designing proscenium arch and a pit rail to avoid upward reflection and strong lateral reflection decreasing IACC is described.

2.2.2 Acoustical Measurement for Musicians in Orchestra Pit

The main aim at this work is thus the close investigation of the listening attributes experienced by performers in the orchestra pit for the sound emitted by sources on the stage. Several combinations of sound sources on the stage and listeners (as musicians) in the pit are considered and the resulting sound fields are analyzed as well as the previous subsection.

Procedure

Measurements were conducted in changing the location of a sound source on the stage. Locations of sound sources and receivers were determined according to the possible locations of a singer on the stage and players in the pit as shown in Figure 2.14. Three locations of the sound source P1, P2, and P3 on the stage and ten locations of the receiver (M01-M10) in the orchestra pit were selected. The P1-P3 were selected as possible locations for the singer on the stage. The P1 was located at middle-front of the stage. The P2 was located just under the proscenium arch and 6-m from the centerline. The P3 is located 2.5 m behind from P1. The height of the sources was 1.5 m considering standing singers on the stage. Ten receivers were distributed with its grid 2.5-m in the pit as shown in the figure. The height of the human receiver (the location of the ears) was about 1.2 m. The receiver always sat on a chair and directed toward to the conductor's position. Reference measurements were conducted at a distance of 1 m for all sources. Note that the locations of the sources P1 and P3, and the receivers were 1 m away from the centerline axis for the reason as well as the previous measurement.

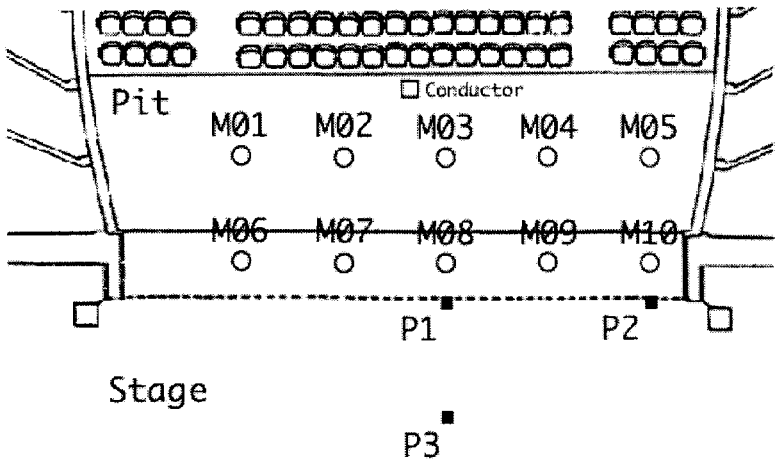

Figure 2.14 The locations of sound sources (P1-P3) and receivers (M01-M10).

Results and discussions

Figure 2.15(a-e) shows binaural impulse responses as typical examples of the measurements. Note that the receivers always faced toward the conductor's position (middle front in the pit). As shown in Figure 2.15(a), the amplitude of the direct sound at the left ear is smaller than the initial reflection, because the receiver M02 faced toward the conductor's position and a human head obstructs the direct sound path for the left ear. Except for such cases, the largest amplitude appears in the initial reflections for the receivers in the rear row (M06-M10) for all source positions, although it appears as a direct sound for the receivers in the front row (M01-M05). This phenomenon is deeply connected to the sight line between the sound source and each ear of the receivers. As there is no obstacle between P1 and the receiver M03, the direct sound has the maximum amplitude as shown in Figure 2.15(b). Although the receiver turns his back upon the source, well-balanced impulse responses were obtained. Figure 2.15(c, d) show typical examples of impulse responses for which the amplitude of Δt_1 is larger than the direct sound (M06 and M08 for P1, respectively). As shown in Figure 2.15(e), the first strong reflection, which arrived from the proscenium arch close to M05, arrived within 1 ms at M05 for P2.

Figure 2.16(a), Figure 2.17(a), and Figure 2.18(a) show the results of *LL* (500 Hz) for P1, P2, and P3 respectively. The averaged *LL* (500 Hz) for all receivers' positions for P2 and P3 was 1.8 dB and 4.0 dB smaller than that for P1, respectively. This value is mainly due to the attenuation by the distance between the source and the receiver. The differences of averaged *LL* values between the front row and the rear row were not so long as 1.3, 0.4, and 1.2 dB for P1, P2, and P3, respectively. Figure 2.19 shows the results of *LL* as a function of frequency for each source position. Each plot indicates the average *LL* for each row. As the averaged *LL* is different for the front and rear row, values of *LL* among each row are averaged in the figure. Empty plots and filled plots indicate the results for front and rear row, respectively. Circles, triangles and squares indicate the average *LL* values of five receivers for P1, P2, and P3. And empty and filled symbols represent the results in the front and rear rows. For P1, there was a monotone increase as the frequency increased. There is no specific peaks or dips. For the cases of P2 and P3, large dips can be found at 2 kHz. For P2, small dips at 500 Hz were also observed.

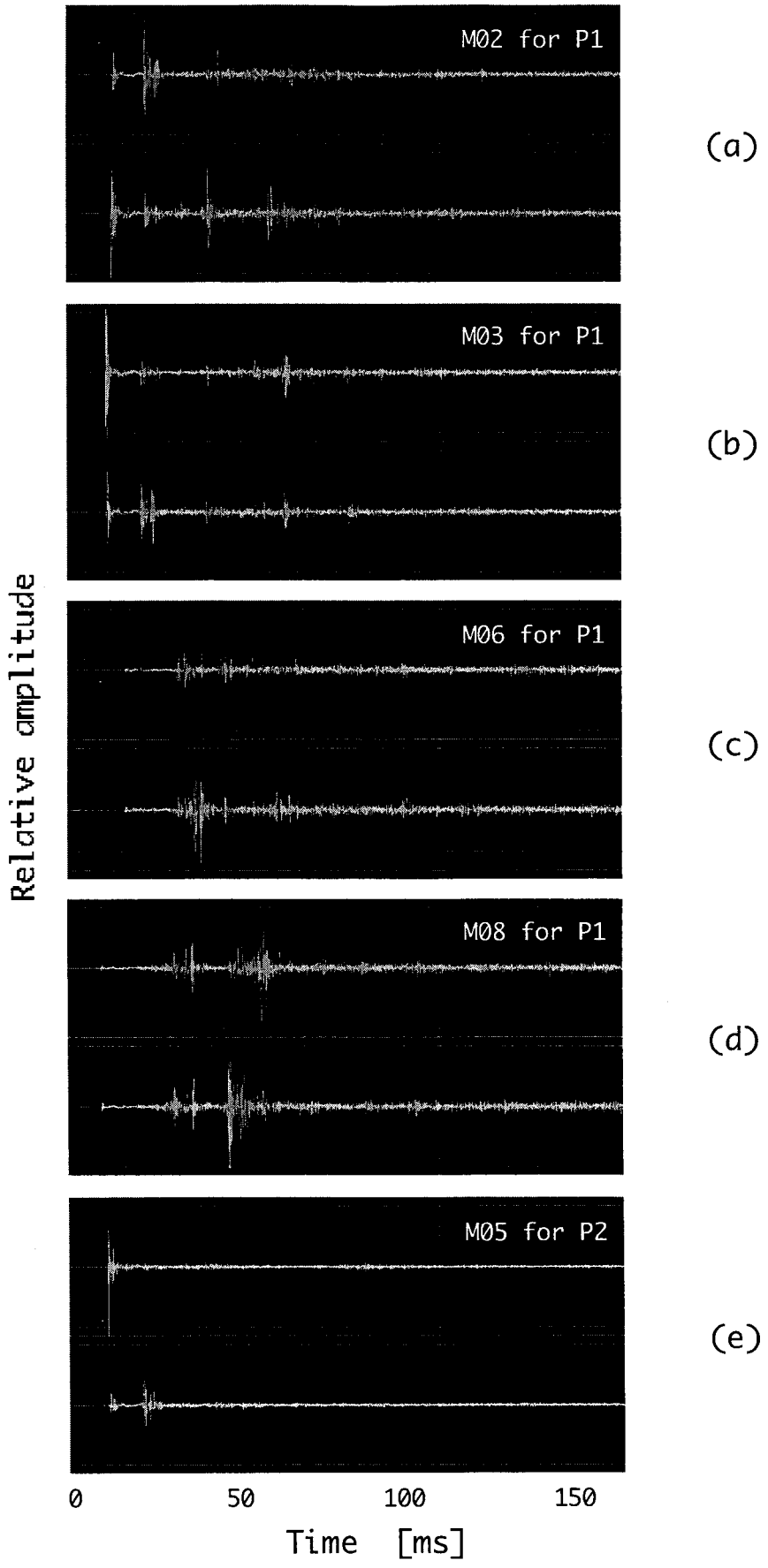

Figure 2.15. Binaural impulse responses as typical examples of the measurements. Initial 150 ms part is shown. (a): M02 for P1; (b): M03 for P1; (c): M06 for P1; (d): M08 for P1; and (e): M05 for P2.

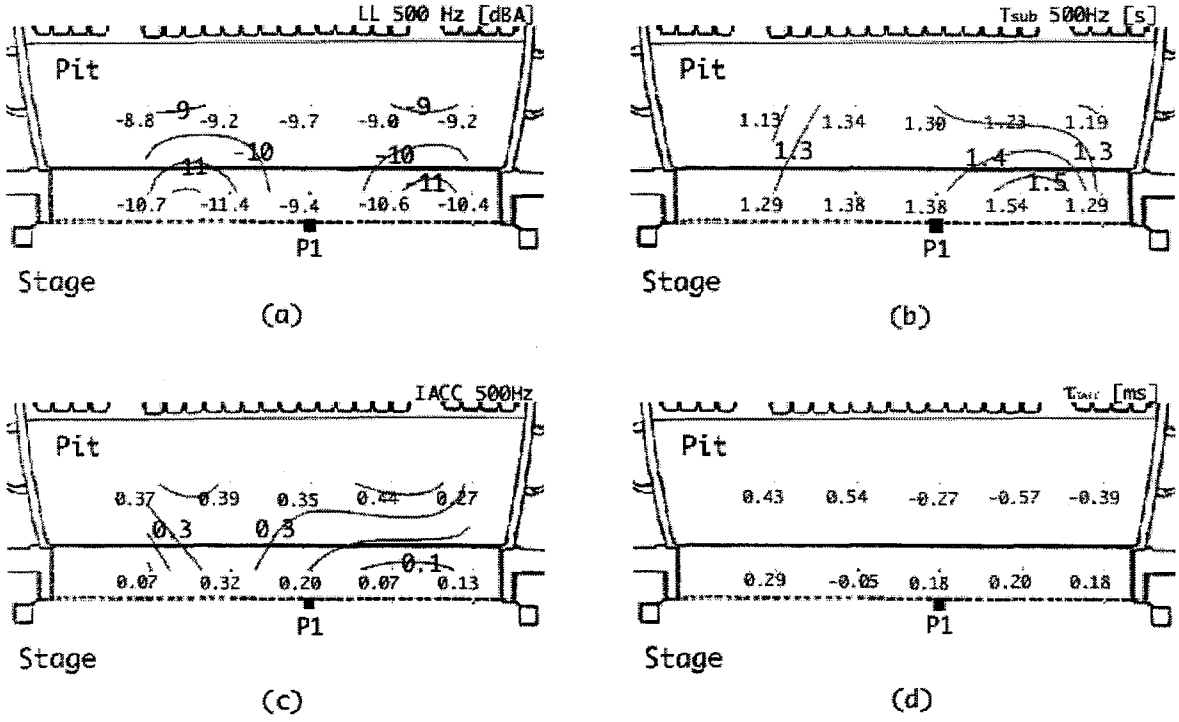

Figure 2.16 Contour lines of measurement results for P1. (a): *LL* (500 Hz); (b): T_{sub} (500 Hz); (c) IACC (500 Hz); and (d): τ_{IACC}.

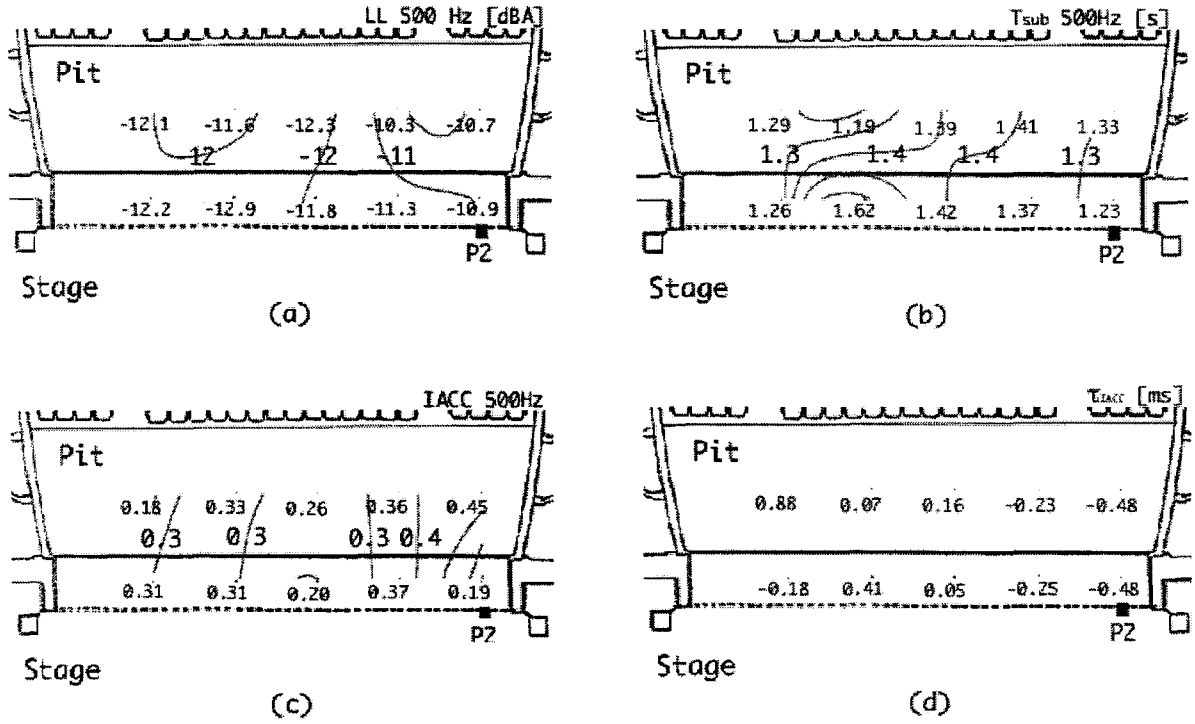

Figure 2.17 Contour lines of measurement results for P2. (a): *LL* (500 Hz); (b): T_{sub} (500 Hz); (c) IACC (500 Hz); and (d): τ_{IACC}.

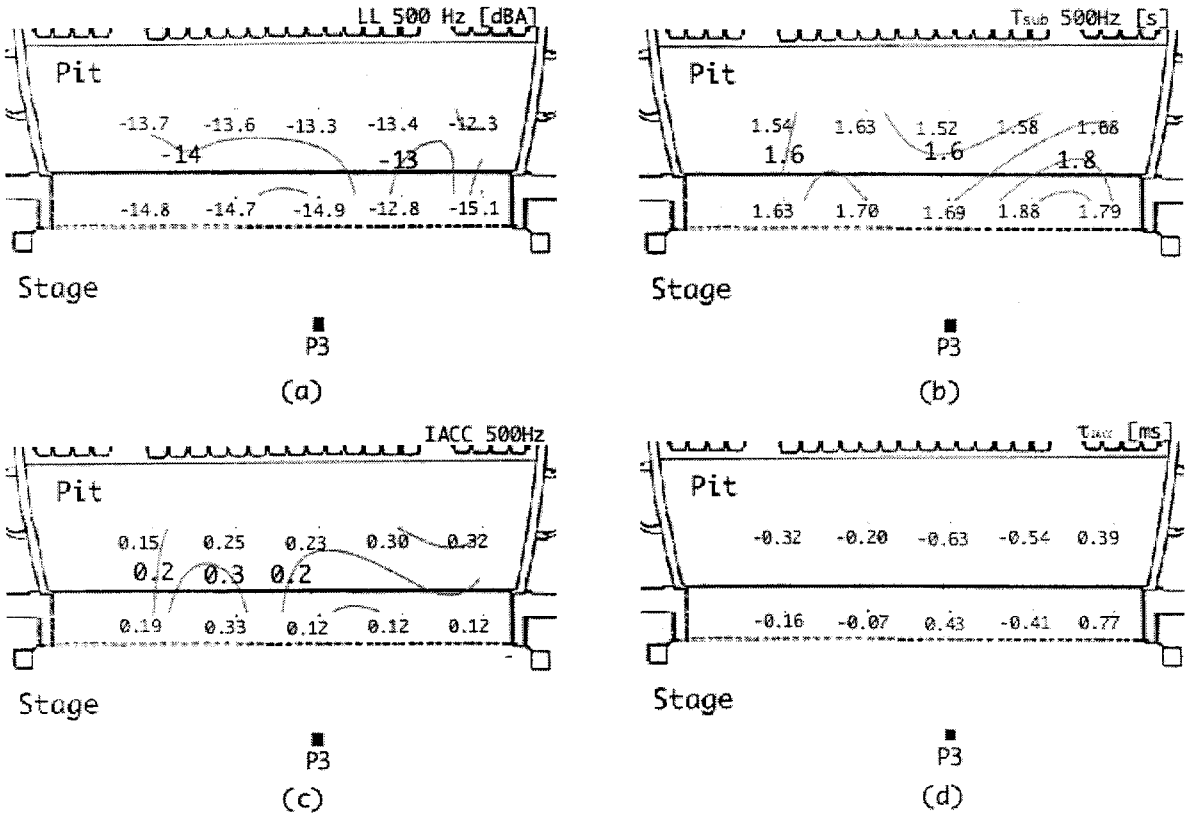

Figure 2.18 Contour lines of measurement results for P3. (a): *LL* (500 Hz); (b): T_{sub} (500 Hz); (c) IACC (500 Hz); and (d): τ_{IACC}.

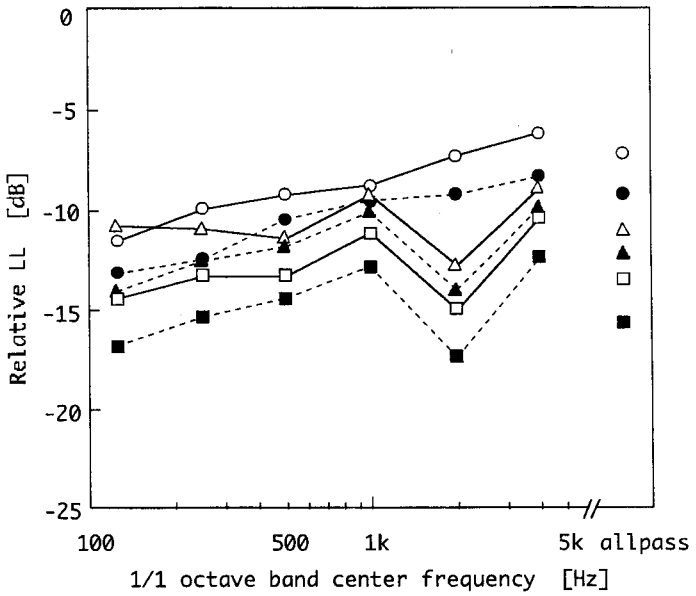

Figure 2.19 Results of relative *LL* as a function of frequency. Each plot indicates the average value of *LL* at each row. Right side plots without lines are the results for allpass band. ○: front row (M01-M05) for P1; ●: rear row (M06-M10) for P1; △: front row for P2; ▲: rear row for P2; □: front row for P3; and ■: rear row for P3.

The value of Δt_1 is defined as a delay time of reflection whose amplitude become the maximum for impulse response at each ear. Generally, the first reflection becomes the maximum reflection in the case of the stall of a theater or a concert hall. However, in a sound field including the stage and the orchestra pit, this relation is not kept because of the overhanged stage in the pit and the existence of a stage house. Table 2.3 shows the results of Δt_1 for the each source. As the different Δt_1 were obtained at both ears in some receivers as shown in binaural impulse responses in Figure 2.15, both left and right Δt_1 values were calculated. Especially for P1 and P2, the initial reflections arriving at each receiver are much complicated. For this reason, contour lines were unable to make for Δt_1.

For P1, Δt_1 of 7-10 ms for the front row and 15-20 ms for the rear row come from the pit rail considering the geometry of the pit. The longer Δt_1 (26 ms for left channel at M01; 28 ms for left channel at M02) was obtained. The Δt_1 at such receivers arrived from the proscenium arch. In overhanged rear row, the longer Δt_1 (for example 47 ms for left channel at M08; 54 ms for left channel at M09) was obtained. The Δt_1 at such receivers arrived from the lateral walls in the hall part. Thus, Δt_1 does not vary successively inside the pit. For the other source locations, the reflections from lateral walls in the pit, proscenium arch, and walls in the hall part, become the strongest reflection at some receivers. As described above, the Δt_1 does not vary successively due to the different reflective surface determining Δt_1.

Table 2.3. Results of Δt_1 [ms] for each receiver locations. This table contains the results for source locations on the stage, P1, P2, and P3 respectively. Range means the difference between the maximum and minimum value.

	Δt_1 for P1 [ms]		Δt_1 for P2 [ms]		Δt_1 for P3 [ms]	
Receiver	Left	Right	Left	Right	Left	Right
M01	8	26	5	4	9	33
M02	9	28	6	4	10	11
M03	53	10	26	3	30	11
M04	10	9	2	9	29	10
M05	5	7	1	10	27	9
M06	16	20	25	15	19	19
M07	39	18	17	17	36	46
M08	47	38	21	22	47	22
M09	54	31	25	20	34	21
M10	20	17	26	22	24	19
Range	49	30	26	19	38	37

Figure 2.20 shows the relationship between left and right A values. A values were large, especially at the receivers in the rear row as represented in Table 2.4. A values were more than 15 in the rear row for all source positions. For S2 and S3, left A values were more than 30. This means the small amplitudes of direct sound in the rear row. For example, when a sound source was on the stage in the same theater, left A value averaged all around in the stall (21 positions) were 2.3 (SD = 0.49) (Sakai et. al, unpublished).

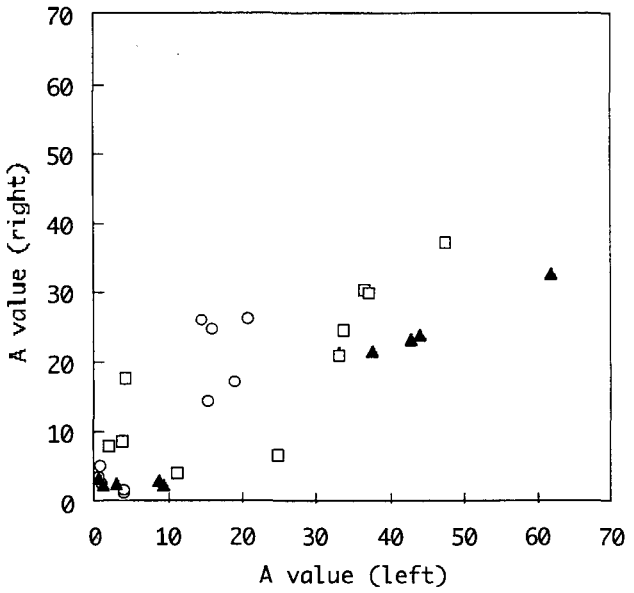

Figure 2.20. Left and right A values for each receiver location. ○: P1; ▲: P2; and □: P3.

Table 2.4. Results of A value for each receiver locations. This table contains the results for source locations on the stage, P1, P2, and P3 respectively.

	A value for P1		A value for P2		A value for P3	
Receiver	Left	Right	Left	Right	Left	Right
M01	4.26	1.07	9.00	2.98	25.00	6.37
M02	4.34	1.60	9.59	2.33	11.39	3.76
M03	1.15	2.28	3.30	2.62	4.00	8.30
M04	1.04	4.96	1.38	2.45	2.32	7.79
M05	0.78	3.44	0.81	3.53	4.38	17.41
M06	19.14	16.97	43.13	23.23	47.75	36.85
M07	16.08	24.41	44.36	23.76	33.36	20.61
M08	14.58	25.75	62.15	32.57	33.92	24.37
M09	21.00	25.89	37.78	21.54	36.81	29.98
M10	15.36	14.17	33.30	21.30	37.53	29.69

Figure 2.16(b), Figure 2.17(b), and Figure 2.18(b) show the results of T_{sub} (500 Hz) for P1, P2, and P3, respectively. For all sources, range of T_{sub} was around 0.2 s at 500 Hz in the pit. Averaged T_{sub} among 10 receivers for P3 becomes the largest as 1.66 s (standard deviation SD: 0.08 s). Those for P1 and P2 were 1.31 s (SD: 0.08 s) and 1.35 s (SD: 0.09 s), respectively. Figure 2.21 shows the results of T_{sub} as a function of frequency for P1, P2, and P3. Each T_{sub} value is averaged among each row for all sources. For all sources, the values of T_{sub} almost monotonically decrease as the frequency range become large. Comparing between the results at front and rear rows, averaged T_{sub} in the front row at 500 Hz (1.24 s) was smaller than that in the rear row (1.38 s) for P1. In the rear row for P1, there was a dip (1.45 s) at 125 Hz with uncertain cause. Those in the front row at 500 Hz (1.32 s) were smaller than that in the rear row (1.38 s) for P2. And those for P3 in the front row at 500 Hz and in the rear row were 1.59 s and 1.74 s, respectively. In the front row for P1, there was a peak (1.45 s) at 125 Hz. In the rear row, there was a dip (1.90 s) at 125 Hz.

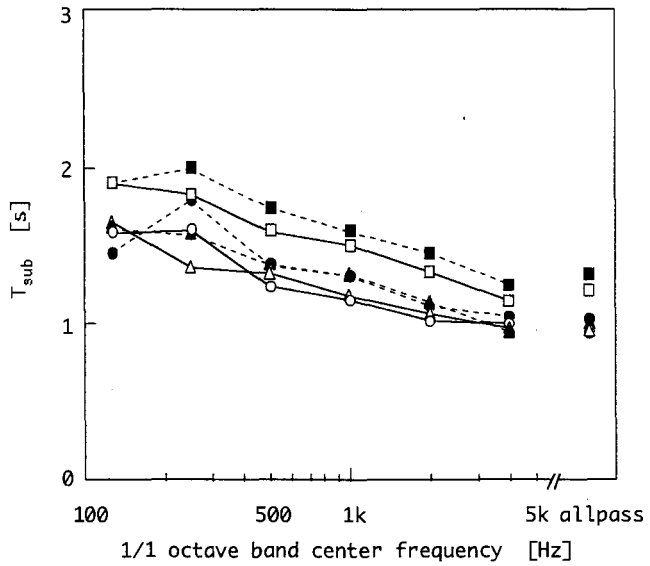

Figure 2.21 Results of T_{sub} as a function of frequency. Each plot indicates the average value of T_{sub} at each row. Right side plots without lines are the results for allpass band. ○: front row (M01-M05) for P1; ●: rear row (M06-M10) for P1; △: front row for P2; ▲: rear row for P2; □: front row for P3; and ■: rear row for P3.

Figure 2.16(c), Figure 2.17(c), and Figure 2.18(c) show the results of IACC (500 Hz) for each source. For all source positions, in the side at rear row, IACC were relatively small by lateral reflections in the pit. Figure 2.22 shows the results of IACC as a function

of frequency for each row of P1, P2, and P3. Average IACC in the front row for P1 has a specific peak at 1 kHz (0.36). On the contrary, the average IACC in the rear row for P1 has a rapid increase at 500 Hz. The IACC is larger above 1 kHz at front law for both P1 and P2. For P2, those at 500 Hz and 1 kHz at the first row are about 0.3 larger than other receivers' locations. Some dips were observed at lower ranges at the rear row for all source locations.

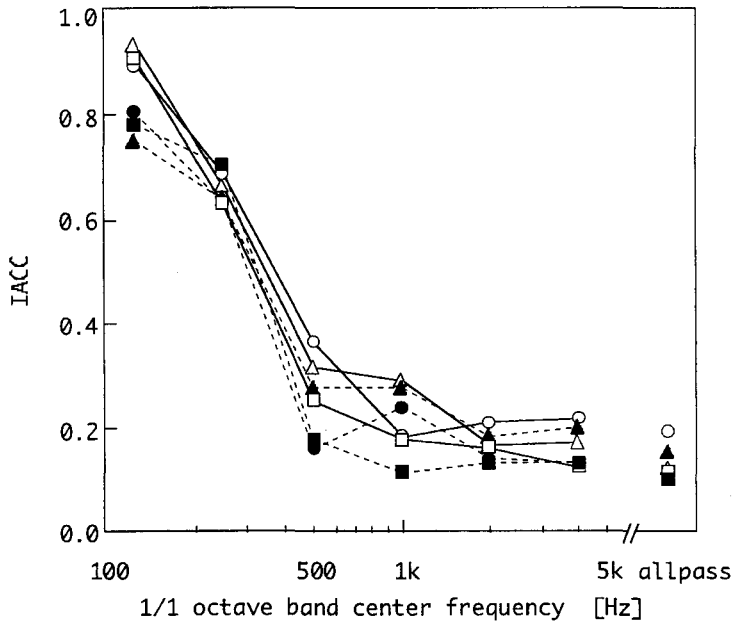

Figure 2.22 Results of IACC as a function of frequency. Each plot indicates the average value of IACC at each row. Right side plots without lines are the results for allpass band. ○: front row (M01-M05) for P1; ●: rear row (M06-M10) for P1; △: front row for P2; ▲: rear row for P2; □: front row for P3; and ■: rear row for P3.

Figure 2.23(a-c) shows examples of interaural crosscorrelation functions. For P1, as shown in Figure 2.23(a), the τ_{IACC} was –0.27 ms at M03. It means the sound source is located at the left side for the frontal direction of the receiver. For P2, as shown in Figure 2.23(b), the τ_{IACC} was –0.25 ms at M09. Figure 2.23(c) shows the example with minor peaks of interaural crosscorrelation functions (M03 for P3). Clear direction may not be perceived for this case. Figure 2.16(d), Figure 2.17(d), and Figure 2.18(d) show the results of τ_{IACC} for P1, P2, and P3 respectively. When the interaural crosscorrelation functions has no specific peaks like M03 for P3 as shown in Figure 2.23(c), the values of τ_{IACC} become difficult to determine. So contour lines were unable to make in these figures. Average values of W_{IACC} at each source location were almost constant as 0.04 (standard deviations are less than 0.01 for all receiver locations).

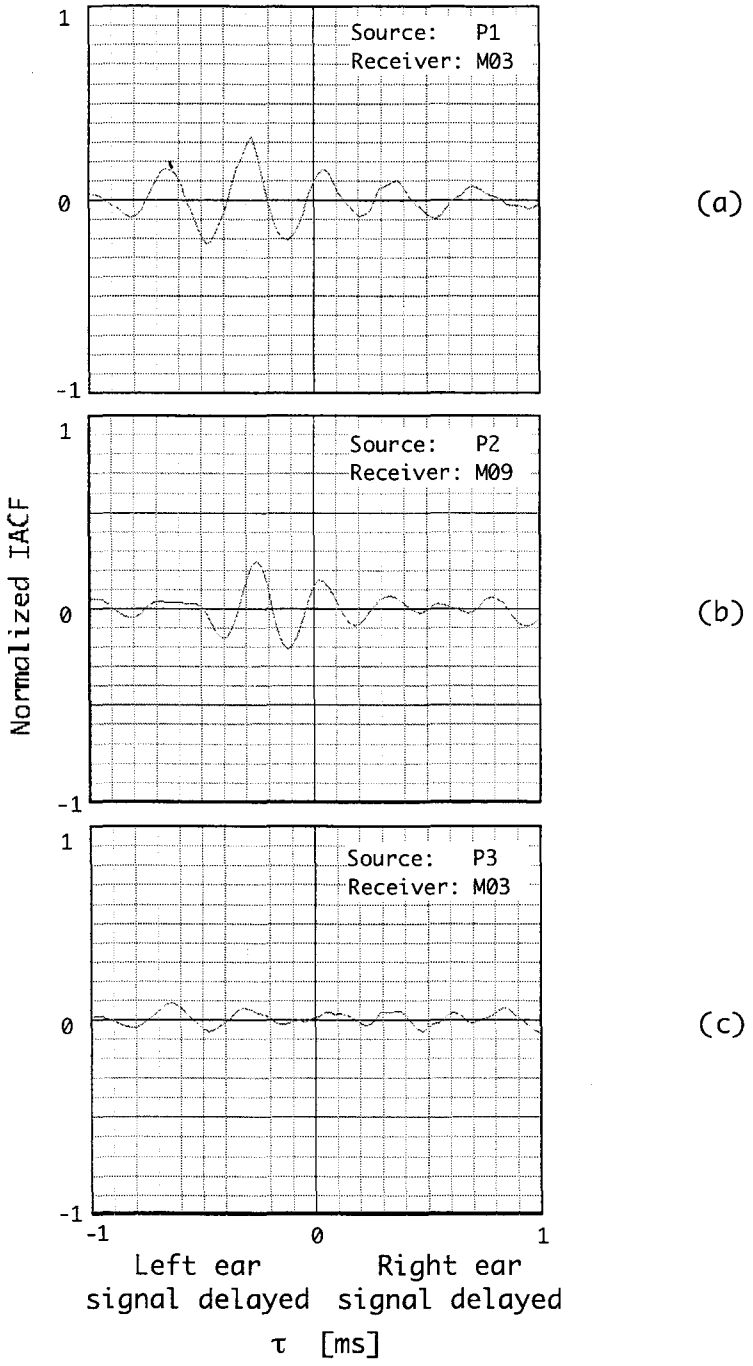

Figure 2.23 Examples of interaural crosscorrelation functions. (a): M03 for P1; (b): M09 for P2; (c): M03 for P3.

For P2 and P3, *LL* has a dip at 2 kHz as shown in Figure 2.19. When a singer performs at P2 or P3 (not center-front), the singing formant (Marshall and Meyer, 1984) may be suppressed more or less. If the location of a singer is constant, the difference of *LL* between the front and rear row is negligible. And specific enhanced *LL* at the low frequency range due to the standing wave between the pit floor and the stage (Sakai et. al, unpublished) was not observed even if the receiver placed under the stage in this

measurement.

As shown in Figure 2.21, the variety of T_{sub} are small at frontal source positions (P1 and P2) by a singer's movement for lateral direction. At rearer position such as P3, T_{sub} become longer, and the difference of T_{sub} between rows in the pit become larger. And T_{sub} s in the rear row at 250 Hz had dips for all source locations. However, as frequency characteristics of a singing voice is centered around 500 Hz or 1 kHz, this dip may not be problem.

As shown in Figure 2.22, IACCs above 500 Hz were quite small for all the sources. This phenomenon is caused by multiple reflection inside the pit. When the musicians listen to own sound in performance, large value of IACC is preferred. This suggests the necessity of psychological experiments for musicians listening a singing voice or other instruments. Also dip at 125 Hz at rear row for all source positions are uncertain phenomena.

Remarks

The present investigation provides useful knowledge for musicians in the orchestra pit for the sound emitted by sources on the stage in a typical historical opera house. Conclusions are obtained as following.

For the sources P2 and P3, large dips of *LL* can be found at 2 kHz. This may cause the suppression of the singing formant enhancing the singing voice at higher frequency range.

A values were quite large especially at the receivers in the rear row as more than 15 (up to 30) in the rear row for all source positions, although averaged *A* value in the stall (21 positions) were 2.3 in the same theater.

The variety of T_{sub} between the rows was negligible at frontal source positions (P1 and P2) by a singer's movement for lateral direction. At rearer position such as P3, T_{sub} become longer, and the difference of T_{sub} between rows become large as 0.2 s.

IACCs above 500 Hz were quite small for all the sources. This phenomenon is caused by multiple reflection inside the pit. By the unstable τ_{IACC} in the pit, the musicians in the pit perceive vague directivity for a singer singing on the stage, especially below overhang.

Thus, these data gives valuable and information in designing a stage and an orchestra pit inside opera houses. These results suggest the necessity of the psychological experiments for musicians in a laboratory especially regarding to the complicated initial reflections.

2.2.3 Acoustical Measurement for Conductor

The main aim at this work is thus the close investigation of the listening attributes experienced by a conductor in the orchestra pit for the sound emitted by sources in the orchestra pit and on the stage. Several combinations of sound sources and listeners in the pit are considered and the resulting sound fields are analyzed as well as the previous subsections.

Procedure

Locations of sound sources were determined according to the possible locations of musicians in the pit and a singer on the stage, as shown in Figure 2.24. The receiver was standing on the conductor's stage and faced toward to the stage-house. The receiver is located at same position throughout the measurements. Twelve sound sources (P1-P6 in the pit and S1-S6 on the stage) located as illustrated in the figure with its grid 2.5-m. The height of the sources was 1.2-m for those in the pit and 1.5-m for those on the stage.

Results and discussions

Figure 2.25 and Figure 2.26 show initial part (0-160 ms) of binaural impulse responses for each sound source in the orchestra pit (P1-P6) and on the stage (S1-S6), respectively. Amplitudes of left channel were generally larger than those of right ones, as all of the receivers located at left side of the conductor. For the sources in the pit (P2-P6), complicated multiple reflections between walls inside the pit were seen around initial 50 ms. For S2 and S5 on the stage, clear reflections were arrived around delay time of 30 ms.

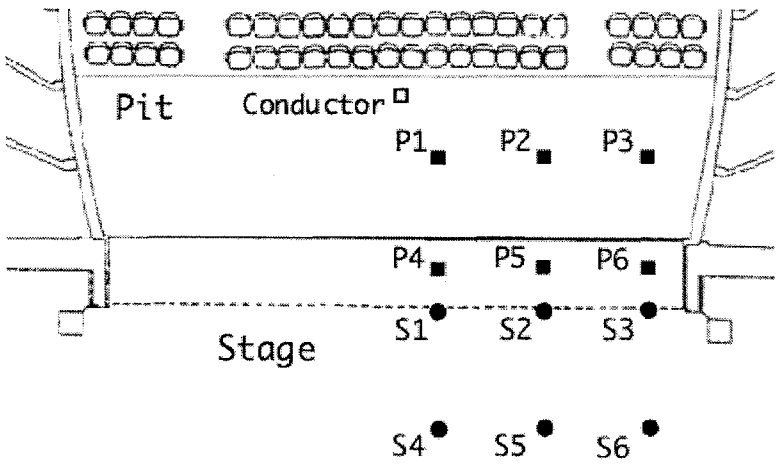

Figure 2.24 The locations of a receiver at a conductor's position and sound sources in the orchestra pit (P1-P6) and on the stage (S1-S6).

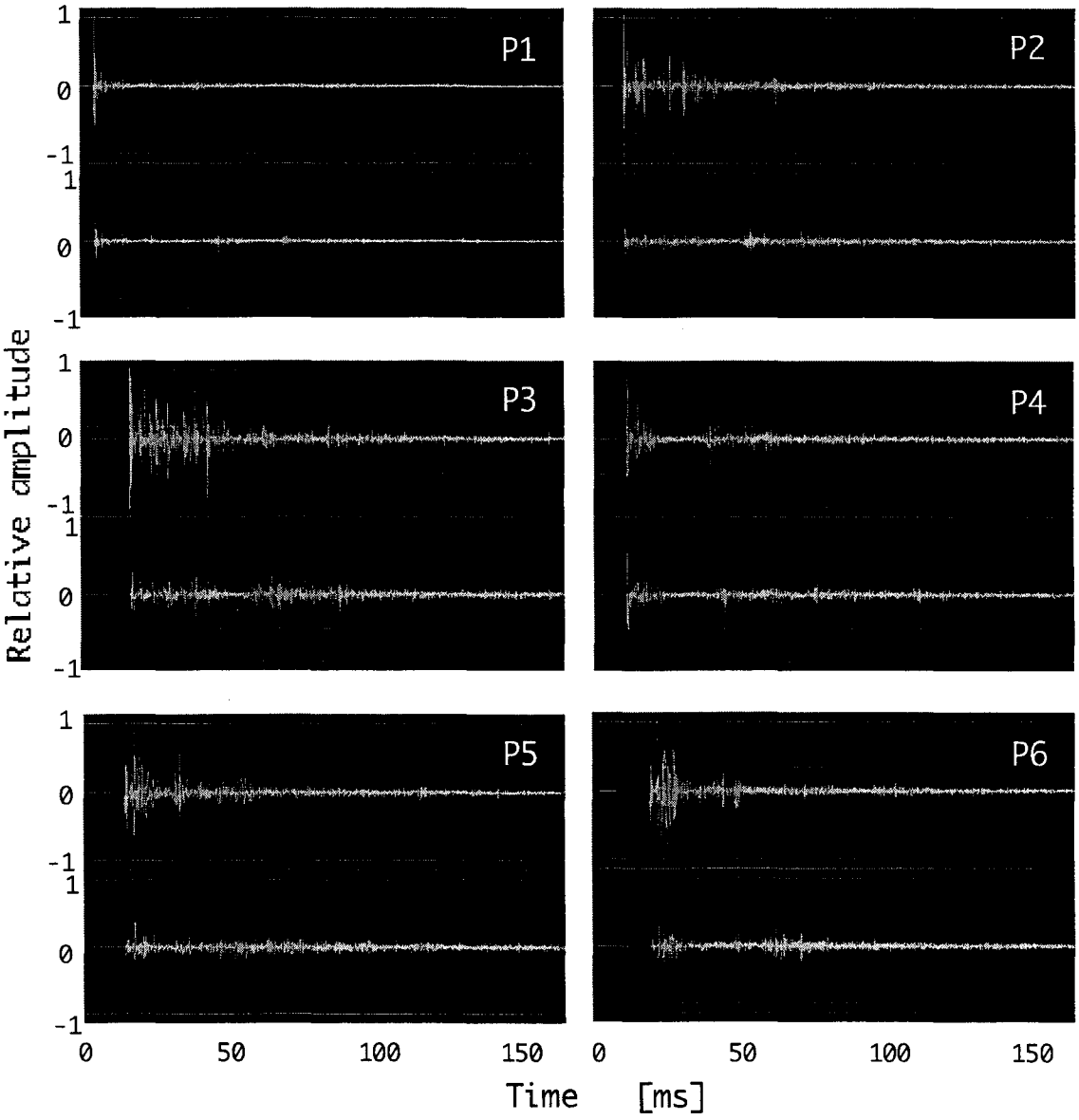

Figure 2.25 Binaural impulse responses at a conductor's position for each sound source in the orchestra pit (P1-P6). Upper: impulse response at left ear; Lower: impulse response at right ear.

Figure 2.27(a) shows the contour lines of *LL* (500 Hz). The difference of averaged *LL* (500 Hz) between the pit sources and the stage sources was 7.0 dB. Averaged *LL* values at 500 Hz were –6.2 dB for the pit sources and –13.2 dB for the stage sources. Ranges of *LL* were 2.4 dB for the pit sources and 5.0 dB for the stage sources. In the case that reflective surface existed near the sound source as P3, P6, and S3, *LL* kept large even if the distance between the source and the conductor was further. Other statistical values for *LL* are indicated in Table 2.5, as well as T_{sub} and IACC. Figure 2.28(a, b) show the results of *LL* as a function of frequency for the pit sources and the stage sources, respectively. Open circles with a straight line indicate the average *LL* for the pit sources or the stage sources. And the other different symbols indicate the results at each receiver. The values of *LL*

monotonically increase as the center frequency increases for both sources. For the pit sources, the dips were observed at 250 Hz, especially for P6 (-12.5 dB). This may be caused by the interference effects between the direct sound and strong initial reflections from a pit rail or from lateral or rear walls inside the pit, because the P6 located at a rear corner in the pit. Similar dip at 250 Hz can be found for P1. For only P2, there was a peak at 250 Hz and a dip (-9.9 dB) was shifted to lower frequency range at 125 Hz. For S3 and S6 on the stage, dips were observed at 1 kHz, and a peak (-10.6 dB) was observed at 500 Hz for S3.

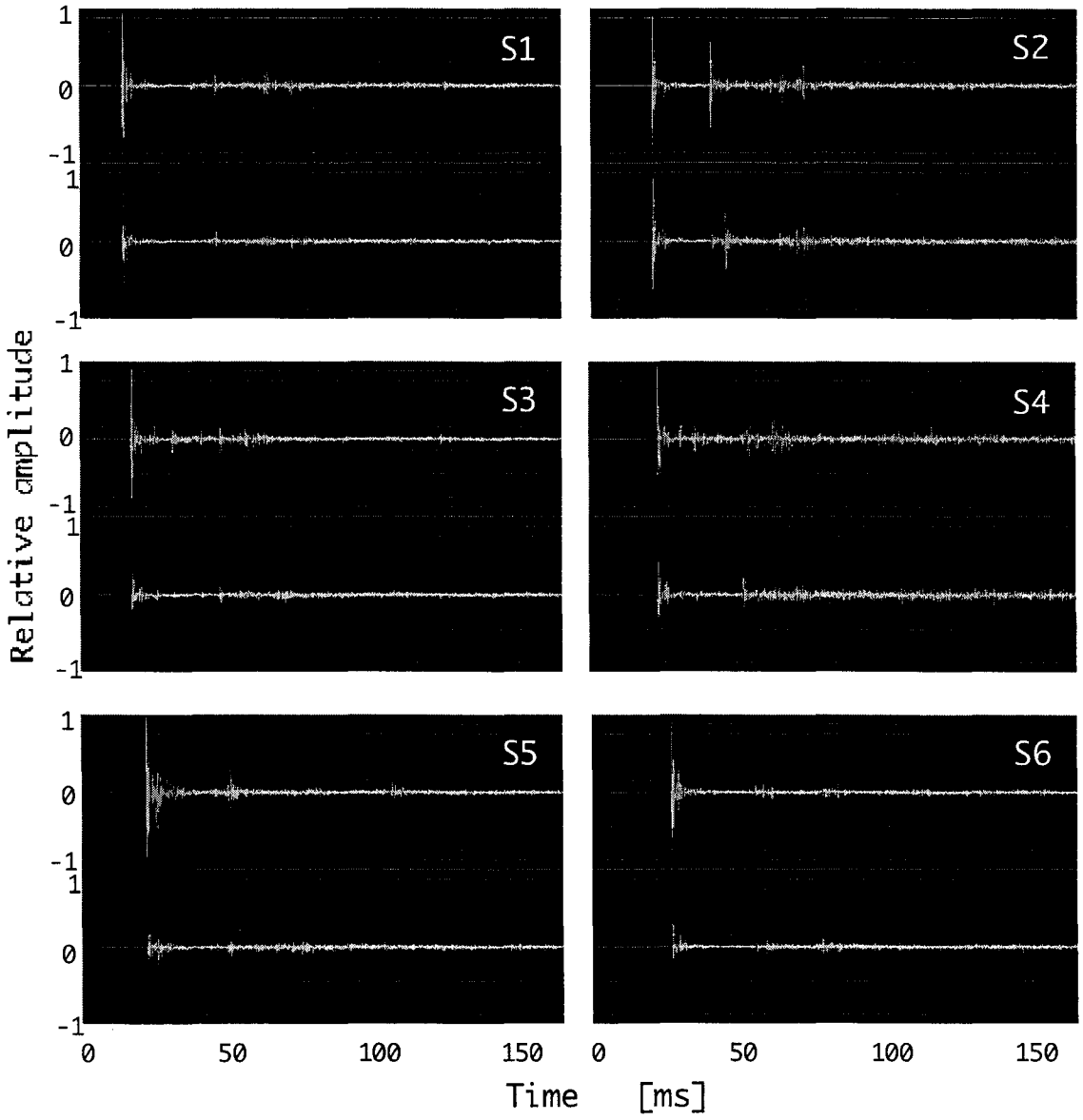

Figure 2.26 Binaural impulse responses at a conductor's position for each sound source on the stage (S1-S6). Upper: impulse response at left ear; Lower: impulse response at right ear.

Generally, the first major reflection becomes the reflection with the maximum amplitude in a concert hall. However, in a sound field including the stage and the orchestra pit, this does not happen because of the stage overhang, the orchestra pit, and the stage house. For this reason, Δt_1 is defined as a delay time of the reflection with maximum amplitude here. As the different Δt_1 values were obtained at both ears for some receivers, both left and right Δt_1 values were calculated. Figure 2.27(b) shows the contour lines of left and right Δt_1 at each source location. At audience area in concert halls, Δt_1 orderly varies, because the first reflection arrives from the large lateral walls. In other words, in an opera house, it is important to know the reflective surface providing the Δt_1 in order to adjust Δt_1.

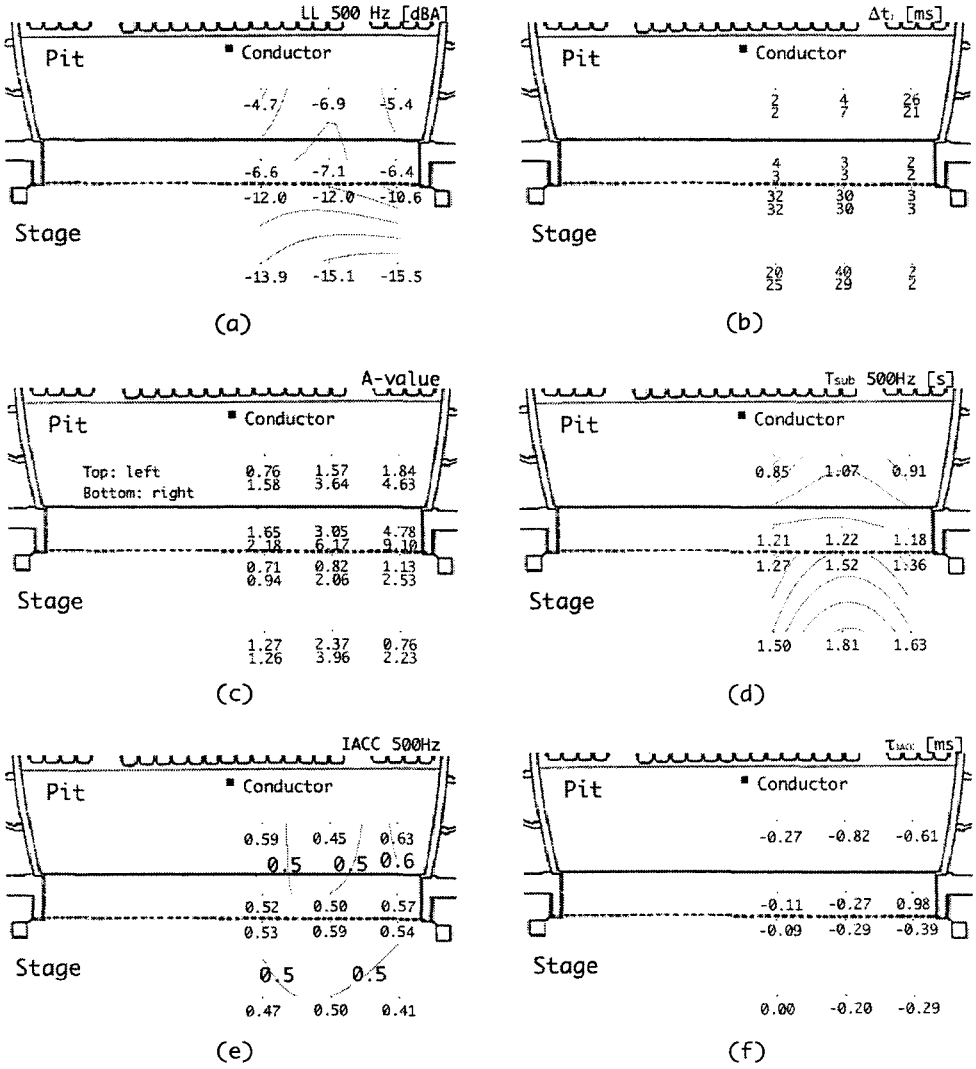

Figure 2.27 Contour lines of measurement results for each source location. (a): *LL* (500 Hz); (b): Δt_1 [ms]; (c): A value; (d):T_{sub} (500 Hz); (e) IACC (500 Hz) and; (f): τ_{IACC} [ms].

At all positions in the pit without P3, the first maximum reflection appeared around 3 ms. Such short reflections come from the pit rail just behind the conductor. As shown in impulse responses in Figure 2.25, multiple reflections between walls inside the orchestra pit were observed especially at the left channel of P2 and P3. The Δt_1 for P3 (left: 26 ms; right: 21 ms) was from the lateral wall in the pit. The Δt_1 at right channel for P2 (7 ms) was considered to come from the pit floor. Generally, the reflection from the floor should be excluded as Δt_1 in a concert hall. However, this reflection from the pit floor is included as Δt_1 here, because the reflection from the pit rail around 3 ms is shorter than this. Amplitudes of the direct sound for P5 and P6 were smaller than those of the first reflection around 3 ms. These boosts of the first reflection may be caused by the interference effects of strong initial reflections. As shown in Figure 2.26 for the stage sources, the Δt_1 was observed around 3 ms for S3 and S6, where are the positions near a sidewall of the proscenium arch. For the other source locations, first maximum reflections came from the lateral wall inside the hall or the proscenium arch. For S3 and S6, similar delay time values to the other positions were also observed (both left and right Δt_1 values for S3 were 29 ms; those for S6 were 29 ms), but they were not maximum amplitudes as Δt_1.

Table 2.5 Statistical values of the measurements. Average, standard deviation (SD) and range (maximum minus minimum values) of measured relative *LL*, T_{sub}, and IACC.

Factor	Source location		Allpass	1/1 octave band center frequency [Hz]					
			(A)	125	250	500	1k	2k	4k
LL	Pit	Average	-2.9	-7.1	-8.3	-6.2	-4.6	-3.8	-2.5
[dB]		SD	1.0	1.3	1.6	0.8	0.9	0.8	1.1
		Range	4.1	5.9	6.6	2.4	3.7	3.3	4.3
	Stage	Average	-9.8	-13.5	-14.1	-13.2	-13.4	-10.2	-9.1
		SD	2.0	1.5	1.4	1.6	1.5	1.8	2.3
		Range	6.1	5.1	4.6	5.0	6.4	4.9	7.5
T_{sub}	Pit	Average	0.82	0.98	1.05	1.07	1.00	0.92	0.82
[s]		SD	0.06	0.23	0.20	0.13	0.11	0.05	0.08
		Range	0.15	0.81	0.59	0.37	0.38	0.20	0.21
	Stage	Average	1.23	2.01	1.71	1.52	1.41	1.34	1.22
		SD	0.15	0.38	0.21	0.14	0.15	0.13	0.16
		Range	0.43	1.02	0.58	0.54	0.53	0.46	0.42
IACC	Pit	Average	0.19	0.87	0.73	0.54	0.35	0.27	0.21
		SD	0.09	0.07	0.08	0.05	0.07	0.11	0.06
		Range	0.32	0.18	0.30	0.18	0.22	0.42	0.17
	Stage	Average	0.38	0.94	0.77	0.51	0.33	0.43	0.36
		SD	0.09	0.02	0.06	0.05	0.08	0.07	0.11
		Range	0.35	0.05	0.22	0.18	0.35	0.25	0.48

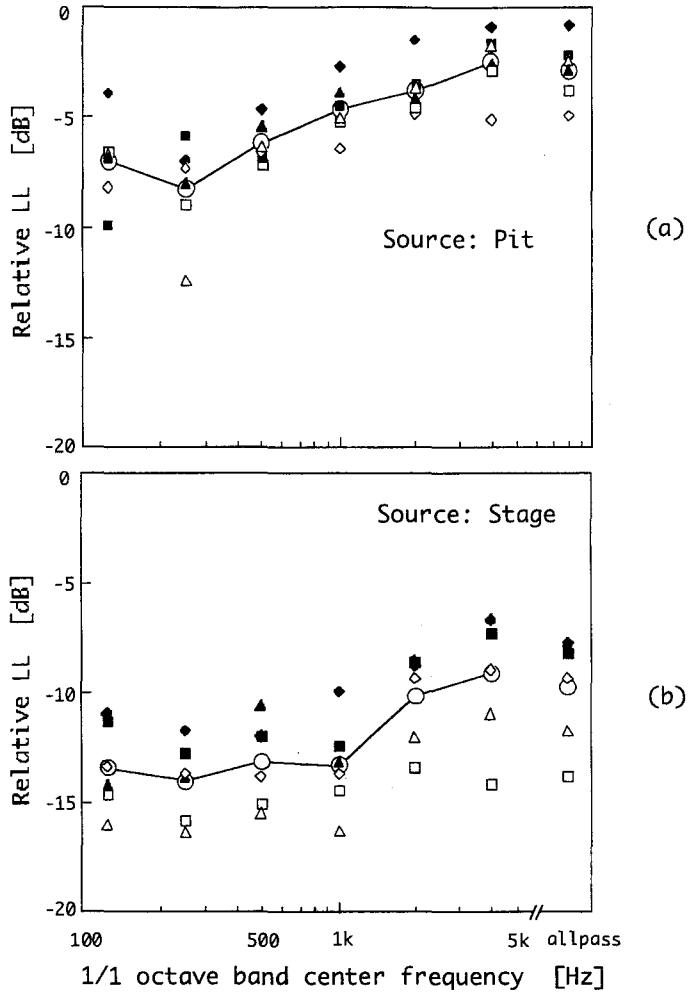

Figure 2.28 Results of relative *LL* as a function of frequency. (a): *LL* for the sources in the pit; and (b): *LL* for the sources on the stage. ○: average *LL* for all source locations in the pit or on the stage. Right side plots without lines are the results for allpass band. ◆: P1 or S1; ■: P2 or S2; ▲: P3 or S3; ◇: P4 or S4; □: P5 or S5; and △: P6 or S6.

Figure 2.27(c) shows the contour lines of A value. Generally, A value became larger, as the distance from the conductor was farther. A value for the distance was rapidly increase, especially in the pit, due to the multiple reflections inside the pit. Namely, A value was 1.58 at right channel of P1 and 9.10 at same channel of P6. Maximum A value was 3.3 in the stall of the same theater (Sakai et al., unpublished). A value at S6 was relatively small because strong initial reflections were absorbed inside the stage house. For all sources, A values at left channel become larger than right ones as the left channel of the conductor were always nearer than right one.

Figure 2.27(d) shows the contour lines of T_{sub} (500 Hz) for each source location. The average T_{sub} (500 Hz) for the stage sources was 1.52 s, which was longer than the values for the pit sources 1.07 s. This longer T_{sub} is due to the stage house. Differences between maximum and minimum T_{sub}s were 0.37 s for the pit sources and 0.54 s for the

stage sources. Figure 2.29(a, b) show the results of T_{sub} as a function of frequency for the pit sources and the stage sources, respectively. Although the frequency characteristics of T_{sub} were almost flat for the pit sources, T_{sub} increases at lower frequency ranges for the stage source. This longer T_{sub} at lower frequency range is caused by the effect of a large volume of a stage house. Statistical values for T_{sub} is indicated in Table 2.5.

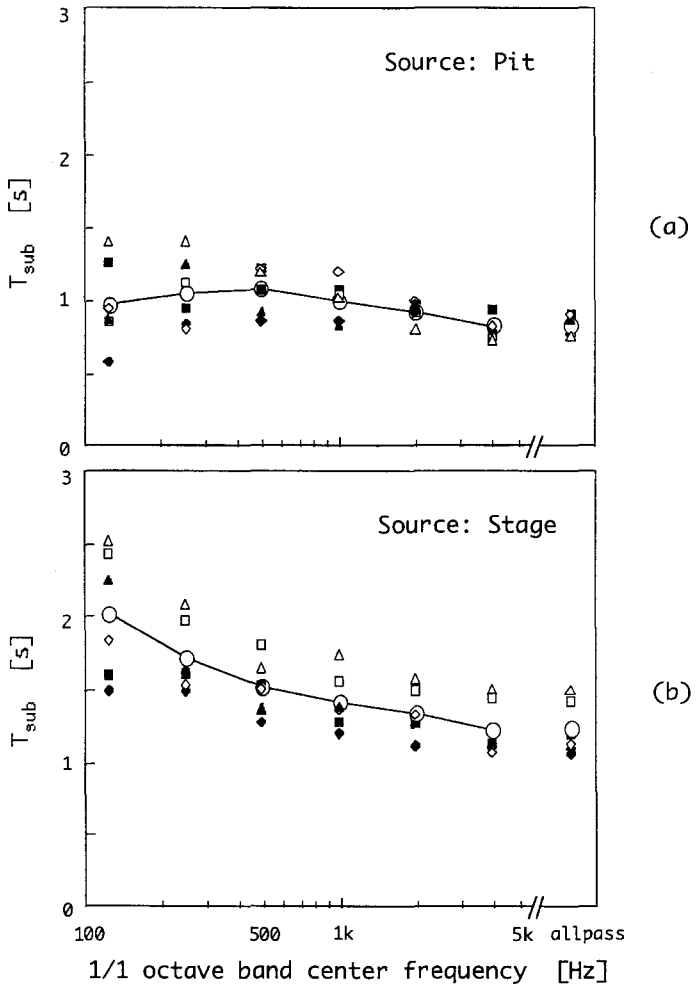

Figure 2.29 Results of T_{sub} as a function of frequency. (a): T_{sub} for the sources in the pit; and (b): T_{sub} for the sources on the stage. ○: average T_{sub} for all source locations in the pit or on the stage. Right side plots without lines are the results for allpass band. ◆: P1 or S1; ■: P2 or S2; ▲: P3 or S3; ◇: P4 or S4; □: P5 or S5; and △: P6 or S6.

Figure 2.27(d) shows the contour lines of IACC (500 Hz) for each source location. The average of IACC for the pit source was 0.54, which was as large as that for the stage source 0.51. For each source, IACC was larger above 0.4. Figure 2.30(a, b) show the results of IACC as a function of frequency for the pit source and the stage source, respectively. For the pit sources, IACC decrease as the center frequency increase. For P6, there was a dip at 250 Hz. For P2 and P4, IACC at 125 Hz become smaller than that at 250 Hz. The complicated initial reflections inside the pit walls may give some interference effects between the direct sound and strong initial reflections or the standing wave (Meyer, 1998) between the overhanged stage and the pit floor. On the other hand, IACC at 2 kHz (0.43) was higher than that at 1 kHz and 4 kHz, although IACC decreased monotonically up to 1 kHz. IACC above 500 Hz kept large values for S1.

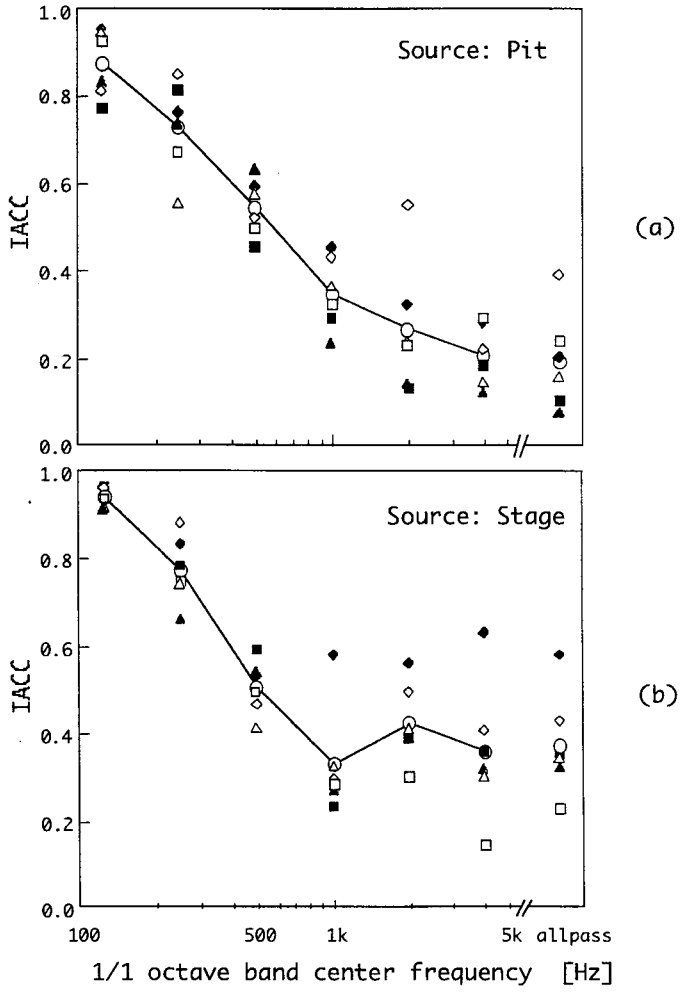

Figure 2.30 Results of IACC as a function of frequency. (a): IACC for the sources in the pit; and (b): IACC for the sources on the stage. ○: average IACC for all source locations in the pit or on the stage. Right side plots without lines are the results for allpass band. ◆: P1 or S1; ■: P2 or S2; ▲: P3 or S3; ◇: P4 or S4; □: P5 or S5; and △: P6 or S6.

Figure 2.31 and Figure 2.32 show the interaural crosscorrelation functions for each location of the pit sources and the stage sources, respectively. Figure 2.27(f) shows the counter lines of τ_{IACC}. Although maximum peaks were unstable for the pit sources as shown in Figure 2.31, for the stage sources, clear peaks, which determine IACC, exist as shown in Figure 2.32. The values of τ_{IACC} give the information that the each source locates on the left side of the conductor. Especially for P2, P3, and P6, peaks of IACF were small, and vague directionality may be obtained. According to these results, ordered distribution cannot be obtained for the pit sources comparing with the stage sources. The values of W_{IACC} were almost constant among sources in the pit and on the stage. Average W_{IACC} for pit sources and stage sources were 0.05 (SD: 0.01) and 0.04 (SD: 0.01), respectively.

As shown in Figure 2.27(a), variance of *LL* for the back-and-forth direction was much remarkable at frontal area on the stage than that for the side direction as well as a previous result (Sakai et al., unpublished). As shown in the *LL* for S3, for the source at the side-front on the stage, *LL* kept relatively large at conductor's location due to the strong reflection from the proscenium arch.

Regarding to the music in the orchestra pit, *LL* around 250 Hz had a dip at the conductor's location. Consequently, musician playing instruments with lower frequency range is suggested to be frontal area near the conductor in terms of acoustics.

Averaged *LL* for the pit sources is 7.0 dB larger than that for the stage sources. A trained voice, which can carry power and brilliance at higher frequency range around 2-4 kHz ("singer's formant"), may be carried to a conductor as well as listeners.

For the pit source, Δt_1 was mainly around 2-3 ms, which came from the pit rail just behind the conductor. Considering that a sound field for a conductor should be designed as same procedure for listeners, such values of Δt_1 are too short. To avoid such a short delay time, the pit rail just behind the conductor are removed or have a property degree at which the strong initial reflection do not arrive to the conductor. On the other hand, another idea is that such a short reflection works for the reinforcement of loudness, as a person cannot perceive delay time of 3 ms. It is necessary to clarify whether such a short delay time can work for subjective response of a conductor in the future. For the stage sources, Δt_1 around 30 ms was too long for a conductor in terms of singing voice. Preferred Δt_1 for listeners relates to effective duration of autocorrelation function of a sound source τ_e (Ando, 1998), it can be suggested that τ_e of the source become longer in singing.

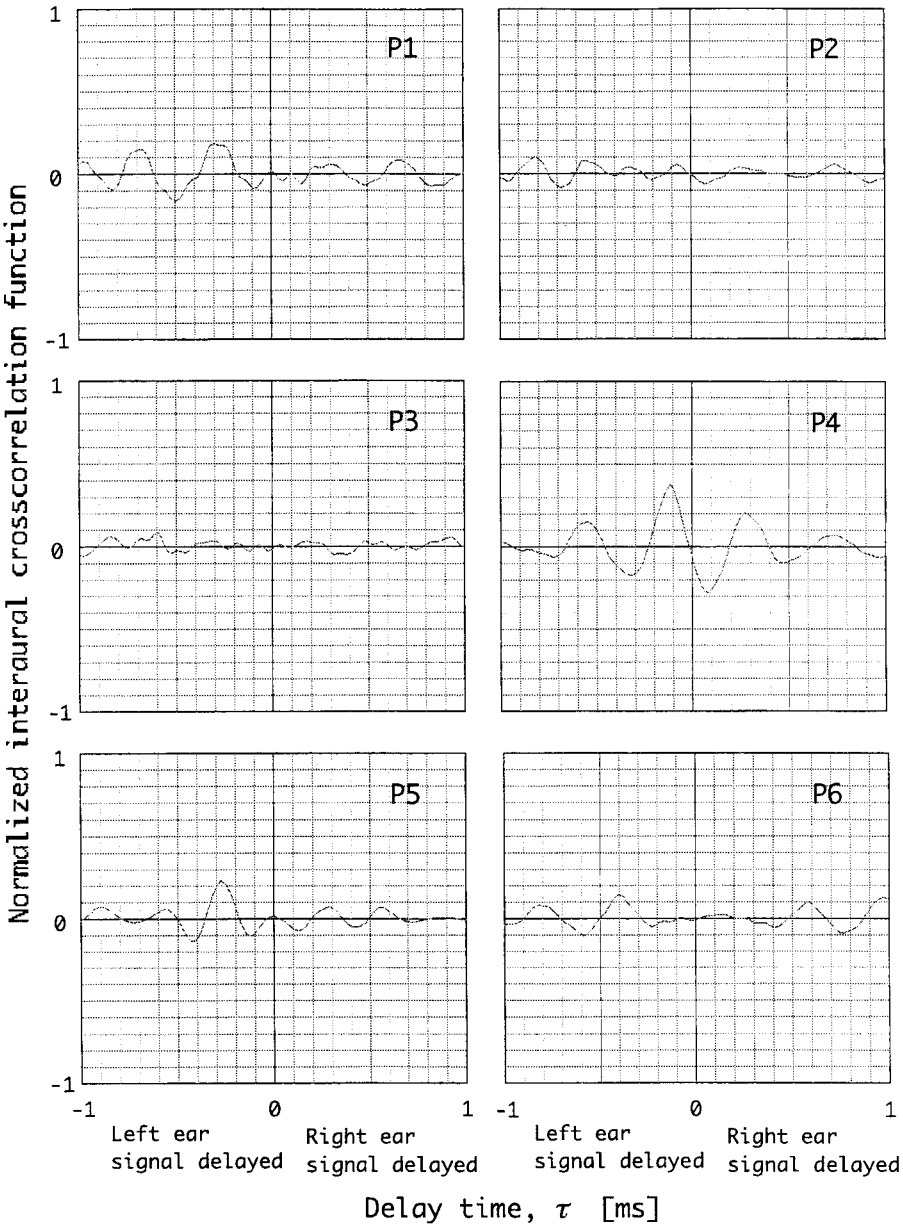

Figure 2.31 Interaural crosscorrelation functions at the conductor's position for each source in the orchestra pit (P1-P6).

T_{sub} for pit source are shorter than that for stage source. Generally, for singing voice, optimum T_{sub} is shorter than that for orchestra (Ando, 1985). Thus, this relation is inconsistent in terms of τ_e of the sound source. Considering the boundary conditions of the sound fields in the orchestra pit and on the stage, this relation is difficult to improve dramatically. If a stage set exists on the stage, T_{sub} may become much shorter, but this may not be enough. Thus, as described here, the suggestion that the sound field for a conductor should be designed as well as that for listeners does not be supported in relation to temporal factors (Δt_1 and T_{sub}), or is difficult to achieve.

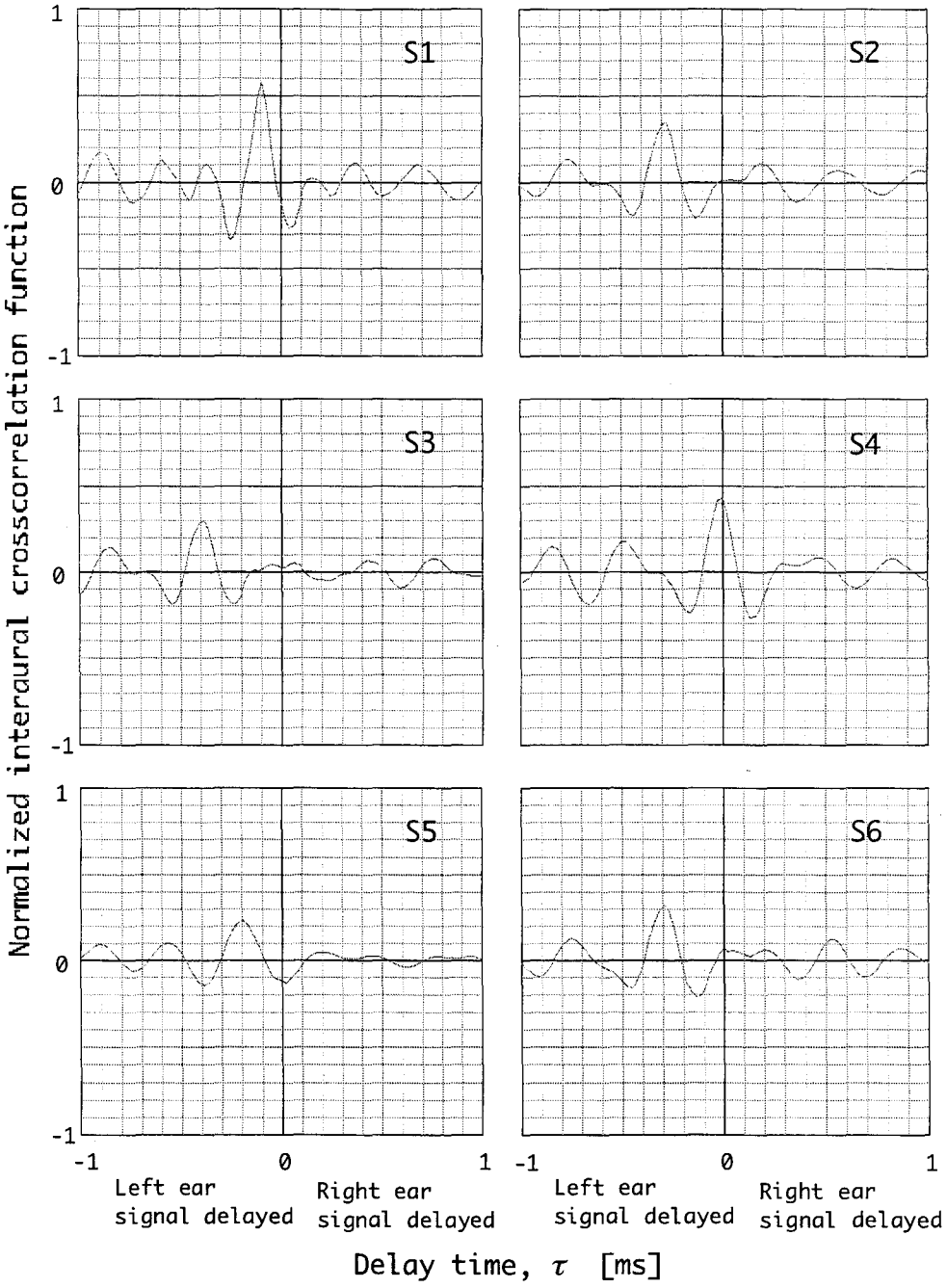

Figure 2.32 Interaural crosscorrelation functions at the conductor's position for each source on the stage (S1-S6).

For the source as a first violin player in front of the conductor, T_{sub} (P1: 0.85 s at 500 Hz) is shorter than that for further source (P5: 1.22 s at 500 Hz). Differences between maximum and minimum T_{sub}s were 0.37 s for the pit sources and 0.54 s for the stage sources. It may be possible for a conductor to rearrange the location of each instrumental player according to such a distribution of T_{sub}. When a singer sing at frontal area on the stage, T_{sub} at conductor's position for the middle position (near S2) become longer than that at center (S1) or side (S3) position.

For both sources in the pit and on the stage, values of IACC were too large, considering that a sound field should be designed similar to that for listeners. For pit sources, as the sources are very close to the conductor and the direct sound component is larger, it should be difficult to improve IACC. But, if the degree of the pit rail or lateral wall in the pit are well designed, IACC should become smaller (namely, better). For the stage sources, it may be possible by adjusting the degree of the surface of proscenium arch or the lateral walls in the hall, which is same for the frontal area in the stall for listeners.

Remarks

The present investigation provides useful knowledge for a conductor for the sound emitted by sources in the orchestra pit and on the stage in a typical historical opera house. Conclusions are obtained as following.

For the sound sources in the orchestra pit, the dips of relative *LL* were observed at low frequency range (-12.5 dB 250 Hz for P6) due to the interference effects between the direct sound and strong initial reflections inside the pit. Players with lower-frequency instruments are suggested to be frontal area near the conductor in terms of acoustics.

The suggestion that the sound field for a conductor should be designed as well as that for listeners does not be supported in relation to temporal factors (Δt_1 and T_{sub}). Especially, Δt_1 was observed mainly around 2-3 ms, which came from the pit rail just behind the conductor. Also IACC at 500 Hz was large above 0.4, which is quite larger than that in a stall.

T_{sub} for pit source (1.07 s at 500 Hz in average) are shorter than that for stage source (1.52 s). In terms of the optimum T_{sub} for the orchestra music and singing voice, this relation is inconsistent for a listener's condition.

IACC at 2 kHz (0.43 in average) was larger than that at 1 kHz and 4 kHz for the sources in the stage.

Accumulation of such a measurement data in relation to sound fields on the stage and in the orchestra pit inside opera houses, physical characteristics of their sound fields will be known, and they will give valuable and useful information in designing a sound field for a conductor by adjusting the degree of proscenium arch and a pit rail. As well as the procedure for adjusting sound field by a singer on the stage and musicians in the pit according to their preference, a conductor can give orders for their playing location.

2.2.4 Acoustical Measurement for Listeners in a Box

In order to clarify the characteristics of sound fields for listeners inside boxes of a typical historical opera house, acoustical measurements were conducted inside boxes of a typical Italian opera house "Teatro Comunale" in Modena, Italy, as shown in Figure 2.33 and Figure 2.34(a, b). To investigate the effects of head scattering of persons, the number of persons inside a box and the location of a receiver were changed, and physical factors were calculated from binaural impulse responses. Each orthogonal factor (Ando, 1998) is compared to that in a typical location in the stall for the respective configuration. Omnidirectional sound source was located on the stage emulating a singer or in the orchestra pit reproducing the locations of musicians.

Regarding initial time delay gaps (ITDG) inside boxes for listeners, the first reflection arrives from the inside-box walls, but the strongest and most significant reflection arrives later from the lateral wall of the hall (Cocchi et al., 2000). Thus, in the reference, they selected the ITDG at the strongest reflection from the hall.

The theater has a horseshoe-shape in plan, four tiers of boxes plus a gallery on the walls and a vaulted ceiling with a large chandelier suspended in the center. Number of the seats is 900 (2/3 in the five tiers of boxes). Volume of each box is approximately 6 m^3, and opening surface is 1.8 m^2 (height: 1.2 m; and width: 1.5 m).

Figure 2.33 "Teatro Comunale" in Modena, Italy.

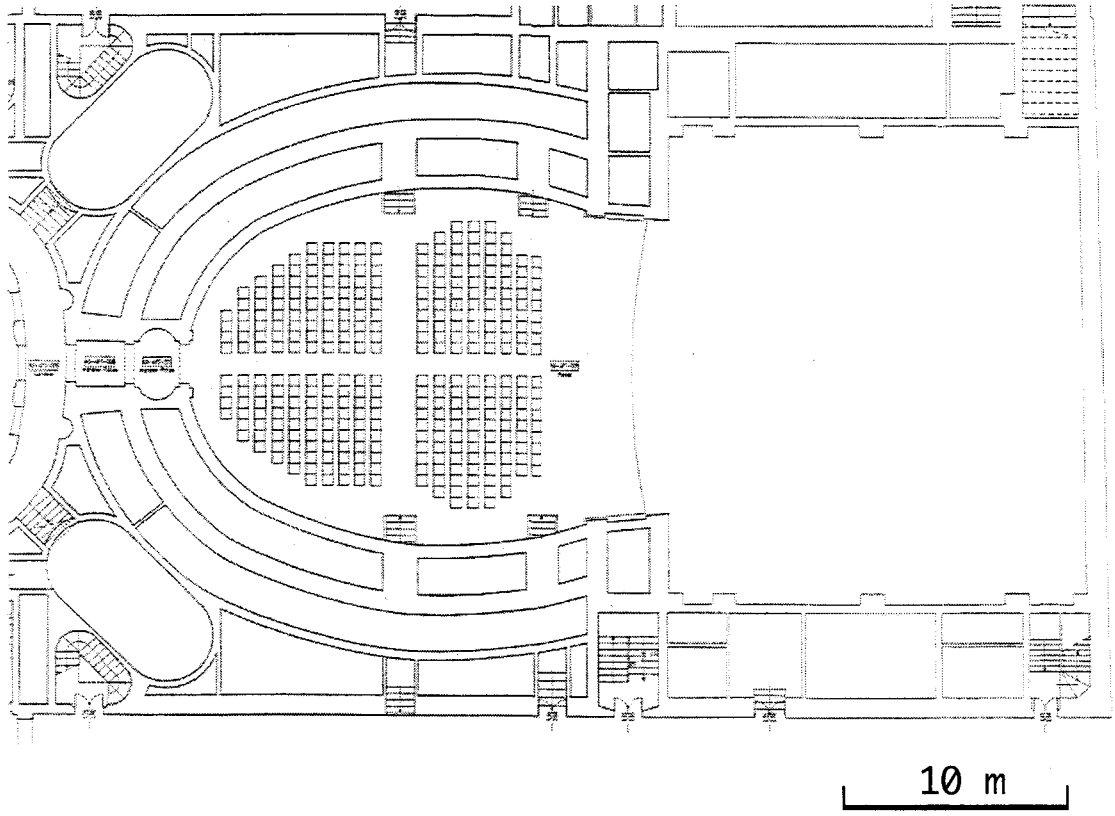

(a)

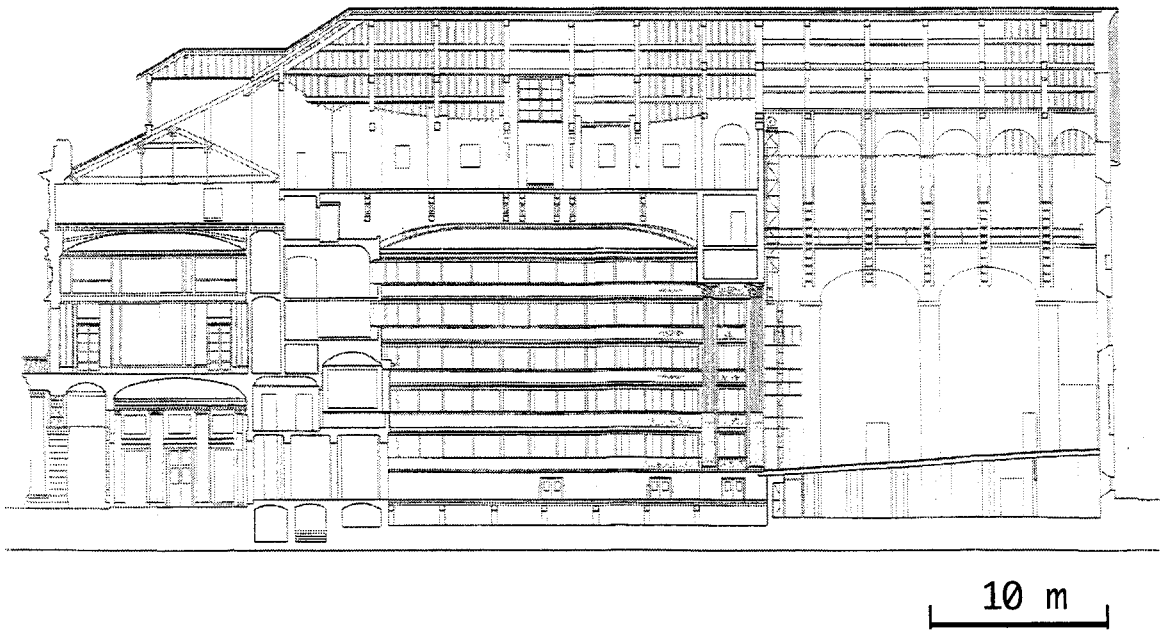

(b)

Figure 2.34 "Teatro Comunale" in Modena. (a): Plan; and (b) Section.

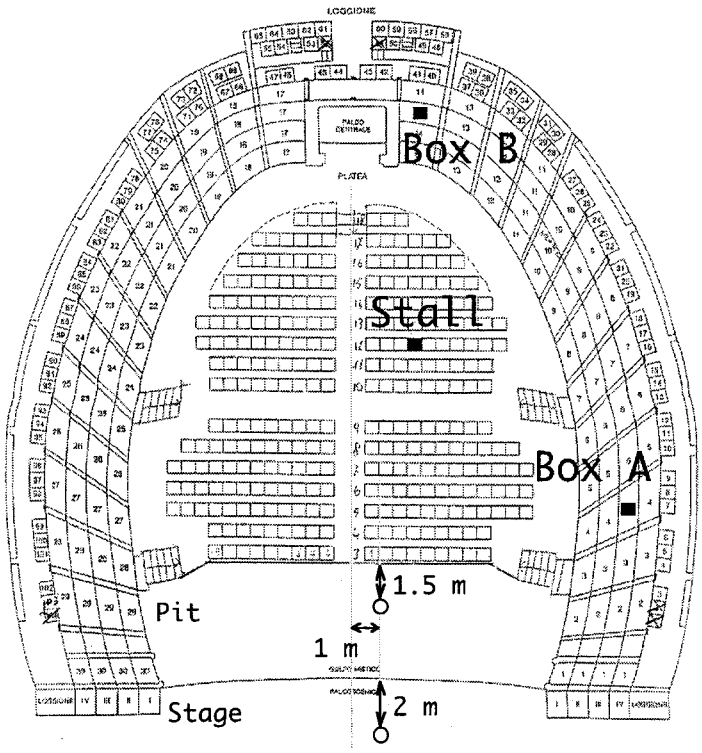

Figure 2.35 Locations of receivers and sound sources. Receiver's locations in the stall, and boxes (Box A and Box B) are indicated in filled squares. Omni-directional sound sources are located on the stage or in the orchestra pit.

Procedure

MLS measurements were conducted to analyze binaural impulse responses for two different source locations as well as previous measurements. Locations of sound sources and receivers are illustrated in Figure 2.35. One source was located at the center of the stage as a typical standing position of a singer (2-m from the stage edge, 1-m from centerline, and 1.5-m high). Another position was located in the orchestra pit (at the position of 1st violin, 1.5-m from a pit rail, 1-m from centerline, and 1.25-m high). An omnidirectional dodecahedron loudspeaker was used as a sound source. Note that the source employed for the measurements does not include the directivity of a singer (Marshall and Mayer, 1985). As receiver's locations, one position in the stall (Row 12; No. 7) and two boxes (a frontal No. 4 and a backward No. 14 box at the 3rd floor) were selected as represented in Table 2.6. No. 4 box and No. 14 box will be called Box A and Box B respectively from now on. The location at the receiver and at other listeners close to him was organized according to four patterns as shown in Figure 2.36 for measurements in the boxes. A hatched circle in the figure represents a real person's head with tiny condenser microphones at both ears. Persons in the boxes were asked to face the sound source during the measurement. In the case of the stalls, Pattern 3 was not measured. Pattern 2 in the stall

was one raw at the rear of Pattern 1 (Row 13; No. 7), and Pattern 4 consisted in four seats around Pattern 1 (Row 12; No. 6-8 and Row 13; No. 7). The setup of the measurement chain is similar to the previous subsections.

Table 2.6 Locations of the source and receivers.

Source location	Receiver location
On the stage	Stall (Row 12; No. 7)
	Box (3rd tiers; No. 4) as "Box A"
	Box (3rd tiers; No. 14) as "Box B"
In the orchestra pit	Stall (Row 12; No. 7)
	Box (3rd tiers; No. 4) as "Box A"
	Box (3rd tiers; No. 14) as "Box B"

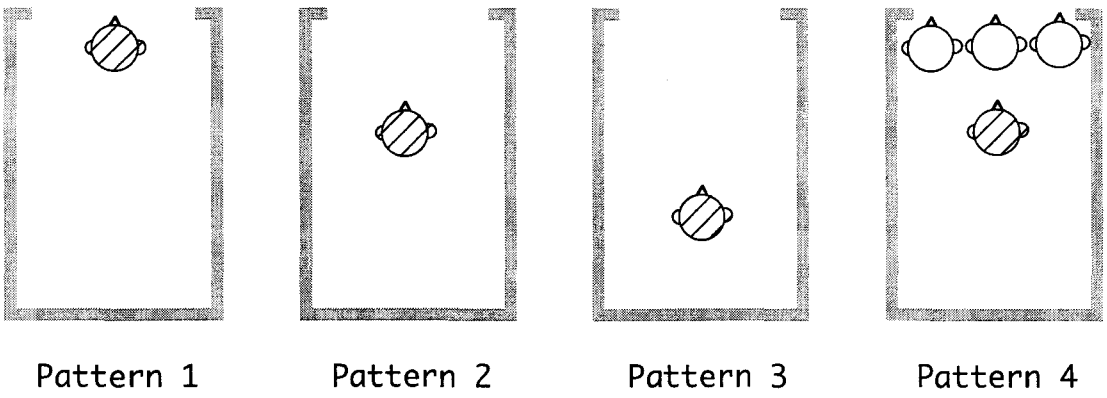

Figure 2.36 Arrangements of persons in a box (Pattern 1–4). Hatched person of each pattern is a receiver with microphone at left and right ears.

Results and discussions

Typical examples of binaural impulse responses (initial 150 ms) in Box B, when the source was on the stage, are shown in Figure 2.37(a-d). As there was no obstacle in the sight line between the source on the stage and Box B, the direct sound has the maximum amplitude as shown in Figure 2.37(a). The strongest reflection with its delay time 26 ms came from a lateral wall of the hall. However, multiple reflections between walls inside the box due to the direct sound component can be observed before arrival of the strongest reflection. As shown in Figure 2.37(b, c), the strongest reflection from the lateral wall of the hall, which appeared for Pattern 1, was weakened or not observed at all due to the screening effect at the sidewalls of the box. Multiple reflections between walls inside the box were relatively

larger than in Pattern 1. In the right impulse response of Pattern 2, a strongest reflection (37 ms), which is different the one in Pattern 1 was observed. As shown in Figure 2.37(d), in addition to the effects of the multiple reflections, initial reflections became so complicated due to the head scattering of the three persons in front of the receiver.

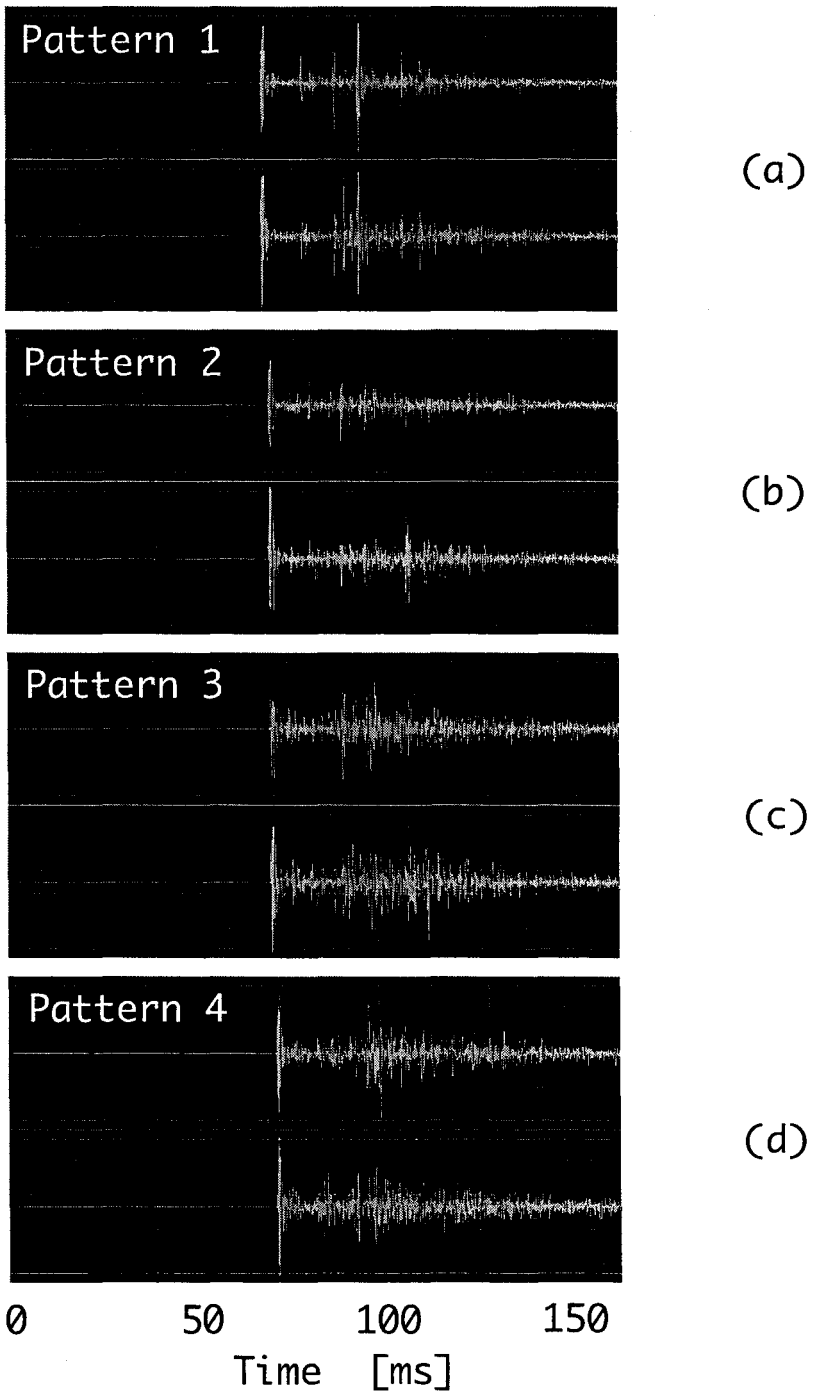

Figure 2.37 Typical examples of impulse responses in Box B at left and right ear when the source was on the stage. (a) Pattern 1; (b) Pattern 2; (c) Pattern 3; and (d): Pattern 4.

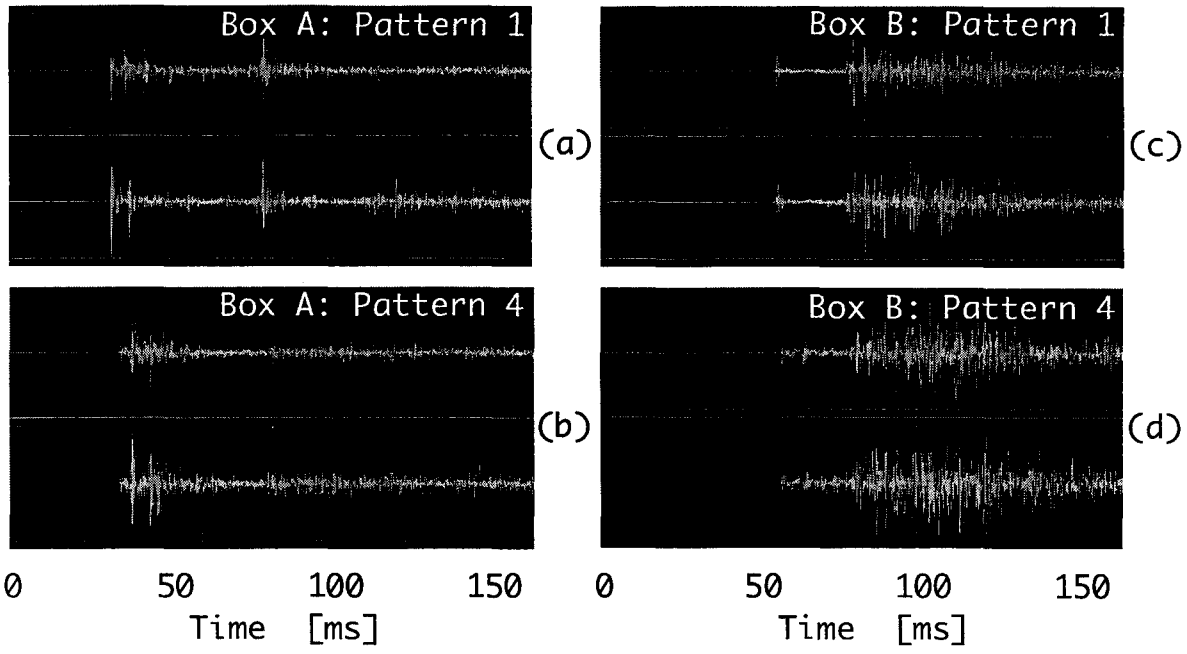

Figure 2.38 Examples of binaural impulse responses in boxes when the source was in the pit. (a): Pattern 1 at Box A; (b): Pattern 4 at Box A; (c): Pattern 1 at Box B; and (d): Pattern 4 at Box B. "S" and "R" indicate source location and receiver location, respectively.

Figure 2.38(a-d) gives initial binaural impulse responses in Box A and Box B when the source was in the pit. Results of Pattern 1 and 4 are shown for both boxes. Except for Patterns 1 of Box A, the front wall of the box or the pit rail interrupted sight lines between the source and the receivers. As shown in Figure 2.38(b), the initial strongest reflection after 4 ms from the weak direct sound might come from the ceiling inside the box. Similarly to the source on the stage, multiple reflections between walls inside the boxes and scatterings by heads are observed in Pattern 4 for both boxes (Figure 2.38(b, d)).

Thus, impulse responses dramatically varied according to the receiver's position, to the number of persons, and to their relative location in the box. That is to say, physical factors are also expected to vary.

Results of relative LL as the function of 1/1 octave band center frequency from 125 Hz to 4 kHz are shown in Figure 2.39(a–f). Left figures are the cases of the source on the stage, and right ones is in the pit. Top row is the cases of the receivers in the stall, middle is in Box A, and bottom is in Box B. Different symbols represent each pattern of arrangements. Right-side plots of each figure without a line are the results for A-weighted allpass band. Note that results between different source locations cannot be directly compared, although the source power was same for both source locations. This id because these LL results are relative levels to each source. Comparing the LL values for the source on the stage with

that in the pit, LL values for the stage source were smaller than for the pit source. When the source is placed on the stage, the output signal radiated from the loudspeaker is equally distributed in all directions. And the main reflective surface close to the stage source is the stage floor. Radiation for the loudspeaker and the reflection from the stage floor are spread into partly the absorptive stage house and partly in the hall. On the other hand, for the source in the pit, there are five reflective surfaces near the source, namely the pit floor, the pit rail, the sidewalls, and the rear wall in the pit. Furthermore the reflections against the rear wall at the pit are mainly radiated into the hall, as there is no pit overhang.

Values of LL at 125 Hz were boosted for the pit source, especially at the receiver in the stall (up to -14 dB). This phenomenon is considered to be by a couple-room effect between the orchestra pit and the hall. For Pattern 3 in Box A, LL was locally boosted at 250 Hz when the source was on the stage.

The maximum LL at allpass band for each condition was observed at frontal position (Pattern 1) in both boxes, and LL for Pattern 2, 3, and 4 were smaller than that of Pattern 1 (up to 5 dB differences), although LL was almost constant for each pattern in the stall. This should be related with the smaller number of reflections than in the Pattern 1 for the inner boxes. In Figure 2.39(b), in comparing with the others, distribution of LL for the pit source was quite small in the stall. Their standard deviation was less than 0.5 dB for all frequency bands. In this case, the pit rail shielded the sight line between the source and the receiver. And as already described above, many components of strong reflections are radiated into the hall by the reflections from flat and hard surface of the rear wall in the pit. These reasons make possible to such a tight distribution of LL.

Results of Δt_1 are represented in Table 2.7. Values of Δt_1 at both ears were calculated separately, because the Δt_1 values at each ear were quite different, especially in the boxes. Values of Δt_1 in the stall for the stage source were almost constant as 39-40 ms. In this case, the delay times of the maximum reflections at both ears almost coincided, because the reflections' paths by way of the sidewall of the hall were same. On the other hand, values of Δt_1 in the stall for the pit source were different at left and right ears. In this case, left Δt_1 was shorter than right one, because the paths were different and also further complicated by the diffraction around receivers' head.

In comparison between Δt_1s for the source on the stage and in the pit, for example, Δt_1 in the stall for the stage source (40 ms) was shorter than that for the pit source (65 ms) at left ear of Pattern 1.

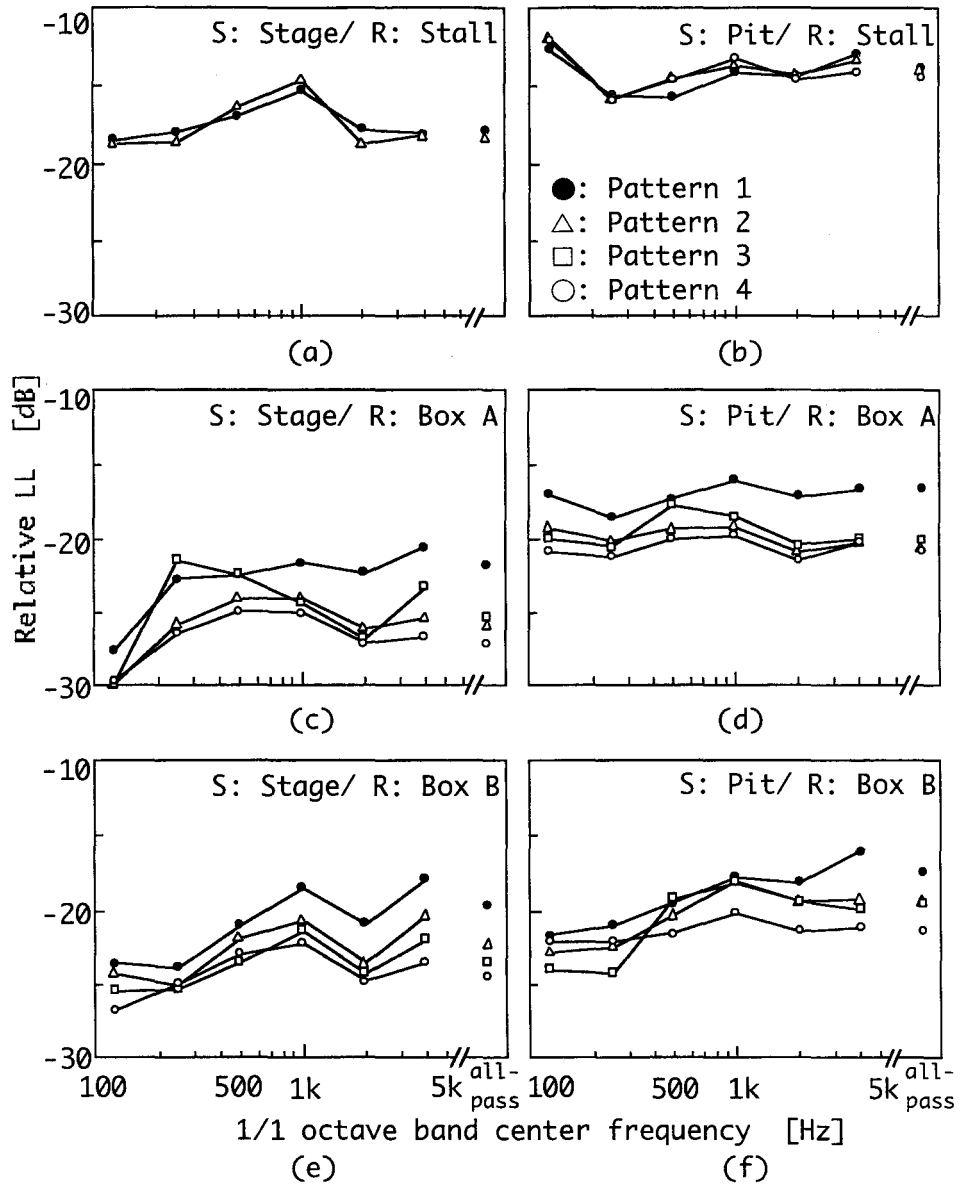

Figure 2.39 Results of relative LL of 1/1 octave band center frequency. Extreme right plots in each figure are results of allpass band (A-weighted). ●: Pattern 1; △: Pattern 2; □: Pattern 3; and ○: Pattern 4. S: Source location; and R: Receiver location.

In Box A for the stage source, Δt_1 values were also quite different between the ears. This is due to its asymmetrical shape of the box close to the stage. The first maximum reflection arrived from the sidewall or ceiling in the hall (Δt_1 > 40 ms), walls inside boxes (7–12 ms), stage or pit floor (4 ms), and human head (1–3 ms). In Box A for the pit source, similar tendency was observed. However, the strong reflections from the flat and hard surfaces of a pit wall arrived as a first reflection with 48 ms for Pattern 1. In Box B for the stage source, such a tendency was not observed because this box is almost symmetric for the centerline of the theater.

Table 2.7 Results of left and right Δt_1 and their ranges, which are the difference between maximum and minimum values.

Receiver	Source	Δt_1 [ms]			
		Stage		Pit	
	Pattern	Left	Right	Left	Right
Stall	1	40	40	65	77
	2	39	39	57	77
	4	---	---	101	77
	Range	1	1	44	0
Box A	1	17	42	48	48
	2	7	11	10	4
	3	8	7	10	10
	4	7	11	9	4
	Range	10	29	39	44
Box B	1	26	26	28	43
	2	19	37	33	33
	3	28	26	27	26
	4	19	37	48	30
	Range	9	11	21	17

In Box A, the maximum reflection came from the wall inside the box for Pattern 2-4 (Δt_1 < 11 ms), whereas the first reflection for Pattern 1 came from the sidewall of the hall as described above. In opposite, dominant reflection came from the lateral walls in the hall for Box B. Thus, different characteristics for this parameter were seen in the different boxes. This can be interpreted as a more uniform listening environment for the rear box compared to the frontal one.

As represented in Table 2.8, values of A for the pit source were larger than for the stage source, although there are some exceptions. The differences of average value were 0.39 in Box A, and 1.32 in Box B. For Box A, A values of Pattern 2-4 were larger than that of Pattern 1 for both source locations. This means the increase of the reflection components by multiple reflections between walls or scattered reflections by the heads at the other listeners at rear positions inside the box. But, such a clear tendency could not be seen for those in Box B.

Table 2.8 Results of left and right A value and their ranges, which is the difference between maximum and minimum values.

Receiver		A value			
		Stage		Pit	
	Pattern	Left	Right	Left	Right
Stall	1	1.27	1.54	1.28	1.22
	2	1.39	1.53	1.98	1.25
	4	---	---	0.84	1.37
	Range	0.49	0.23	1.14	0.15
Box A	1	1.02	0.70	1.20	1.44
	2	2.65	1.64	2.57	4.86
	3	2.87	2.80	2.33	2.43
	4	3.06	1.76	2.38	5.09
	Range	2.04	2.10	1.37	3.65
Box B	1	1.14	1.00	2.87	1.44
	2	1.26	0.82	2.64	2.34
	3	1.05	1.15	2.94	2.91
	4	1.83	0.90	1.57	3.32
	Range	0.78	0.33	1.37	1.88

The parameter T_{sub} is not distributed into a wide range between the patterns. So the results are indicated as the average among patterns as shown in Figure 2.40(a, b). Values of T_{sub} for 500 Hz and 1 kHz are 1.4 s and 1.3 s for the stage source, and 1.3 s and 1.3 s for the pit source, respectively. For both source locations, T_{sub} above 250 Hz in Box A was larger than that in the stall and in the Box B. For example, values of T_{sub} at 500 Hz in the both boxes were 1.5 s for the both sources, and those at 1 kHz were 1.6 s. One of the reasons is that the location of the receiver is closer to the stage house than the others. So the characteristics of stage house with large volume enhancing longer T_{sub} affects the T_{sub} values in the Box A. Values of T_{sub} in the stall and Box B are more similar, though the latter was smaller for the source on the stage.

Figure 2.41(a-f) shows the results of IACC. In the stall, difference of IACC was generally small. Effects of head scattering could not be seen as shown in Figure 2.41(a, b). In the boxes, multiple scattering by interior box surfaces could be to reduce IACC.

For average IACC values (above 500 Hz) for the stage source, IACC in the stall is largest, that in Box B is second, and that in Box A is smallest. One of the main reasons is the existence of sight line between the source and the receivers without some exceptions for the receivers inside boxes (Pattern 2, 3, and 4). In fact, by arrivals of strong direct sounds at the receivers, IACC keep large values.

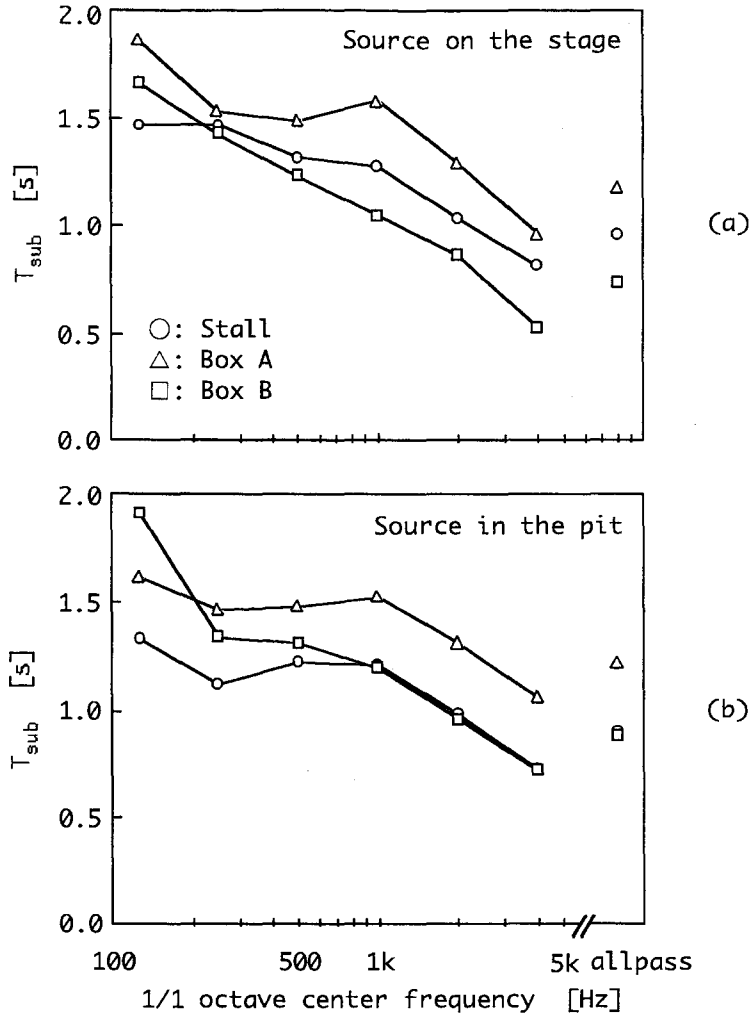

Figure 2.40 Results of T_{sub} of 1/1 octave band center frequency. Extreme right plots in each figure are results of allpass band (A-weighted). (a) Source on the stage; and (b) Source in the pit. ○: Stall; △: Box A; and □: Box B.

For the both source locations, IACC dramatically decreased between 250 Hz and 500 Hz in boxes comparing to that in the stall. In general, IACC values for the pit source were smaller than on the stage.

In both boxes, IACC has a dip at 125 Hz for all receivers. As shown in Figure 2.41(e), IACC was boosted at 1 kHz and 4 kHz for Pattern 1. In general, IACC values are large at lower frequencies as shown in the results of the stall. However, IACC decreased in both boxes at lower frequency ranges. The cause of this is considered to be related phase differences at the two ears, which are especially evident in Pattern 2, 3, and 4.

In terms of IACC at allpass band, IACC become less than 0.2 for locations at which the path of the direct sound was shielded as in rear locations of a box. For the source on the stage, IACC in the stall (0.23: Pattern 1) become smaller than that in Box A (0.33: Pattern 1) and in Box B (0.43: Pattern 1).

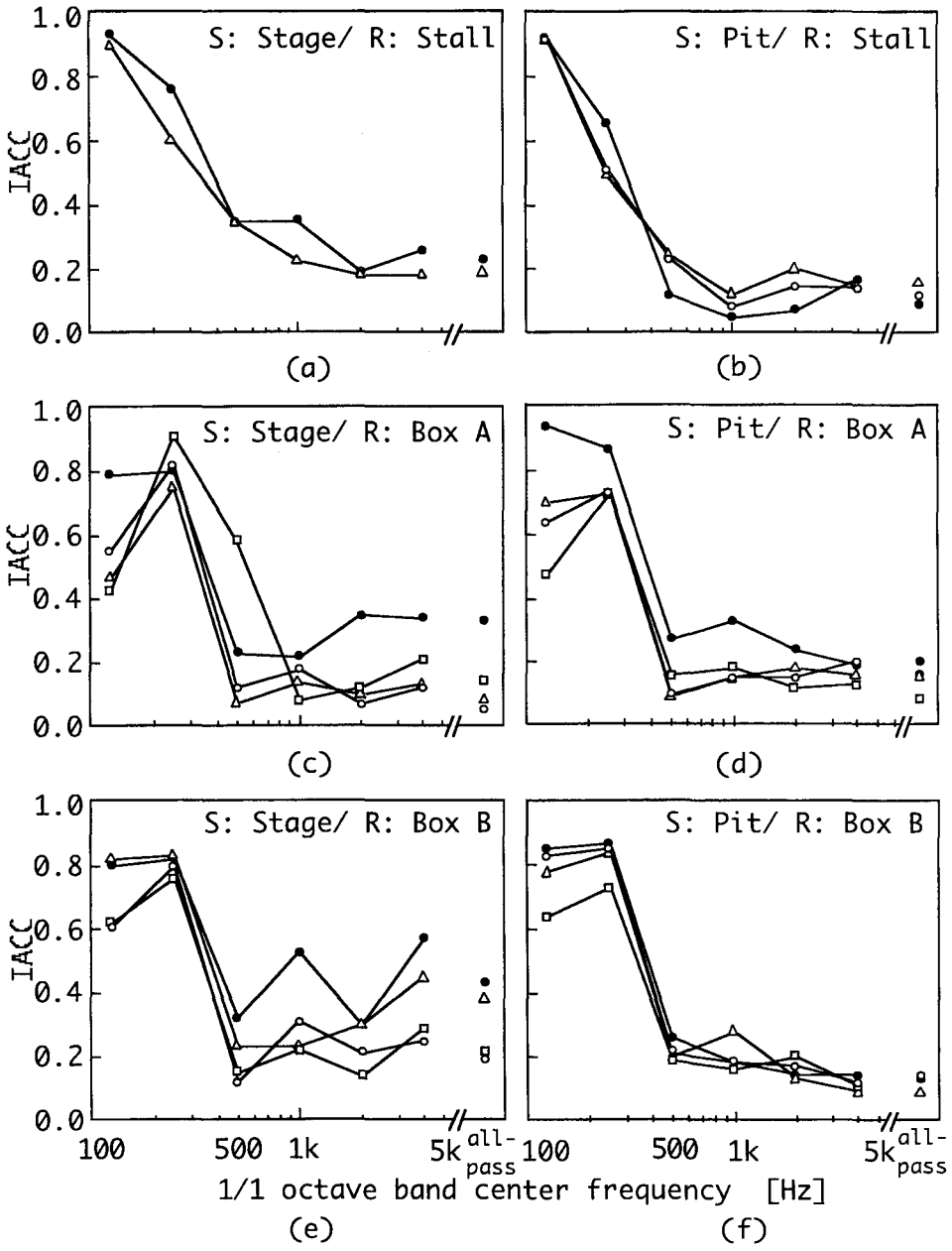

Figure 2.41 Results of IACC of 1/1 octave band center frequency. Extreme right plots in each figure are results of allpass band (A-weighted). ●: Pattern 1; △: Pattern 2; □: Pattern 3; and ○: Pattern 4. S: Source location; and R: Receiver location.

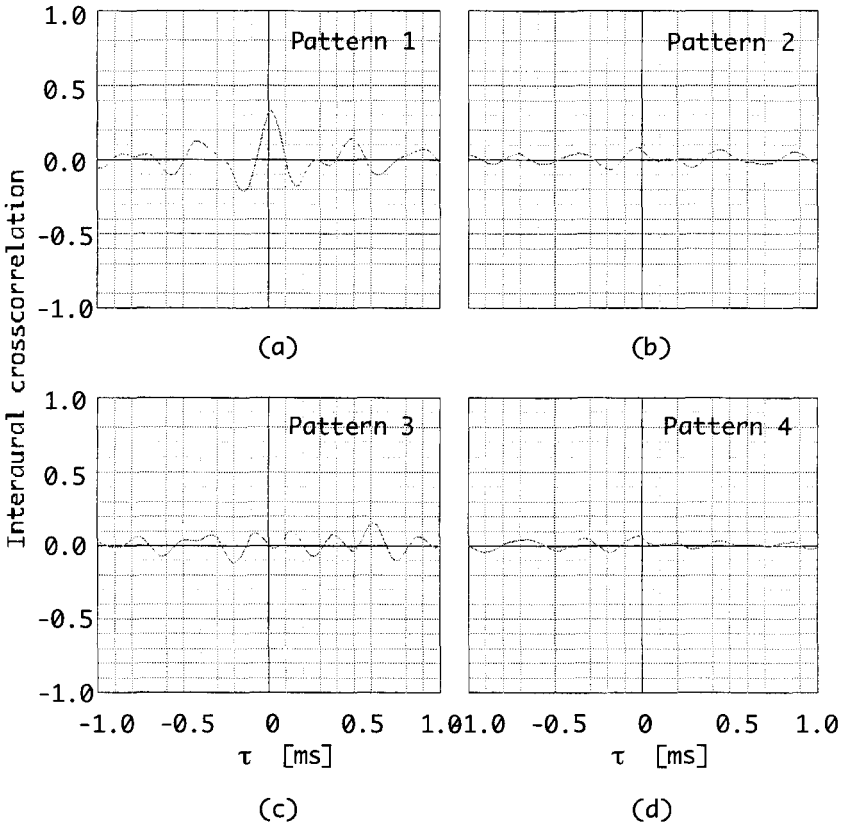

Figure 2.42 Interaural crosscorrelation functions (IACF) in No. 4 box (front) when the source was on the stage. (a): Pattern 1; (b): Pattern 2; (c): Pattern 3; (d): Pattern 4.

Table 2.9 represents the results of τ_{IACC} obtained from IACF at each receiver. If the τ_{IACC} is zero at the range between –0.1 and +0.1 ms, the clear frontal direction of the source should be perceived. If IACC is below 0.15, a person perceives subjectively diffused sound field (Ando, 1998). In the measurements, larger τ_{IACC} values were obtained in some cases. For example, τ_{IACC} for Pattern 3 of Box A for the stage source and the pit source were 0.61 ms and 0.95 ms, respectively. All these cases have some minor IACF peaks. Namely, in such cases, IACC values are small (less than 0.15). The IACF peaks (but not maximum) exist also near origin. W_{IACC} was almost constant around 0.4 for all conditions. This parameter in relation to white noise as well as MLS signal is not so significant, because it is deeply related to the sound source itself.

Regarding LL, if the output power of a singer on the stage and at a musical instrument in the pit is same (although this is not realistic), the resulting balance in the hall will be in favor at the instrument. However, according to the study using a professional tenor singer, a "singing formant" around 3 kHz has been discovered (Sundberg, 1977). By means of the singing formant, singing voice may safely reach with instruments to the listener's positions,

even if LL for the stage source is smaller than that for the pit source.

It is interesting to note that the left and right Δt_1 values of Pattern 2 and 4 measured in the two boxes for both source positions were quite similar, with the only exception at Box A for the pit source. This means that the Δt_1 is almost the same value for a person at rear seats almost independently, even if some persons in the front row exist or not when the listener is at second row.

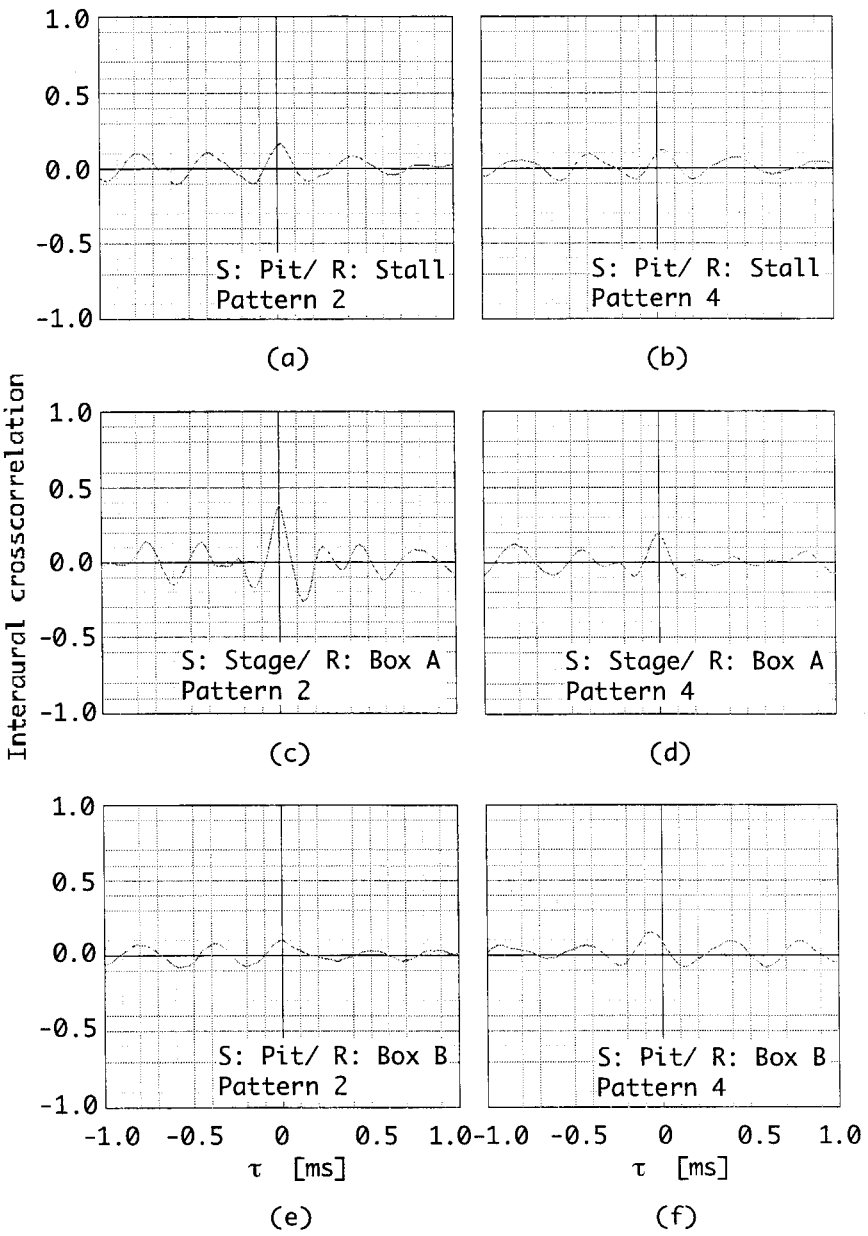

Figure 2.43 Interaural crosscorrelation functions (IACF). (a): Pattern 2 in the stall (source in the pit); (b): Pattern 4 in the stall (source in the pit); (c): Pattern 2 in the No. 14 box (rear) (source on the stage); (d): Pattern 4 in No. 14 box (rear) (source on the stage); (e): Pattern 2 in No. 14 box (rear) (source in the pit); (f): Pattern 4 in the No. 14 box (rear) (source in the pit).

Thus, clearly Δt_1 values were different for the number of the persons or their location. In general, anyway, the binaural analysis shows that the presence and location of the listener and of "dummy" listeners implies the change in Δt_1, which may introduce different listening condition.

According to the preference theory, the maximum amplitude is dominant as a Δt_1 even if there are some initial reflections (Ando and Gottlob, 1979). But in the previous investigation of this reference, conditions for amplitudes of reflections were limited with close amplitudes. In the present investigation, reflections arrived from not only sidewalls in the hall, but also from the walls inside boxes. At the present stage, there is no expanded study about this effect of the dominant reflection based on the psychological activity. Especially, the earlier first reflections like reflections between walls inside boxes have neglected as a reflection from stage floor in a concert hall acoustics, though there are many early reflections at a receiver inside a box. Psychological experiments are necessary to establish which reflection is dominant for subjective preference, for such complicated situation of the difference at left and right ear.

Table 2.9 Results of τ_{IACC}. The range is the difference between maximum and minimum values.

		τ_{IACC} [ms]	
Receiver	Pattern	Stage	Pit
Stall	1	0.02	0.02
	2	0.09	0.02
	4	---	0.05
	Average	0.04	0.03
	Range	0.09	0.03
Box A	1	0.02	0.05
	2	-0.02	0.11
	3	0.61	0.95
	4	-0.02	0.07
	Average	0.15	0.30
	Range	0.63	0.90
Box B	1	-0.05	-0.07
	2	0.00	0.00
	3	-0.02	-0.05
	4	0.00	-0.07
	Average	-0.02	-0.05
	Range	0.05	0.07

In these measurements, T_{sub} was about 1.5 s at middle frequency range. According to the subjective preference theory, optimum T_{sub} is related to the source signal. For a vocal source, 1.5 s is considered to be too long. However, for opera performance, experiential listening condition may be included through history of opera. Anyway, psychological data for the source, which consist of orchestra and a vocal, is lack at the present stage.

For the source on the stage in the stall, sharp peaks of IACF, which determine IACC values, are clearly obtained in the stalls. In Box A, IACC for Pattern 1 has a major peak, but for the other patterns, peaks become vague as shown in Figure 2.42(a-d). Regarding to the maximum peaks of IACF, which determine spatial factors, a clear and sharp peak was obtained when a pit rail does not shield direct path as shown in Figure 2.43(a-f). In opposite, a vague and minor peak is obtained when the direct sound path is shielded by the pit rail.

In concert hall acoustics, in order to evaluate a hall, preference scale values are analyzed by use of orthogonal factors at each seat. However, it is quite difficult to evaluate the sound field inside boxes. This is because characteristics of the temporal factors (Δt_1 and T_{sub}) differ from concert halls. For Δt_1, a part of initial reflections come from walls inside a box, and characteristics of the source signals are quite complicated to identify. That is why the scale values were not calculated in this paper to evaluate sound field inside boxes.

Remarks

In these measurements, the characterization for listening conditions in boxes in the opera theatre is partly clarified by use of orthogonal factors. Comparing the LL values for the source on the stage with that in the pit, LL values for the stage source were smaller than for the pit source. Values of LL at 125 Hz were boosted for the pit source, especially at the receiver in the stall (up to -14 dB). The Δt_1 values were quite different at both ears in the boxes. It is interesting to note that the left and right Δt_1 values of Pattern 2 and 4 measured in the two boxes for both source positions were quite similar. This means that the Δt_1 is almost the same value for a person at rear seats almost independently, even if some persons in the front row exist or not when the listener is at second row. More uniform listening environment for the rear box compared to the frontal one. The parameter T_{sub} is not distributed into a wide range between the patterns. For both source locations, T_{sub} above 250 Hz in Box A was larger than that in the stall and in the Box B. For the both source locations, IACC dramatically decreased between 250 Hz and 500 Hz in boxes comparing to that in the stall.

2.3 Acoustical Measurement in Outdoor Space

2.3.1 Acoustical Measurement in a Forest

The original acoustic space for humans might well have been a sound field in a forest. Since then we have experientially determined that such an outdoor space has excellent acoustic properties. A forest consists of various randomly distributed trees of different diameters. Obviously, it is difficult to calculate impulse response at present, because complicated reflections are scattered from the trunks of trees. In this paper, measurements were made to determine the acoustic properties of sound fields in a forest as well as those in a concert hall.

In these measurements, values for Δt_1 could not be identified in the forest other than for reflection from the ground, because of weak scattered reflections from the trees. The Δt_1 as an orthogonal factor is defined as a time interval between a direct sound and a first reflection from a sidewall except a reflection from a floor. Hence, the first reflections coming from the ground were neglected in accordance with the definition.

Procedure

The acoustical measurements were performed in a forest owned by Kirishima Shrine in Kagoshima, Japan. The diameters of trees which consisted mainly of deciduous trees and various shrubs were classified into three categories; i.e., 0.3, 0.6 and 1.0 m as shown in Figure 2.44. The heights of all trees were about 18.5 m. In the center of the forest, there was a 5-meter wide path made of asphalt where the loudspeaker and receivers were placed.

Wind was not present during the measurements in the forest. The humidity and temperature near to the ground were almost constant for about 20 minutes measurements. A wave-guide from the upper portion of the forest (Embleton, 1996) was not considered, because the measurements were conducted so far as 40 m from the source.

Sound fields obtained in the Kirishima International Concert Hall, Kagoshima, Japan were compared with results obtained in the forest. The location of the sound source and measuring points indicated by the gray seats are illustrated in Figure 2.45.

An omnidirectional dodecahedron loudspeaker, S, and receiving points were arranged as shown in Figures 2.44 and Figures 2.45. The height of the center of S was 1.5 m above the ground surface or the stage floor. The heights of the receiving points were 1.7 ± 0.05 m (in the forest, standing) or 1.15 ± 0.05 m (in the concert hall, sitting), respectively.

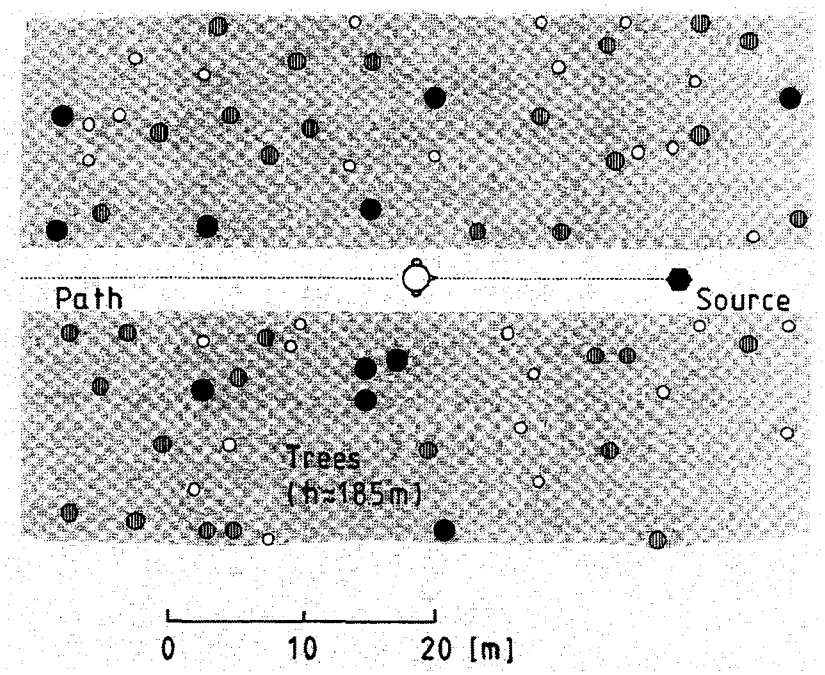

Figure 2.44 The main path of the forest investigated over a total area of about 200,000 m^2. The symbols indicate different diameters; ●:1.0; ○:0.6; ○:0.3 [m]. A loudspeaker was set as a sound source S. The person with two condenser microphones placed at ear-entrances was applied to each receiving point.

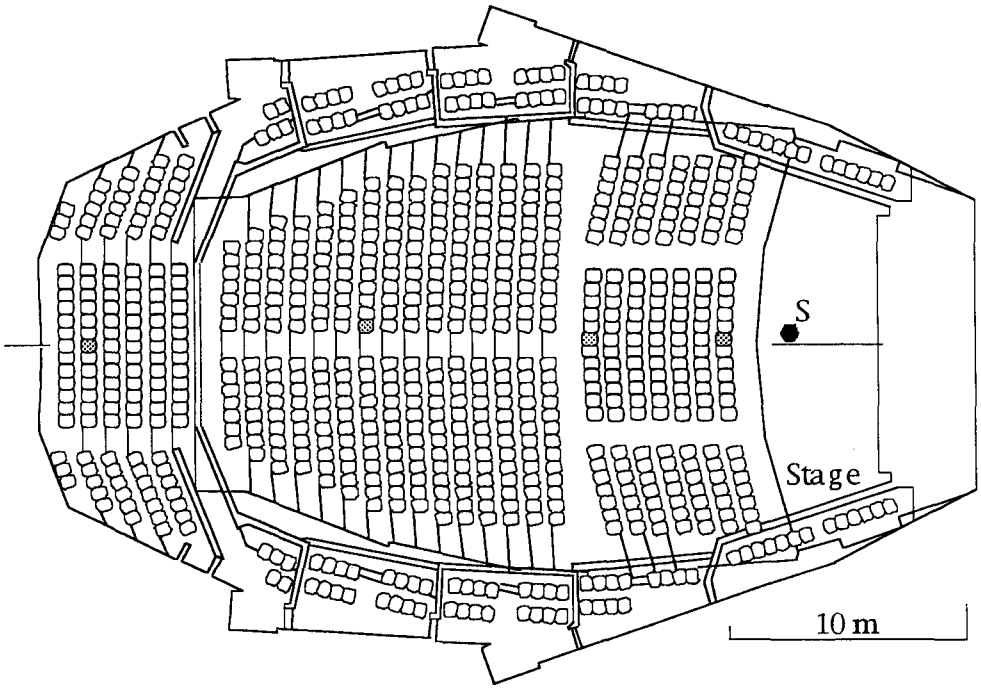

Figure 2.45 Concert hall measured for comparison. It has a volume of 8475 m^3 and 770 seats. The loudspeaker was set on the stage as a sound source S. The receiving point was set at the height of 1.15 ± 0.05 m above the seating floor.

The measurement setup is illustrated in Figure 2.46. The MLS signal radiated from the sound source S. The LL was about 100 dBA at the 5-meter-reference point. Two microphones were placed at the ears of a person who faced the loudspeaker during measurement. The microphones were of the 1/2-inch condenser type.

The four physical factors and three additional factors previously mentioned were analyzed using binaural-impulse responses. In order to obtain impulse responses, first of all, signals after A/D conversion into microphones were analyzed using a fast Hadamard transform (FHT). After obtaining binaural-impulse responses, physical factors were calculated for each 1/1 octave-band center frequency between 125 Hz and 4 kHz. The signal's duration was 2.7 s, and the sampling frequency was 48 kHz. In order to improve the signal to noise ratio, the sequenced signals were repeated 8 times.

Results

Binaural-impulse responses obtained at a distance 20 m in the forest are shown in Figure 2.47(a). The initial 30 ms of impulse responses at each receiving point are illustrated in Figures 2.47(b)-(e).

The measured relative LLs for 1/1 octave band frequencies between 125 Hz and 4 kHz are shown in Figure 2.48, as a function of the distance. In general, LL attenuates according to the inverse-square law in a free sound field as shown by the straight line in Figure 2.48. However, the LL in the forest decreased much more than the LL for the inverse-square law except for 125 Hz.

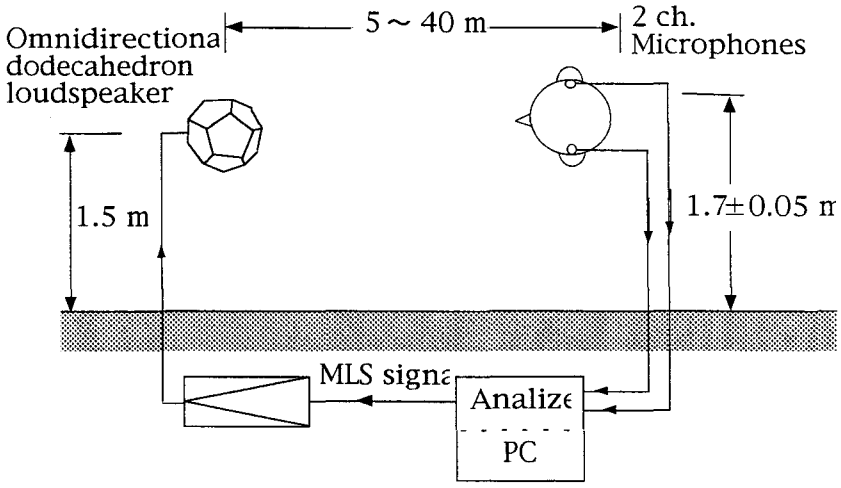

Figure 2.46 Schematic illustration of measurement with a dodecahedron loudspeaker and the real head.

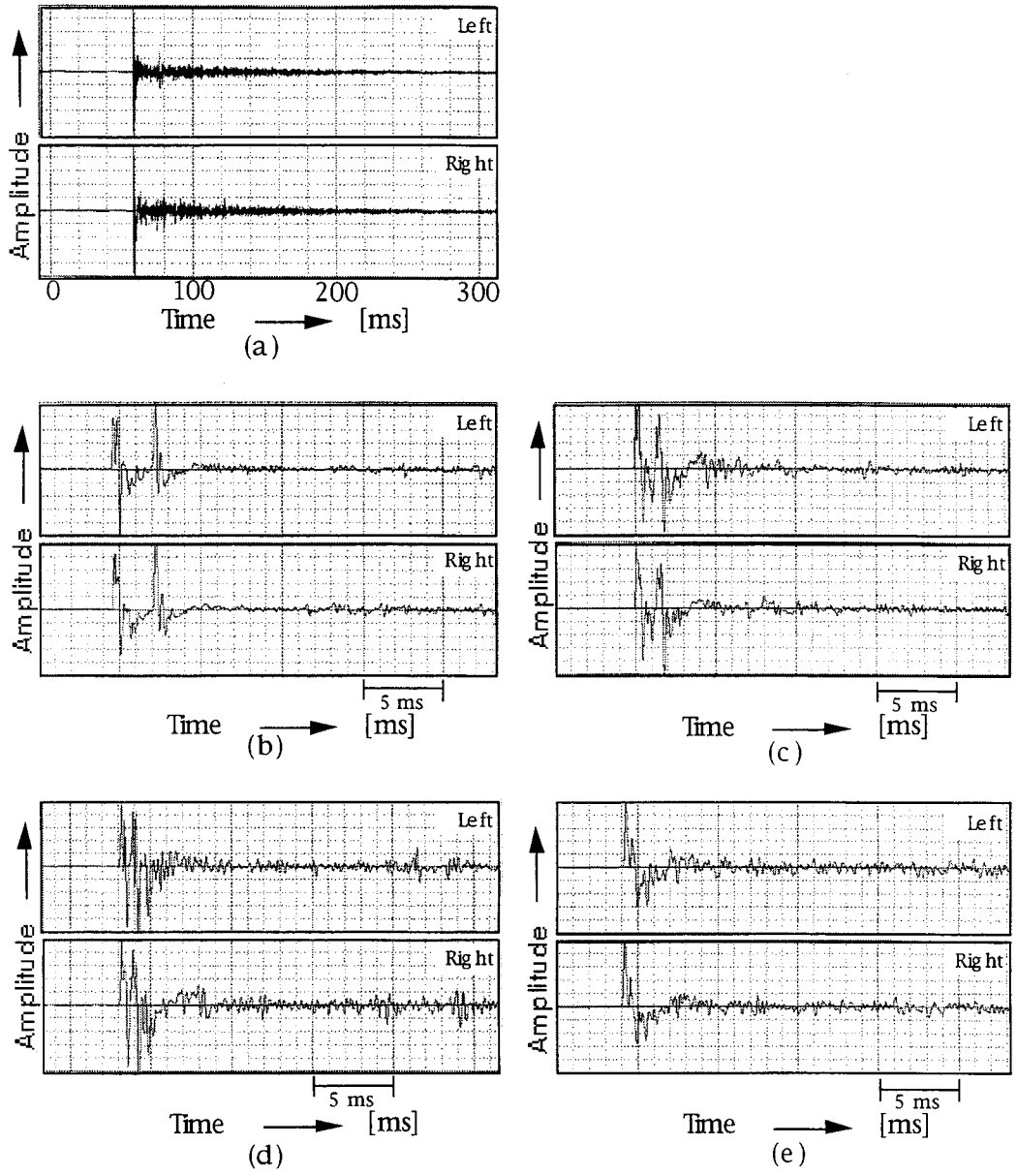

Figure 2.47 Normalized impulse responses analyzed in the forest. Binaural-impulse responses at 20 m from the source point for (a) 0-300 ms; (b) initial binaural impulse responses at 5 m for 0-30 ms; (c) at 10 m; (d) at 20 m; (e) at 40 m.

The results of LL at 500 Hz are compared with those in the concert hall as shown in Figure 2.49. In the sound field of the hall the LL was remarkably higher than the inverse square law due to the multiple reflections of walls and ceilings.

Figure 2.50 shows values of total reflections A in the forest and the hall. The longer the distance between the sound source and the receiver is, the greater the values of A are in both cases. The room radius defined by A = 1 which means there is equal energy between direct sound and early reflection-plus-subsequent reverberation, is found near 40 m in the forest, while that in the room is about 4 m.

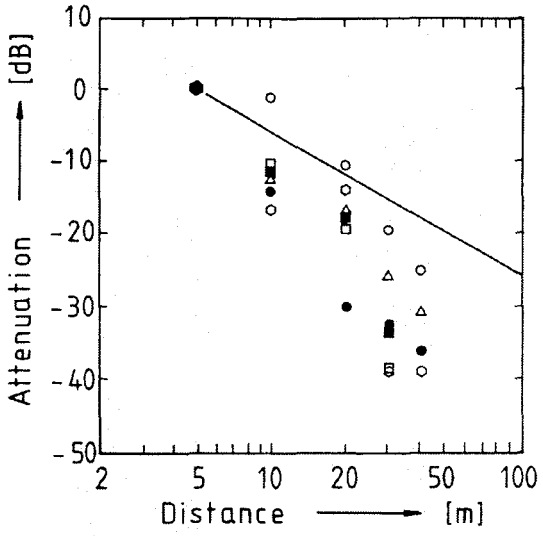

Figure 2.48 LL attenuations in the forest measured as a function of the distance. ○: 125 Hz; △: 250 Hz; ●: 500 Hz; □: 1 kHz; ■: 2 kHz; :4 kHz of 1/1-octave-band center frequency, —: inverse square law.

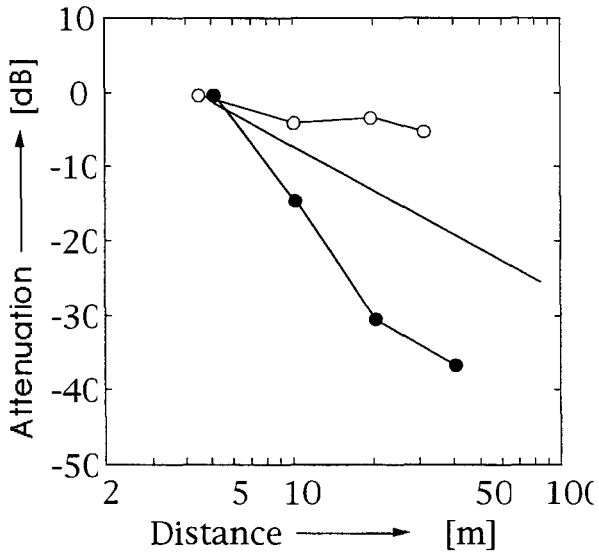

Figure 2.49 Comparison of LL attenuations in the forest with those in the concert hall at 500 Hz. ●: in the forest; ○: in the hall; —: inverse square law.

Figure 2.51 shows examples of the decay curves of reverberation in the forest and in the concert hall. Figures 2.51(c) and (d) show examples of the decay curves at 500 Hz and 1 kHz at a point 19.1 m from the source in the concert hall (Sato et al, 1994). As shown in Figure 2.51, the decay curve in the decibel scale decreased almost linearly in the concert hall. However, in the forest, the curves were not linear, maintaining their level after 0.4 s (Figs. 2.51(a) and (b)).

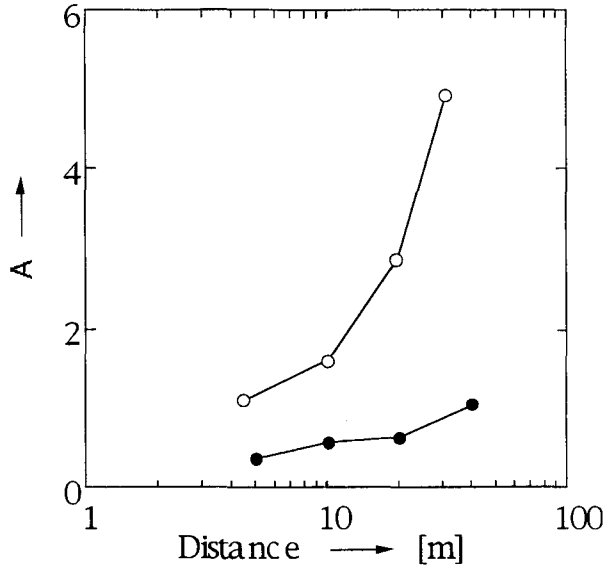

Figure 2.50 Comparison of total amplitudes of reflections in the forest with those in the concert hall.●: in the forest; ○: in the hall.

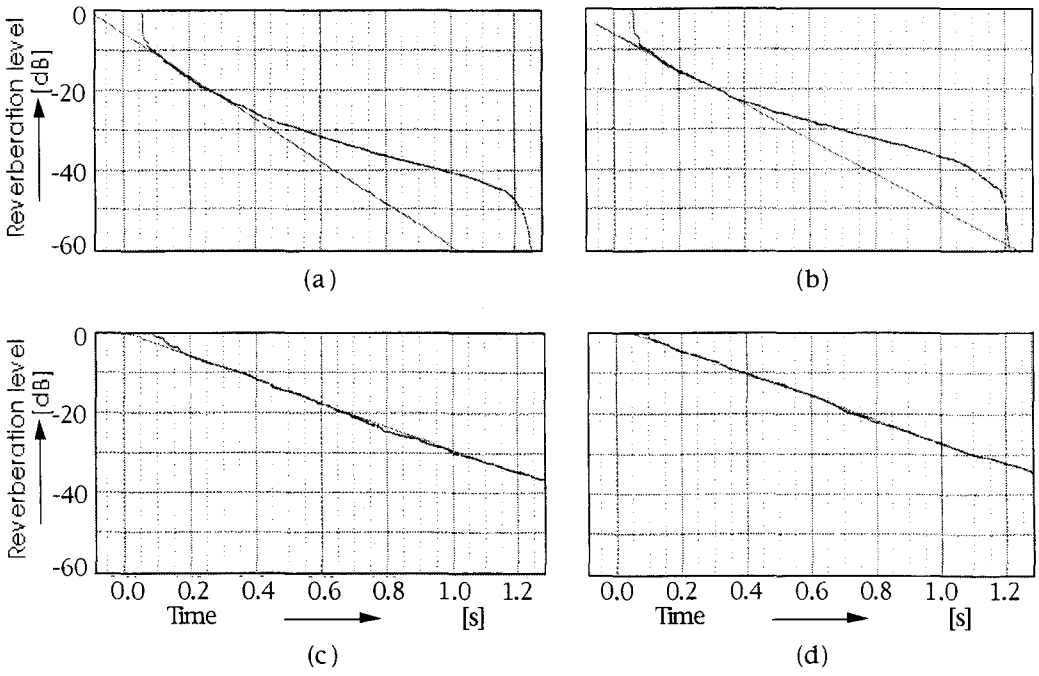

Figure 2.51 Comparisons of decay curves for reverberation at the left ear 20 m in the forest obtained by Schroeder's method. (a) Forest, 500 Hz; (b) Forest, 1 kHz; (c) Concert hall, 500 Hz; (d) Concert hall, 1 kHz.

The results of measured T_{sub} in the forest are shown in Figure 2.52. It is remarkable that the values of T_{sub} at 250 Hz are the shortest of those of the other frequencies measured. The maxima of T_{sub} appeared near the frequency band around 500 Hz particularly at distances longer than 10 m; i.e., 1.66 s at 500 Hz and 1.60 s at 1 kHz at the 40-m point.

The normalized interaural cross-correlation functions ($-1 \leq \tau \leq 1$ ms) at each receiving point in the forest are shown in Figure 2.53. The values of τ_{IACC} and the W_{IACC} were obtained from them. The results of measured IACC are shown in Figure 2.54. Here, it is interesting that the IACC is small at distances further than 20 m for higher frequency ranges above 500 Hz, for example, 0.53 (2 kHz, 20 m), and 0.44 (1 kHz, 40 m). At low frequency below 250 Hz, the IACCs are around 0.95.

Since the values for τ_{IACC} at all measuring points nearly equal zero in the forest as shown in Figure 2.53. This means that a frontal direction for the sound source can be perceived. Figure 2.55 compares the W_{IACC} between the forest and the hall at the allpass band as a parameter of distance. The W_{IACC} in the forest is always smaller than that of the room. The W_{IACC} gradually increases further away from the sound source in both cases. This indicates that the ASW should be perceived to be wider at far field points.

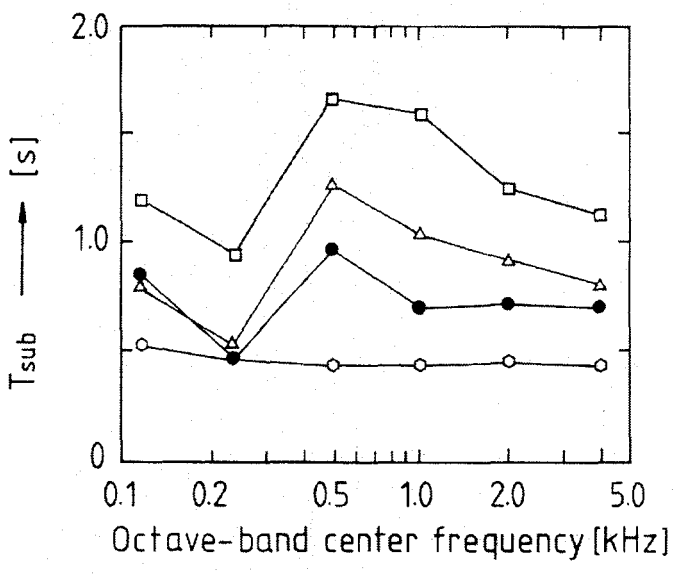

Figure 2.52 Subsequent reverberation time as a factor of the center frequency of the 1/1 octave band obtained by the 0-10 dB curve after the direct sound in the forest. : 5; ●:10; △:20; □:40 [m].

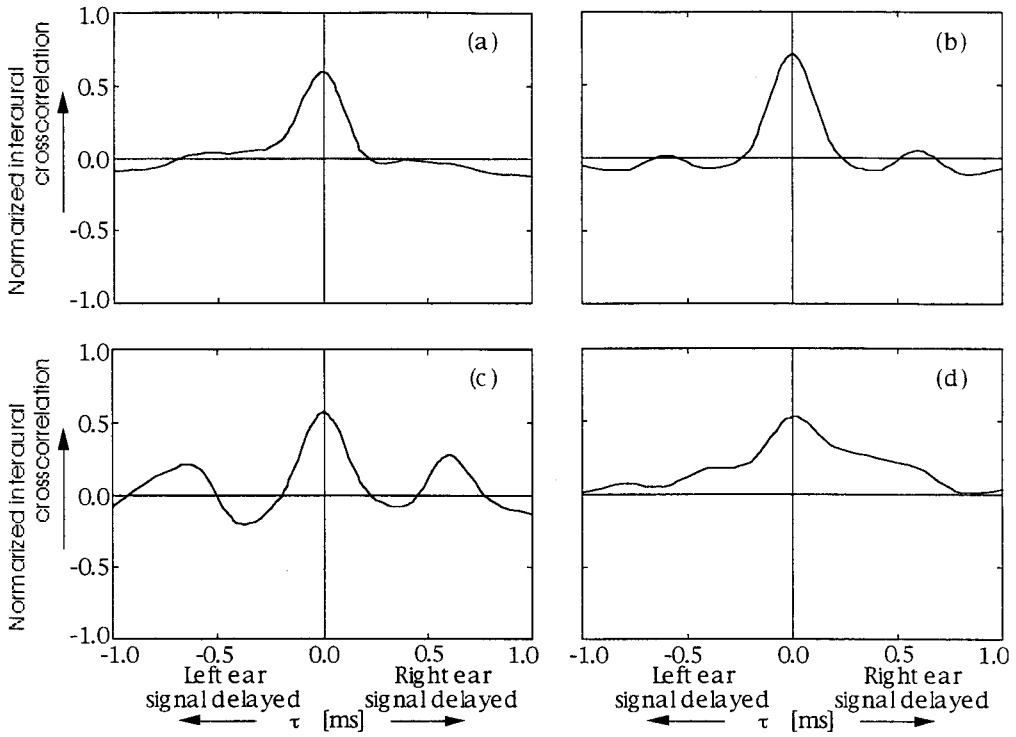

Figure 2.53 Normalized interaural cross-correlation function at each receiving point in the forest. (a) 5; (b) 10; (c) 20; (d) 40 [m].

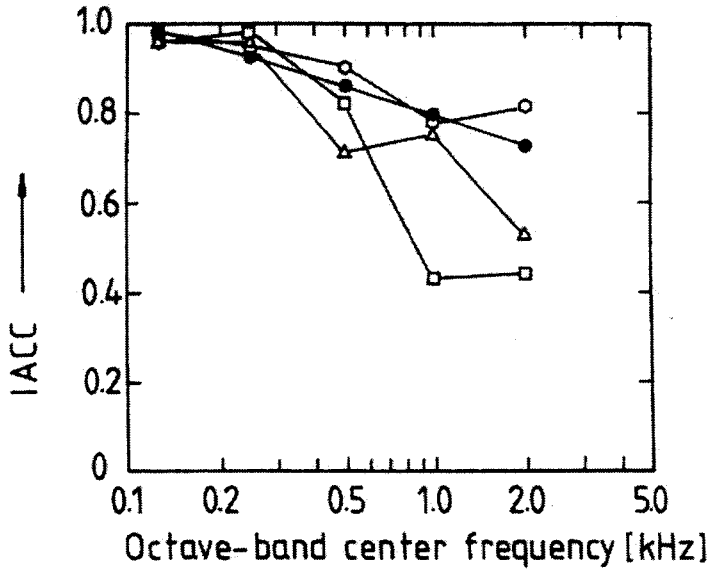

Figure 2.54 IACC as a function of frequency, and as a parameter of the distance in the forest. : 5; ●: 10; △: 20; □: 40 [m].

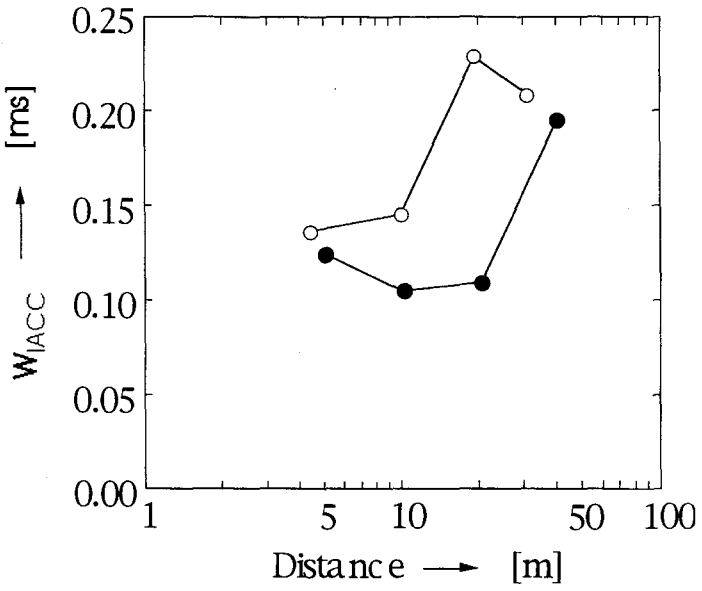

Figure 2.55 The comparison of measured values for W_{IACC} as a function of the distance. ●: in the forest; ○: in the concert hall.

Discussion

The results obtained here may be related to the diameters of trunks of trees. The lack of exponential decay curves shown in Figures 2.51(a) and (b) is considered to be caused by effects of multiple scattering from trees.

About 10 dB of attenuation was found in the initial 50 ms after the direct sound arrived, and subsequent components consistently compared with linear attenuation in a concert hall. These characteristics were found in all decay curves in the forest.

Generally, a person prefers a condition where there are dissimilar sound signals at both ears (a small IACC value). Figure 2.54 shows that IACCs are small at longer distance and higher frequency. It is interesting that the IACC is as small as about 0.4 at 40 m (1 kHz and 2 kHz) in the forest, although the initial reflections are weak as indicated by the impulse responses in Figure 2.47.

The W_{IACC} was almost constant around 0.10-0.12 until it reached 20 m and there was an immediate increase at 40 m in the forest. The W_{IACC} of the room was larger than that of the forest in each measuring point. Regarding the rapid increase at the furthest point (40 m) in the forest, this may be due to the direct sound becoming weaker and coherent multiple scattering reflections.

If music with an effective duration of ACF τ_e values centered on 70 ms (Ando, 1985) is played, then the most preferred value of T_{sub} approaches 1.66 s (23 τ_e, τ_e = 72 ms) at a frequency of 500 Hz. This condition is realized at a distance of 40 m in the forest. At 40 m, the IACC is also small. For instance, the forest would be a fine sound field for string

and wind instruments involving higher frequency ranges. It is found that the forest has excellent acoustic properties, especially for factors of subsequent reverberation time (T_{sub}) and IACC. Music may be better at further points relative to this sound field for large T_{sub} and small IACC.

Conclusion

The excess attenuation by the interference of the direct sound and reflection over the asphalt surface with a high impedance is occurred in the higher frequency range in the forest (Embleton, 1996). But, this interference is not so much effective for the result of the LL than the multiple scattering effects by trunks of trees. The LL at 125 Hz in the forest at 10 and 20 m was greater than that of the inverse-square law as shown in Figure 2.48. This is caused by the interference of the direct sound and reflection arriving at receiver in phase.

In the forest, it is found that the forest has excellent acoustic properties, especially for factors of subsequent reverberation time (T_{sub}) and IACC. The value of T_{sub} was 1.66 s (500 Hz), and IACC was 0.44 (1 kHz) at a point 40 m from the source. Also, it is found that the value of the width of the interaural cross-correlation function, W_{IACC}, was smaller than that in the concert hall.

2.3.2 Acoustical Measurement in a Bamboo Forest

This subsection describes acoustical characteristics in a bamboo forest obtained by using the same procedure for measurements in the forest and in an enclosure. In the previous forest, the wavelength of the frequency band that was effective for T_{sub} and IACC, approximately matched the diameters of the tree trunks. To ensure the validity of the relationship between the effective frequency band and trunk diameter, a bamboo forest, which consists of randomly distributed trunks, was selected. In such a sound field, complicated conditions such as multiple scattering from tree trunks, excess attenuation by the ground, trunk distribution, and many atmospherical factors including temperature, humidity, and wind affect the sound field. Considering these factors, the sound field is difficult to simulate and the impulse responses are too complicated to calculate. At the present stage, therefore, the only effective approach is to use measured results.

Procedure

Acoustical measurements were conducted in a bamboo forest in Kyoto, Japan in June 1997. The measuring procedure was exactly the same as for previous measurements in the forest. In this measurement, the initial time delay gap Δt_1 was not obtained because a strong reflection at the initial part of the impulse responses was not observed due to the effects of multiple scattering.

Acoustical measurements were conducted in part of the bamboo forest. The bamboo is a variety of Phyllostachys pubescens. Receiver positions for sites, 5, 10, 20, and 40 m from the sound source were selected as shown in Figure 2.56. A reference position for LL was set at 5 m away from the source. The density of bamboo in the area was about 50 trunks per 100 m^2. The trunk diameters were all about 13 cm. Although the tree diameters in the previously studied forest were almost random, those in the bamboo forest were almost uniform. The area had a space about 3 m wide in front of the source without any bamboo. The area in front of the source had a gentle slope as shown in Figure 2.56(b). On the day when the measurements were conducted, there was no wind, and the temperature was between 25 and 27 degrees centigrade. Bamboo has a more rigid surface than trees and consists of hollow tubes.

LL at each receiving position was obtained relative to the reference point, 5-m from the source. In these measurements, values for Δt_1 could not be identified in the bamboo forest except for a strong reflection from the ground, because of the weak scattered reflections from the trees. The Δt_1 as an orthogonal factor was defined as the time interval between a direct sound and the first reflection from a sidewall except for

reflections from the ground. Hence, the first reflections coming from the ground were neglected in accordance with the definition.

Results

Initial parts of binaural-impulse responses at each position are indicated in Figure 2.57(a-d). Well-balanced left and right impulse responses were obtained for all receiver positions. The physical factors described in the previous section were calculated from these impulse responses.

Results for LL relative to that at 5 m are shown in Figure 2.58. The abscissa shows the distance from the source on a logarithmic scale. Decreases ranging from 15 to 30 dB for a doubling of distance from 5 to 10 m were observed in the bamboo forest, whereas the decrease given by the inverse square law (solid line) in a free field is 6 dB.

Measured A values are shown in Figure 2.59. Generally, A increases with distance, because it represents the total amplitude of reflections in relation to the direct sound. In the bamboo forest, too, A increased with distance, corresponding to an apparent room radius (the position at A = 1 with the same amplitudes for direct sound and reflections plus subsequent reverberation) of about 10 m from the source.

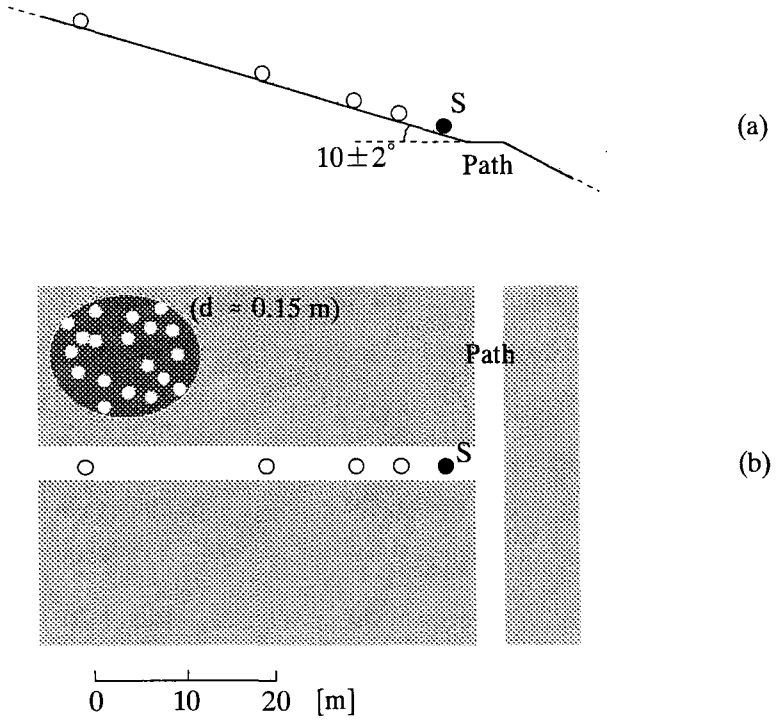

Figure 2.56 The bamboo forest investigated. Locations of the sound source and receivers are indicated. Bamboo within the area was all around 0.13 m in diameter. (a): cross section of the area for measurements and (b): plan of the area for measurements.

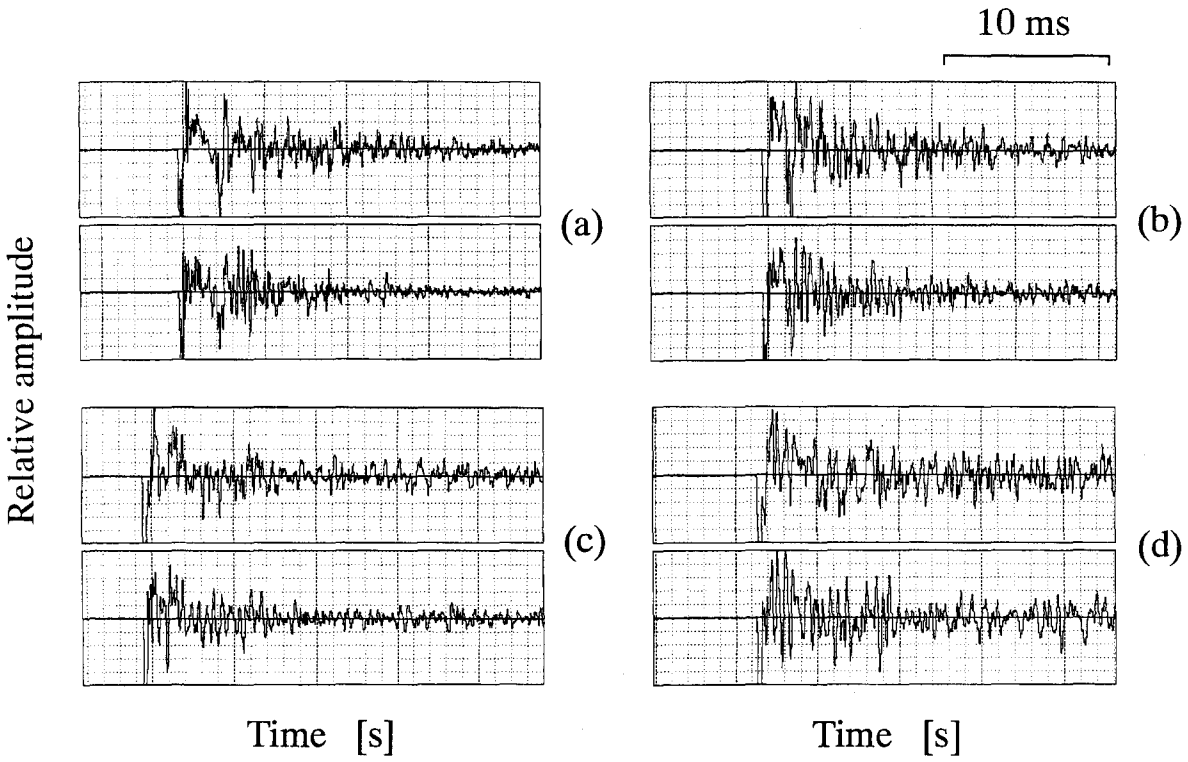

Figure 2.57 Binaural-impulse responses at each measurement point. The vertical axis of each figure is normalized by the maximum amplitude of each impulse response. Top: impulse response at left ear. Bottom: impulse response at right ear. (a) 5 m; (b): 10 m; (c): 20 m; (d) 40 m.

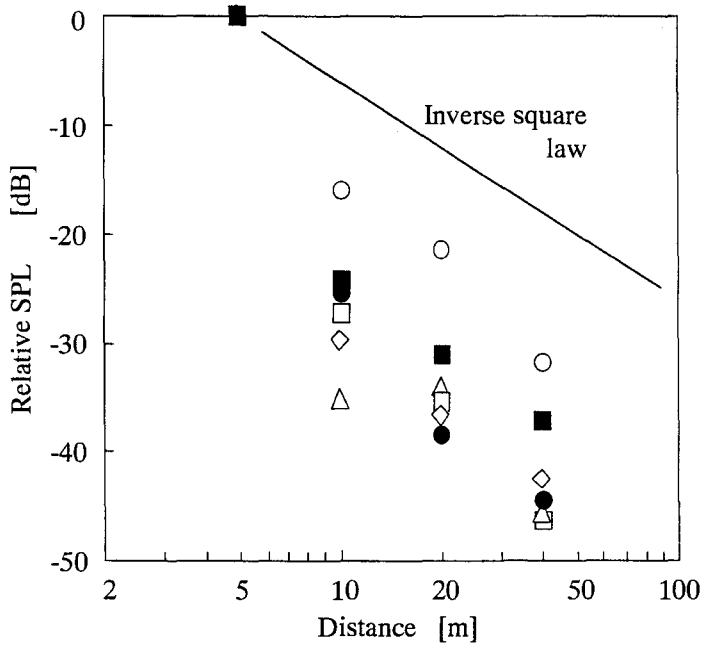

Figure. 2.58 LL values relative to that at 5 m. The solid line shows the inverse square law. ○: 125 Hz; △: 250 Hz; ●: 500 Hz; □: 1 kHz; ■: 2 kHz; ◇: 4 kHz.

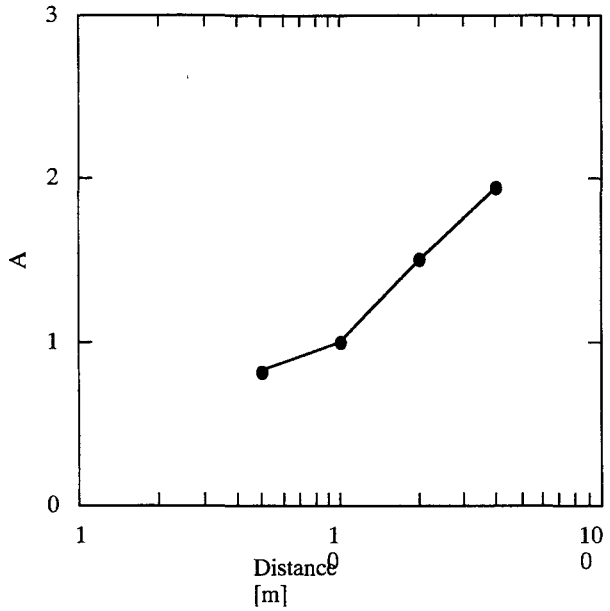

Figure 2.59 Measured A values (allpass band).

Decay curves of reverberation at 500 Hz and 1 kHz at each receiving position are shown in Figure 2.60. Subsequent reverberation components were kept after an initial rapid decrease of 5-10 dB. This tendency is exactly the same as for previous results in the forest. In existing concert halls, decay curves decrease linearly as shown in Figure 2.61 (for the Kirishima International Concert Hall, Japan as an example). Results for T_{sub} are shown in Figure 2.62. T_{sub} increased with distance and frequency for both 5 and 10 m. For 20 and 40 m, T_{sub} became almost constant above 1 kHz or slightly decreased. T_{sub} had a maximum of 1.5 s at 1 kHz (40 m). For 125 Hz in particular, T_{sub} was quite small, 0.2-0.3 s, compared to other frequency ranges.

Results for IACC are shown in Figure 2.63. In the higher frequency range, IACC became smaller and was 0.07 at 4 kHz at 20 m and 0.16 at 2 kHz at 40 m. These results are different from the results in the forest in which IACC was near 0.5 in the higher frequency range.

Results for τ_{IACC} and W_{IACC} are shown in Table 2.10. Interaural cross-correlation functions at each position are shown in Figure 2.64(a-d). Positive τ_{IACC} denote directional perception from the right side and negative values from the opposite side. The τ_{IACC} were obtained within 0.1 ms without exception. τ_{IACC} were between -0.02 and +0.06. Thus, the source should be perceived as being in front of the receiver for all receiver positions. Although we observed a tendency for W_{IACC} to increase with distance, there were some dips at 40 m. Above 20 m, W_{IACC} decreased.

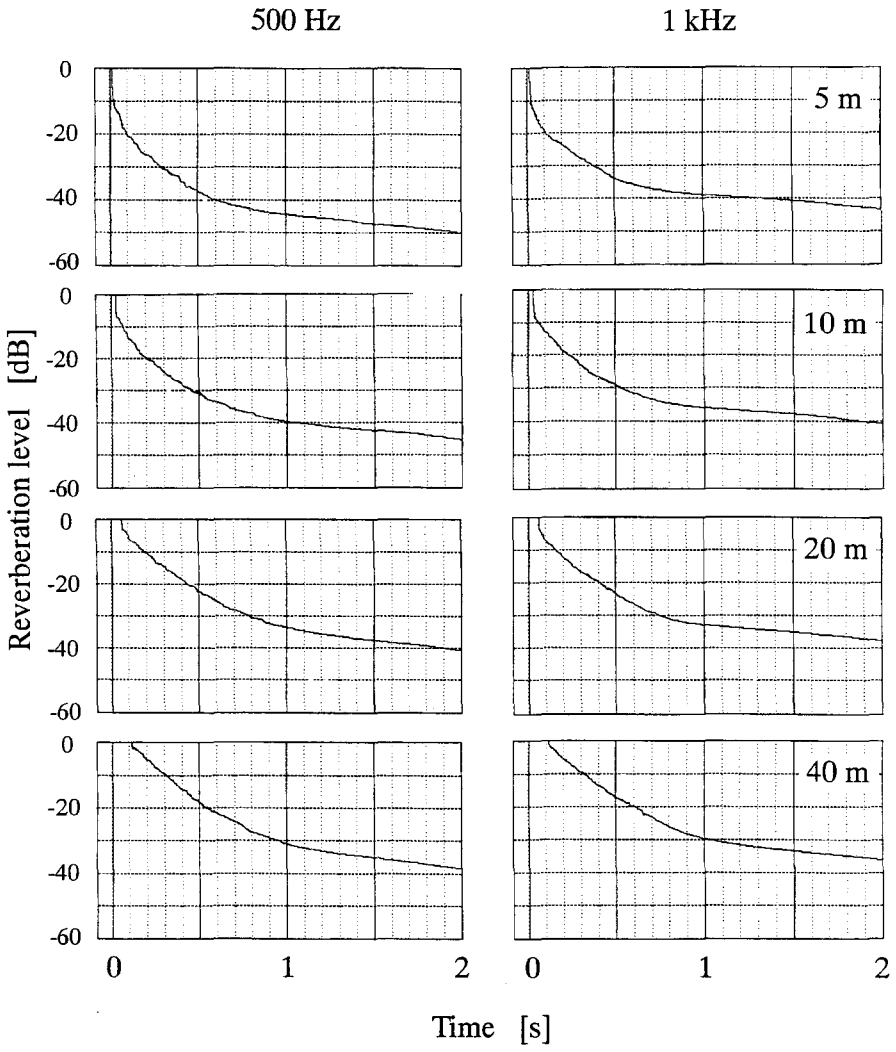

Figure 2.60 Attenuation curves at each measurement point. Left and right columns represent results at 500 Hz and 1 kHz for each receiver position, respectively.

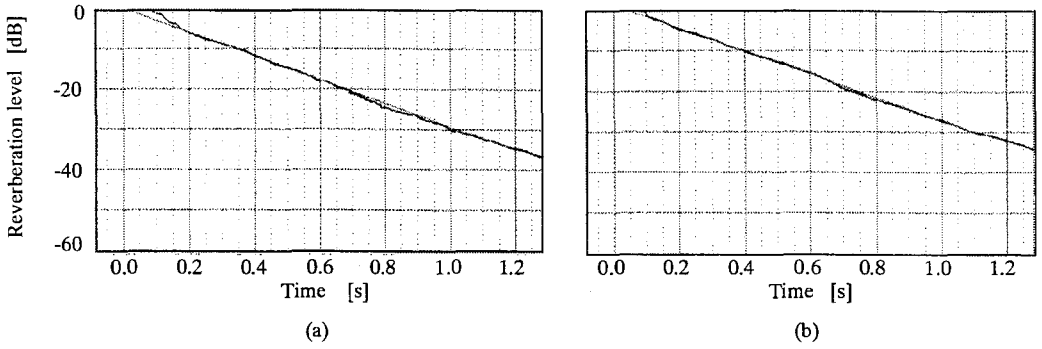

Figure 2.61 Attenuation curves at 20 m from the sound source on the stage of Kirishima International Concert Hall. (a): 500 Hz; (b): 1 kHz.

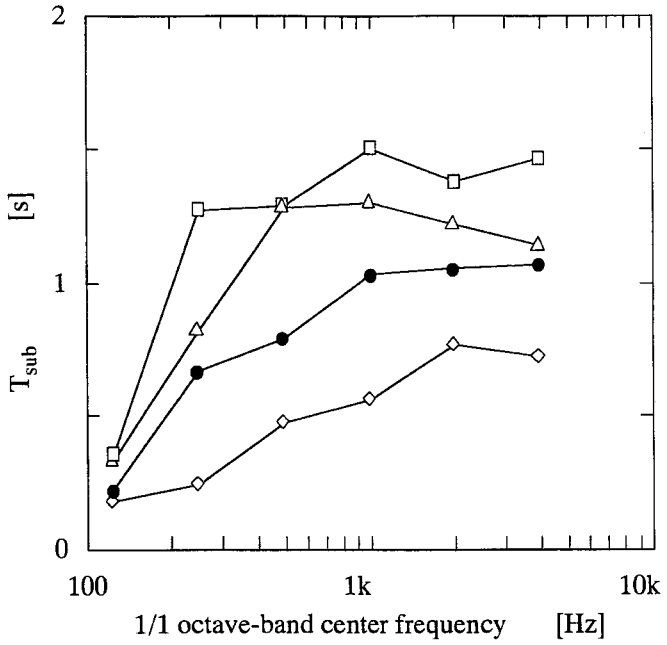

Figure 2.62 Results for T_{sub}. ◇: 5 m; ●: 10 m; △: 20 m; □: 40 m.

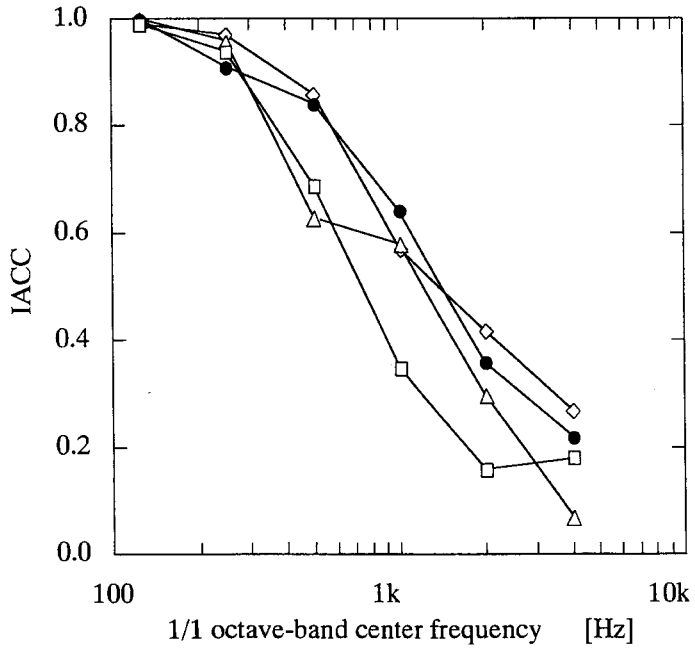

Figure 2.63 Results for IACC. ◇: 5 m; ●: 10 m; △: 20 m; □: 40 m.

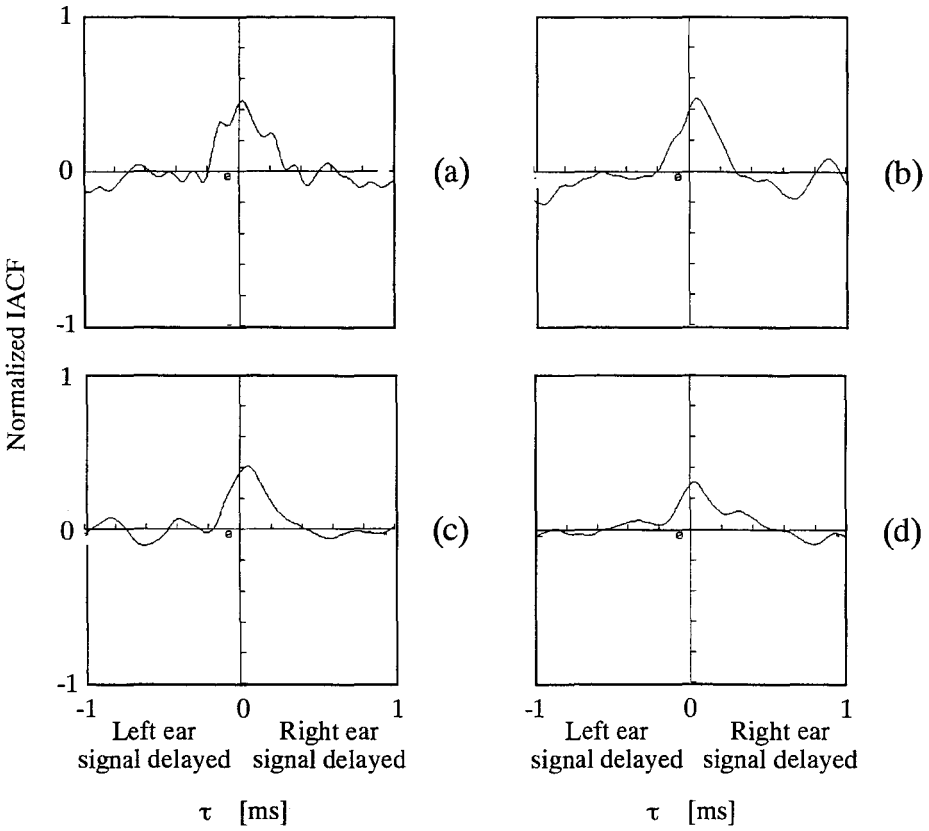

Figure 2.64 Normalized interaural cross-correlation functions at each measurement point. (a) 5 m; (b): 10 m; (c): 20 m; (d) 40 m.

Discussion

The LL results showed a similar tendency to the previous results in the forest in terms of a decrease of more than 15 dB for doubling of the distance, although LL generally decreases by 6 dB for doubling of the distance in a free field. At 40 m, when the source power was about 100 dB, these LLs as having fallen below the level of background noise are regarded. As there are no bamboo in front of the source, this was caused by excess attenuation by the ground and no reflections from above (e.g., from leaves or branches). For the bamboo forest, the rate of decrease was larger than in the case of a forest of ordinary trees. This results is considered to be from excess attenuation from the ground (soil) over wider frequency ranges in the bamboo forest, although there was excess attenuation in the higher frequency range due to the ground, which was made from asphalt, in the case of an ordinary forest (Embleton, 1996).

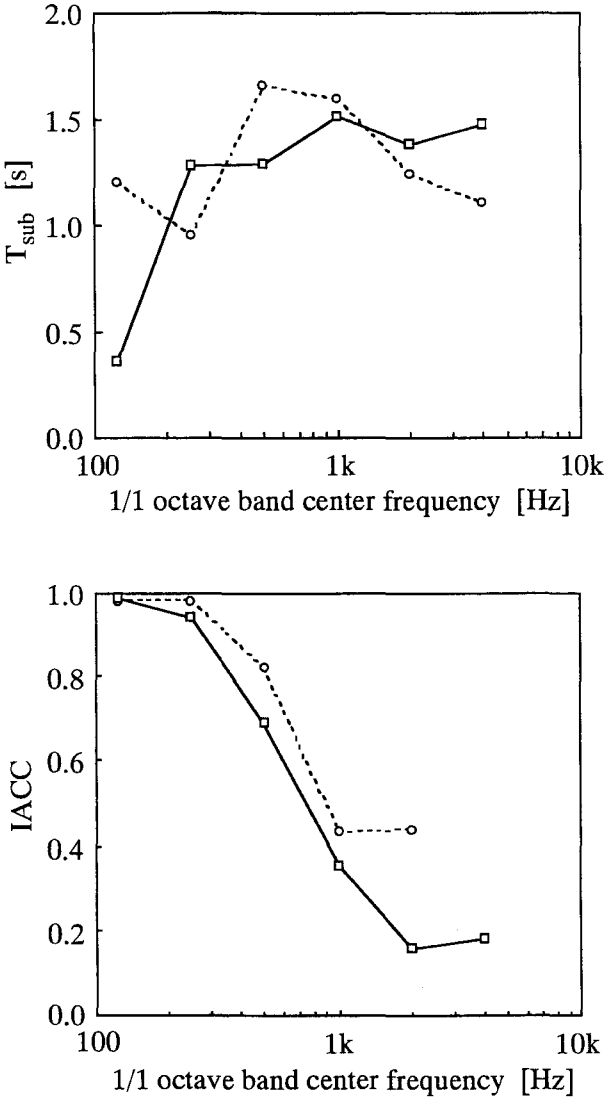

Figure 2.65 Comparison between the bamboo forest and the previous forest. (a): T_{sub} at 40 m; (b): IACC at 40 m. □: results for bamboo forest; ○: results for previous forest.

The maximum value of T_{sub} was shifted to the higher frequency range compared with the results in an ordinary forest, as shown in Figure 2.63(a). This supports the hypothesis we had before the measurements. For the sound field of the bamboo forest, T_{sub} increased with distance, and a maximum peak appeared at 500 Hz without exception. Comparing the sound fields of bamboo and ordinary forests, T_{sub} become maximum at 1 kHz or higher in the bamboo forest compared with 500 Hz in the ordinary forest. And although values of T_{sub} decreased above 500 Hz for an ordinary forest, T_{sub} kept constant with a large LL decreasing above 1 kHz in the bamboo forest. Maximum T_{sub} was obtained at above 1 kHz in the bamboo forest. The difference between sound fields in a bamboo and ordinary forests cannot be compared simply. One reason is that the trunk diameter is

constant (0.13 m) in the former case while it ranges from 0.3 to 1.0 m in the latter case. This raises the frequency range of reveberant components.

T_{sub} itself were smaller than in an ordinary forest (1.6 s at the most). Thus, a bamboo forest is suitable for performances of relatively fast-tempo music. For example, the optimum T_{sub} is 1.2 s for music for which the effective duration of the autocorrelation function of the sound source τ_e is 50 ms, since the optimum T_{sub} is given by 23 times the τ_e value (see Ando 1998 for the definition of τ_e). Music with such a small value of τ_e includes chamber music. However, it is quite difficult to explain the phenomenon because of the complicated sound field, and there is no absorptive material in that specific frequency range. T_{sub} below 250 Hz was small due to absorption by the air and bamboo leaves.

At 20 m, T_{sub} was constant at around 1.3 s above 500 Hz. The τ_e obtained from these values was 53 ms. Thus, jazz music or a clarinet solo would be suitable for this sound field. On the other hand, a cello or violin played with a slow tempo would not be suitable.

It is worth noting that in the higher frequency range, IACC was smaller than in an ordinary forest, as shown in Figure 2.63(b). This may be caused by strong lateral reflections from the rigid surface of the bamboo. IACC generally becomes smaller if strong lateral reflection arrives at the ears. It is worth noting that IACC below 0.1 is the same as in a properly designed concert hall.

Conclusion

It was clarified that the outdoor sound field in a bamboo forest has excellent acoustical properties. Like the sound field in an ordinary forest, the specific sound field was obtained, especially in terms of the factors T_{sub} and IACC. The tendency was found that the effect appears in higher frequency ranges (around 1 kHz) than in the sound field in an ordinary forest. T_{sub} was 1.5 s in the frequency range above 1 kHz at a position 40 m from the source. The effective frequency range for T_{sub} was above 1 kHz. It may be related to the diameter of the bamboo. IACC was as small as 0.07 (4 kHz) and 0.16 (2 kHz) at positions 20 and 40 m from the source. This is caused by the reflective surface of the bamboo.

2.4 Conclusion of Chapter II

It is concluded, from the measurements in historical opera houses, as follows.

From the measurements for a singer on the stage, it is concluded as follows.

As each physical factor greatly varies on the stage for the sources in the orchestra pit, a singer can adjust to the preferred sound field by moving the location on the stage. For

LL and T_{sub}, the variance of these factors are remarkable for the back-and forth direction in the frontal area on the stage. On the other hand, the variance is not so significant for the side direction.

In terms of IACC, it can be suggested for a singer to perform in the middle-front on the stage where has a strong reflection from the frontal direction. On the frontal-center location on the stage, however, an un-preferred upward reflection for a singer from the proscenium arch should be avoided.

From the results of τ_{IACC}, a singer on the stage can localize the direction of the source even for the source under the stage.

These results suggest the necessity of the psychological experiments for a singer in relation to the orchestra music in the orchestra pit in a laboratory regarding to the complicated initial reflections inside an opera house.

From the measurements for musicians in the orchestra, it is concluded as follows.

For the sources P2 and P3, large dips of *LL* can be found at 2 kHz. This may cause the suppression of the singing formant enhancing the singing voice at higher frequency range.

A values were quite large especially at the receivers in the rear row as more than 15 (up to 30) in the rear row for all source positions, although averaged *A* value in the stall (21 positions) were 2.3 in the same theater.

The variety of T_{sub} between the rows was negligible at frontal source positions (P1 and P2) by a singer's movement for lateral direction. At rearer position such as P3, T_{sub} become longer, and the difference of T_{sub} between rows become large as 0.2 s.

IACCs above 500 Hz were quite small for all the sources. This phenomenon is caused by multiple reflection inside the pit. By the unstable τ_{IACC} in the pit, the musicians in the pit perceive vague directivity for a singer singing on the stage, especially below overhang.

From the measurements for a conductor, it is concluded as follows.

For the sound sources in the orchestra pit, the dips of relative *LL* were observed at low frequency range (-12.5 dB 250 Hz for P6) due to the interference effects between the direct sound and strong initial reflections inside the pit. Players with lower-frequency instruments are suggested to be frontal area near the conductor in terms of acoustics.

The suggestion that the sound field for a conductor should be designed as well as that for listeners does not be supported in relation to temporal factors (Δt_1 and T_{sub}).

Especially, Δt_1 was observed mainly around 2-3 ms, which came from the pit rail just behind the conductor. Also IACC at 500 Hz was large above 0.4, which is quite larger than that in a stall.

T_{sub} for pit source (1.07 s at 500 Hz in average) are shorter than that for stage source (1.52 s). In terms of the optimum T_{sub} for the orchestra music and singing voice, this relation is inconsistent for a listener's condition.

IACC at 2 kHz (0.43 in average) was larger than that at 1 kHz and 4 kHz for the sources in the stage.

From the measurements for listeners in a box, it is concluded as follows.

Comparing the LL values for the source on the stage with that in the pit, LL values for the stage source were smaller than for the pit source. Values of LL at 125 Hz were boosted for the pit source, especially at the receiver in the stall (up to -14 dB).

The Δt_1 values were quite different at both ears in the boxes. It is interesting to note that the left and right Δt_1 values of Pattern 2 and 4 measured in the two boxes for both source positions were quite similar. This means that the Δt_1 is almost the same value for a person at rear seats almost independently, even if some persons in the front row exist or not when the listener is at second row. More uniform listening environment for the rear box compared to the frontal one.

The parameter T_{sub} is not distributed into a wide range between the patterns. For both source locations, T_{sub} above 250 Hz in Box A was larger than that in the stall and in the Box B.

For the both source locations, IACC dramatically decreased between 250 Hz and 500 Hz in boxes comparing to that in the stall.

Through the measurements in these opera houses, especially, impulse responses, which the first reflection do not have maximum amplitude, are obtained at many receivers. These results suggest the necessity of the psychological experiments in a laboratory regarding to the complicated initial reflections. Considering actual opera performances, as there are stage sets and some singers on the stage, more complicated sound fields may be constructed. Accumulation of such a measurement data in relation to sound fields on the stage and in the orchestra pit inside a historical opera houses, physical characteristics of their sound fields will be known, and they will give valuable and useful information in designing a stage and an orchestra pit inside opera houses.

In the forest, it is found that the forest has excellent acoustic properties, especially for factors of subsequent reverberation time (T_{sub}) and IACC. The value of T_{sub} was 1.66 s (500 Hz), and IACC was 0.44 (1 kHz) at a point 40 m from the source. Also, it is found that the value of the width of the interaural cross-correlation function, W_{IACC}, was smaller than that in the concert hall.

Also, it was clarified that the outdoor sound field in a bamboo forest has excellent acoustical properties. Like the sound field in an ordinary forest, the specific sound field was obtained, especially in terms of the factors T_{sub} and IACC. The tendency was found that the effect appears in higher frequency ranges (around 1 kHz) than in the sound field in an ordinary forest. T_{sub} was 1.5 s in the frequency range above 1 kHz at a position 40 m from the source. The effective frequency range for T_{sub} was above 1 kHz. It may be related to the diameter of the bamboo. IACC was as small as 0.07 (4 kHz) and 0.16 (2 kHz) at positions 20 and 40 m from the source. This is caused by the reflective surface of the bamboo.

It was clarified that the outdoor sound field in a bamboo forest has excellent acoustical properties. Like the sound field in an ordinary forest, the specific sound field was obtained, especially in terms of the factors T_{sub} and IACC. The tendency was found that the effect appears in higher frequency ranges (around 1 kHz) than in the sound field in an ordinary forest. T_{sub} was 1.5 s in the frequency range above 1 kHz at a position 40 m from the source. The effective frequency range for T_{sub} was above 1 kHz. It may be related to the diameter of the bamboo. IACC was as small as 0.07 (4 kHz) and 0.16 (2 kHz) at positions 20 and 40 m from the source. This is caused by the reflective surface of the bamboo.

It is clarified that the acoustical measurement procedures for a concert hall can be applied for a sound fields in an opera house and outdoor sound fields in forests. Some specific sound fields, which are different from that in a concert hall, are obtained for both sound fields. Especially complicated initial reflections are obtained such sound fields.

CHAPTER III. SUBJECTIVE PREFERENCE TESTS FOR OPERA HOUSE

3.1 Introduction of Chapter III

The theory of subjective preference (Ando, 1985) has been developed by use of psychological experiments for simple simulated sound fields. It is necessary to clarify whether the theory can be applied for existing sound fields. Sato et al. (1997) and Cocchi et al. (1997) indicate the effectiveness of the theory through the investigations in existing concert halls. In this Chapter, the subjective preference test in an existing opera house the "Teatro Comunale" in Ferrara, Italy is described. The activities to preserve and investigate the Italian historical theaters regarded as a cultural heritage is going on (Pompoli and Prodi, 2000).

3.2 Subjective Preference Tests in an Existing Hall

Source Signal

An opera music (Romanza "Tormento" by P. Tosti) which consists of the soprano vocal part in one channel and the piano part in the other channel was used as a source signal. The duration of the signal was 16 s. In subjective preference theory, music source is characterized in terms of the running autocorrelation function (ACF) of the source signal, after passing through an A-weighted network. As described in Subsection 1.2.2, in the ACF analysis, $\Phi(0)$, τ_e, τ_1, and ϕ_1 were calculated with an integration interval $2T$ = 2.0 s, and running step of 100 ms (Figure 3.1). In four factors, the minimum value of the effective duration of the source signal, which is strongly connected to the preferred conditions of temporal factors, is about 16 ms.

Procedure

Two loudspeakers were located on the stage (one was just under proscenium and another was 2.5 m behind) and the other two loudspeakers in the orchestra pit (one was in front of the conductor's box and another was under overhang). The height of the loudspeakers on the stage and in the orchestra pit were 1.5 ± 0.01 m and 1.2 ± 0.01 m above the floor level, respectively as shown in Figure 3.2. These heights simulated the singer on the stage and the sitting performer in the orchestra pit, respectively. A vocal music source is used for

source location on the stage and orchestra music is used for sources in the pit. Four or three listeners are seated in the specified area both in the stall (10 positions) and the box/gallery (5 positions). The number of the subjects is fourty-seven.

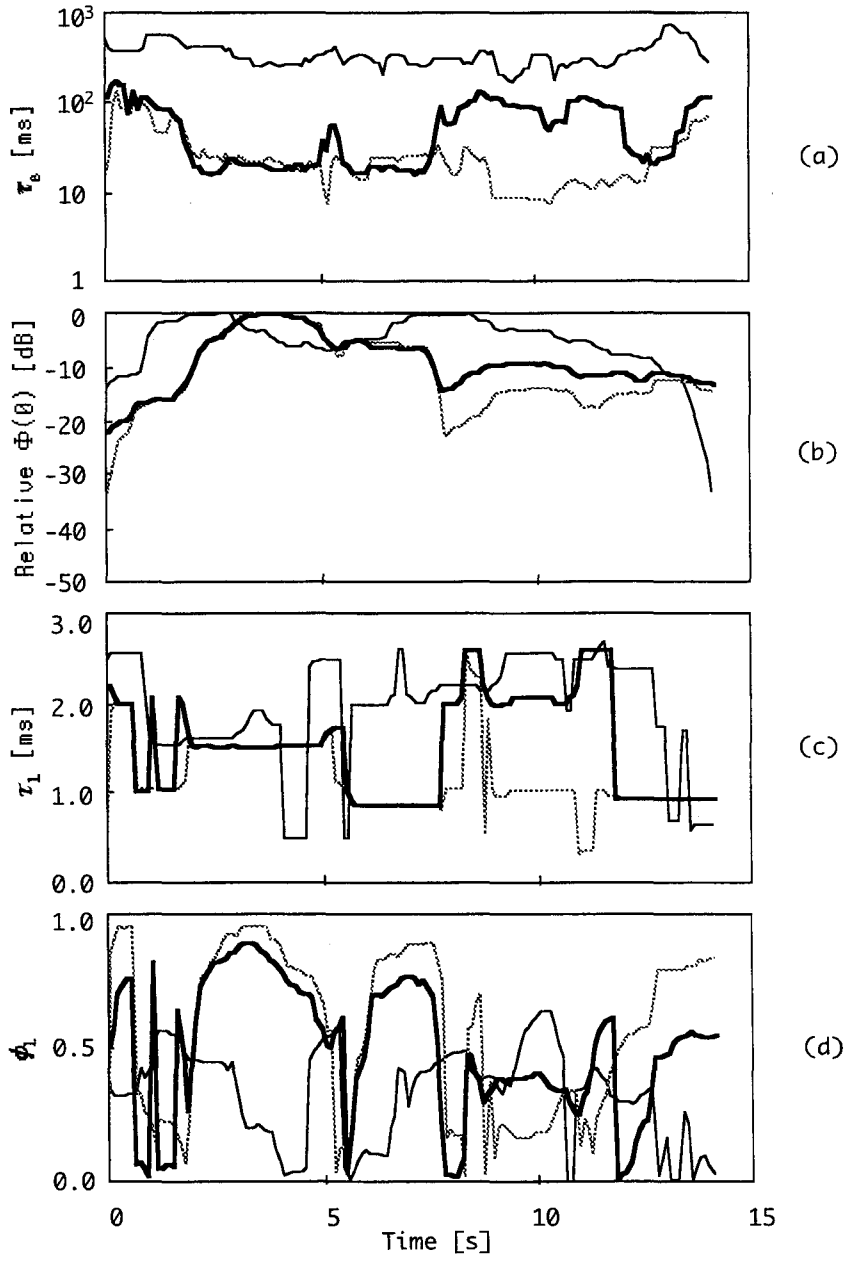

Figure 3.1 Measured factors of running ACF of the source signal used in the experiment with a 100 ms interval as a function of the time. The running integration interval of ACF $2T$ was 2.0 s. (—): piano; (····): vocal; and (—): mixed. (a) τ_e; (b) $\Phi(0)$; (c) τ_1; and (d) ϕ_1.

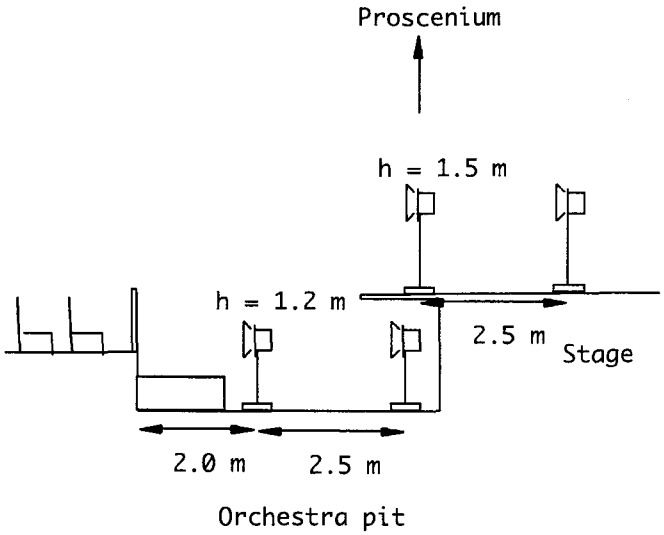

Figure 3.2 Configurations of the loudspeaker settings.

Paired-comparison tests

Paired-comparison test of four sound fields as listed in Table 3.1 were conducted. The duration of each music signal is 16 s, and the silent interval between the stimulus is 2 s. Test consists of six pairs (= $N(N-1)/2$, $N = 4$) of stimuli for a single session. Each pair of sound fields is separated by an interval of 4 s, and the pairs are arranged in random order.

Forty-eight listeners were participated in the experiments. Twenty-one listeners were students of the musical department and twenty-seven listeners were the students of the Faculty of Engineering. Listeners divided into 10 groups were seated at the specified set of seats (Figure 3.3). Five groups were in stalls and another five groups were in the boxes and gallery. The subjects were asked to remain in their seats, and asked to judge which of two sound fields while switching the source locations they prefer to listen. They were advised to judge every pair (not to leave the blank), to face the center of the stage, and not to copy the answer of other person. They were also asked to write down their name, age, sex, and musical experiments (period and instruments) on their answer sheets. Prior to the experimental sessions, exercise session was conducted presenting three pairs of stimuli. The session was repeated five times, changing their seats. It took about four minutes for a single session and about thirty minutes in total including the time for changing their seats.

According to their musical experiment which were given in their answer sheets, listeners were divided into two groups, group of musician, who have musical experiments of more than five years (group M) and others (group N). It was examined whether the listener can discriminate the sound fields presented by test of consistency. The number of the listeners who indicated the significant ability to discriminate preferences were twenty

(eleven for group M and nine for group N) in the stalls and seventeen (eight for group M and nine for group N) in the boxes and the gallery. Scale value of preference was obtained by applying the law of comparative judgment and reconfirmed by goodness of fit (Thurstone, 1927; Mosteller, 1951).

Table 3.1 Conditions of the paired-comparison test.

	Condition 1	Condition 2	Condition 3	Condition 4
Orchestra pit	Front	Front	Back	Back
Stage	Front	Back	Front	Back

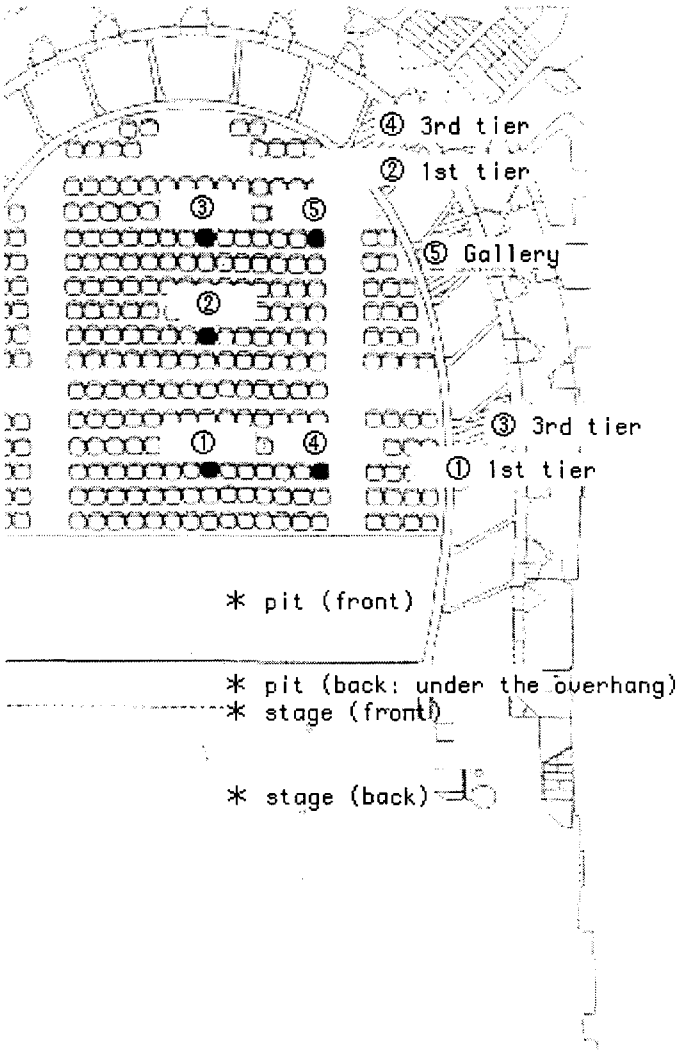

Figure 3.3 Source positions and listener's locations in the theater.

Measurements of acoustical factors

To obtain the factors extracted from the interaural crosscorrelation function (IACF), the musical signals used in the subjective tests were reproduced from the same loudspeaker configurations as the subjective tests and were recorded at each listening position to DAT through the two microphones at both ears of a person who faced the center of the stage. To obtain the impulse responses, MLS signal was reproduced from each loudspeaker and recorded at each listening position in the laptop computer (Sakurai et al. 2000) through the two microphones at both ears of a person who faced the center of the stage.

From the IACF, $\Phi(0)$, IACC, τ_{IACC}, and W_{IACC} were calculated. From the impulse responses, Δt_1 and T_{sub} were calculated.

The Δt_1 is defined by the time difference between the arrival time of the direct sound and that of the reflection which has maximum energy. Shorter one of two Δt_1s obtained from binaural impulse responses was selected as Δt_1 of each loudspeaker configuration and each listener's position.

For T_{sub}, 500 Hz and 1 kHz octave band center frequencies are taken into consideration because these frequencies range are dominant in the τ_1 (first peak of the normalized autocorrelation function) value of the autocorrelation function of the source signal.

Multiple Dimensional Analysis

First of all, correlation coefficients among physical factors were examined as listed in Table 3.2. Of the physical parameters obtained by measurement, total amplitude of reflections (A-value) is not physically independent of the Δt_1 (Ando, 1998). The W_{IACC} is the significant factor on ASW if the dominant frequency range of the source signals are different (Ando et al., 1999) but has minor effects in this experiment. The data were analyzed by factor analysis (Ando, 1998; Hayashi, 1952; Hayashi, 1954). The outside variable to be predicted was the scale values of preference obtained by subjective judgments and the explanatory variables were: (1) the listening level, (2) the IACC, (3) the τ_{IACC}, (4) the Δt_1 normalized by preferred value (for the pit source), (5) the Δt_1 normalized by preferred value (for the stage source), (6) the T_{sub} for the pit source and (7) the T_{sub} for the stage source.

Iteration for possible subdivision of the sub-categories for each factor listed in Table 3.3 and the possible combination of factors was conducted. The results which gives the best correlation between the scale values of preference obtained by subjective judgment and the total score obtained by factor analysis are shown in Figure 3.5.

Table 3.2 Correlation coefficients between orthogonal physical factors obtained from the acoustical measurements in an opera house.

	LL	IACC	τ_{IACC}	W_{IACC}	Δt_1 (pit)	Δt_1 (stage)	T_{sub} (pit)	T_{sub} (stage)
LL	1.00	0.13	0.18	−0.16	−0.26	−0.22	0.19	<0.01
IACC		1.00	−0.21	0.31*	−0.09	0.16	0.49**	0.56**
τ_{IACC}			1.00	0.11	0.06	−0.22	< 0.01	0.07
W_{IACC}				1.00	−0.12	0.50**	< 0.01	0.15
Δt_1 (pit)					1.00	0.03	−0.21	−0.04
Δt_1 (stage)						1.00	−0.05	−0.07
T_{sub} (pit)							1.00	0.54**
T_{sub} (stage)								1.00

*: $p < 0.05$; **: $p < 0.01$.

Table 3.3 Iteration for possible subdivision of the sub-categories for each factor. For example, {−3.5, −0.5} in factor relative LL means that the sub-categories were divided into three groups; (1) less than −3.50 dB; (2) −3.50 to −0.51; and (3) more than −0.50.

Factors	Max	Min	sub-categories
Relative LL [dBA]	−6.30	0.00	{−3.5, −0.5}, {−4.0, −1.0} {−4.5, −1.5}, {−5.0, −2.0} {−5.5, −2.5}, {−6.0, −3.0}, {−5.5, −3.5, −1.5}, {−5.0, −3.0, −1.0}
IACC	0.03	0.65	{0.15, 0.40}, {0.15, 0.50} {0.20, 0.40}, {0.20, 0.50} {0.30, 0.50}
τ_{IACC} [ms]	0.00	0.21	{0.00}, {0.04}, {0.00, 0.10}, {0.00, 0.15}, {0.00, 0.20}
Normalized Δt_1(pit)	0.60	5.28	{1.0, 2.0}, {1.0, 2.0, 3.0}
Normalized Δt_1(stage)	0.31	3.81	{1.0, 2.0}, {1.0, 2.0, 3.0}
T_{sub}(pit) [s]	500 Hz: 1.02	500 Hz: 1.50	{1.1, 1.3}, {1.1, 1.4}, {1.2, 1.5}
T_{sub}(stage) [s]	500 Hz: 0.98	500 Hz: 1.64	{1.1, 1.3}, {1.1, 1.4}, {1.2, 1.5}

Results and discussion

Scale values for each seat position are shown in Figure 3.4. The results in stalls indicate that the frontal source position on the stage (Condition 1 and 3) were preferred by both groups. The range of scale values for group M were greater than that for group N. Preferred condition in boxes and gallery was different between both groups, however, the range of scale values was smaller than that of stalls.

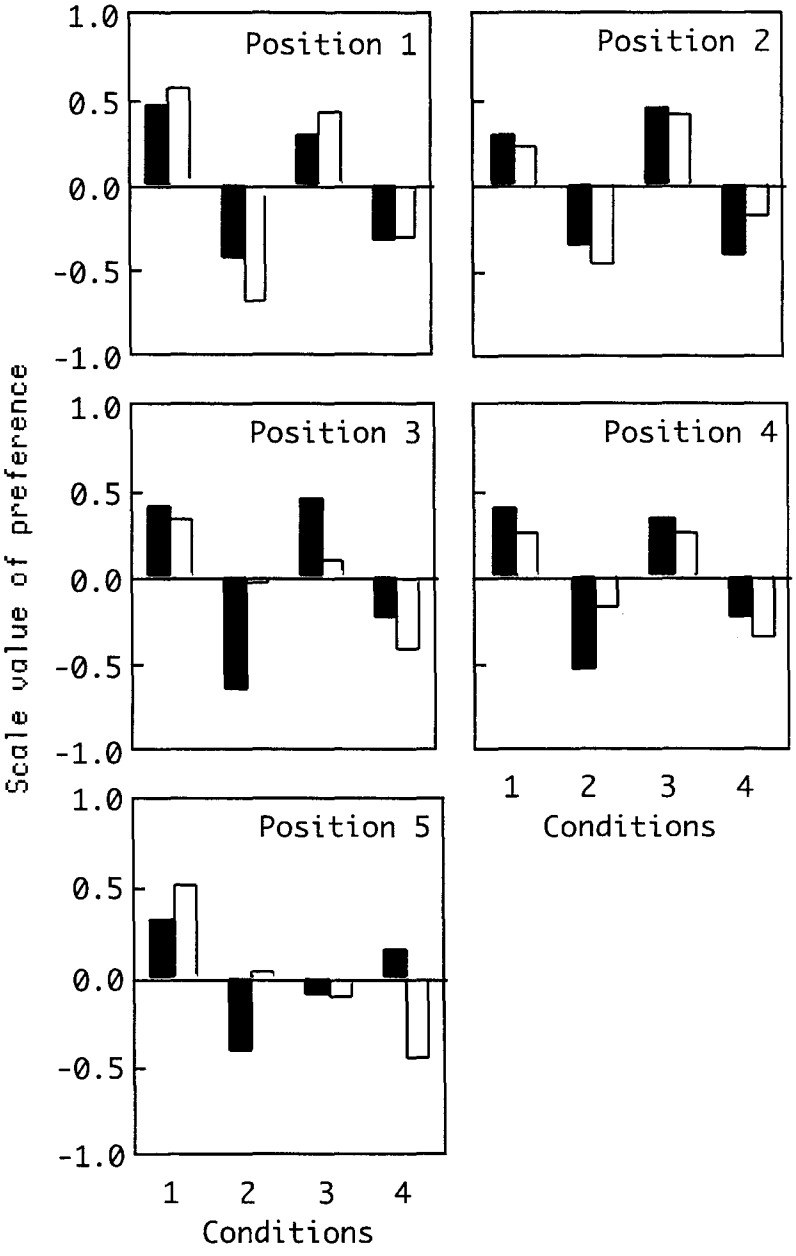

Figure 3.4(a) Results of paired comparison tests at each listener's location in the stall. Filled bar indicates the results for Group M and open bar indicates the results for Group N.

The scores of the listening level indicate a peak at the subcategory of -3.00 to -1.01 dB and decrease the score apart from the preferred listening level (Figure 3.5(a)). Partial correlation coefficient indicates that the effects of listening level were maximum among all factors. For the IACC, the preference score increases with decrease in the IACC (Figure 3.5(b)). The scores of τ_{IACC} become larger when the τ_{IACC} is larger (Figure 3.5(c)). The scores of the above-mentioned three factors are in good agreement with the previous results for a concert hall. In this experiment, all loudspeakers were located on the center axis of the hall and the listeners were asked to face the center of the stage, therefore, the effect of τ_{IACC} on the preference score is small.

The scores of Δt_1 for both the stage and the orchestra pit indicate a peak at a larger value than the most preferred value (Figure 3.5(d) and 3.5(e)). Effects of Δt_1 for stage source were rather minor among all factors. For T_{sub} of the orchestra pit, subcategory of larger T_{sub} indicates larger score. On the contrary, for T_{sub} of the stage, subcategory of smaller T_{sub} indicate larger score (Figure 3.5(f) and 3.5(g)). This may be related to that the source of smaller τ_e (vocal source) fits the sound field with a short reverberation time.

There were little difference between the results for Group M and Group N. This is because the scale values for the listeners in the stall has large range and there is little difference between two groups. The relationship between the scale value obtained by preference judgments and the total score at each listener's position is shown in Figure 3.6. The scale values of preference are well predicted with the total score for four configurations ($r = 0.81, p < 0.01$ for Group M; and $r = 0.82, p < 0.01$ for Group N).

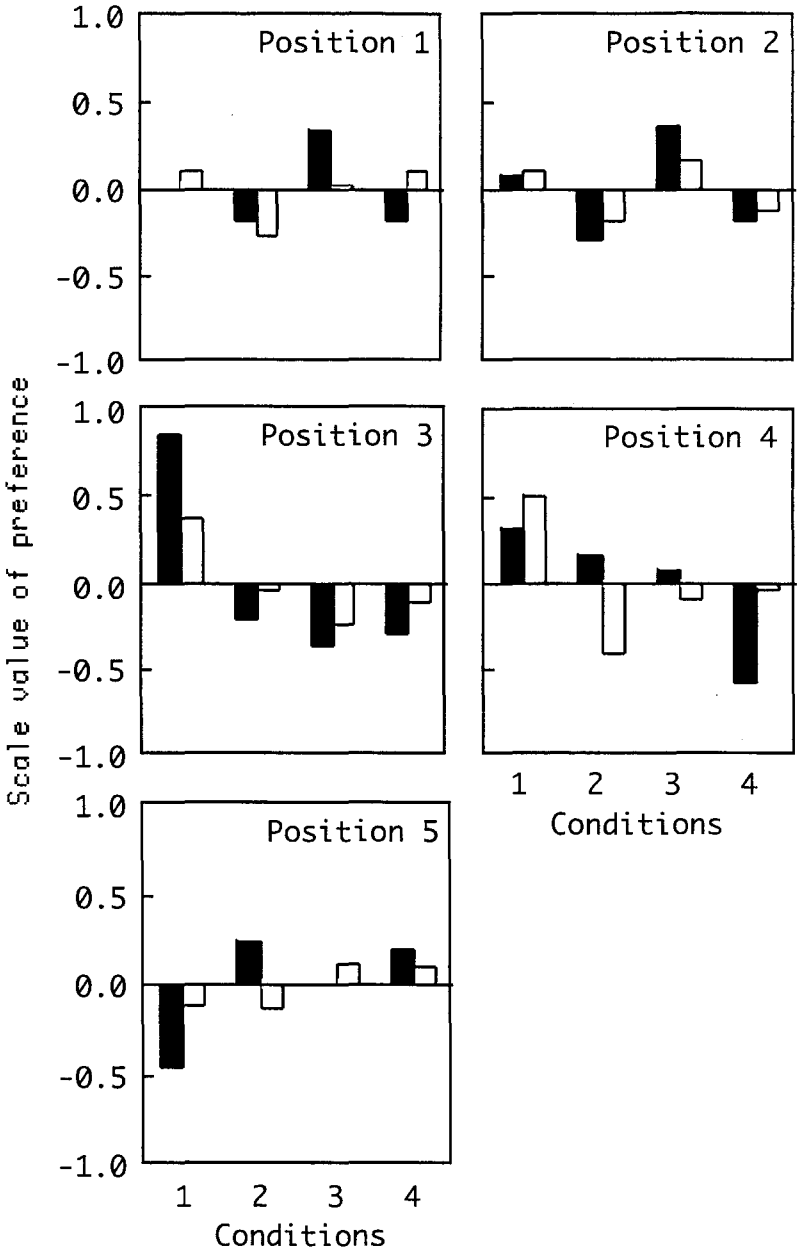

Figure 3.4(b) Results of paired comparison tests at each listener's location in box/gallery seats. Filled bar indicates the results for Group M and open bar indicates the results for Group N.

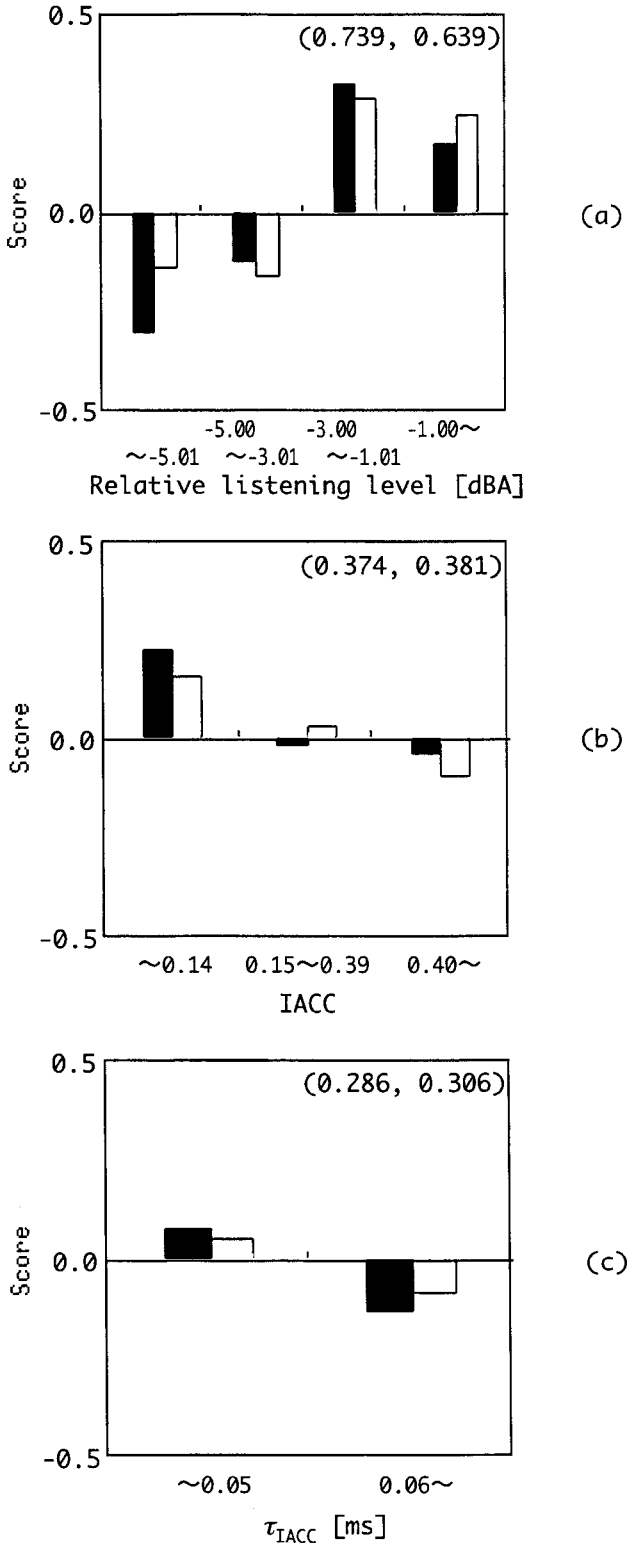

Figure 3.5(a-c) Scores for each category of physical factors obtained by factor analysis. The number signifies the partial correlation coefficient between the score and each factor. Filled bar: Group M; and Open bar: Group N. (a) Listening level; (b) IACC; and (c) τ_{IACC}.

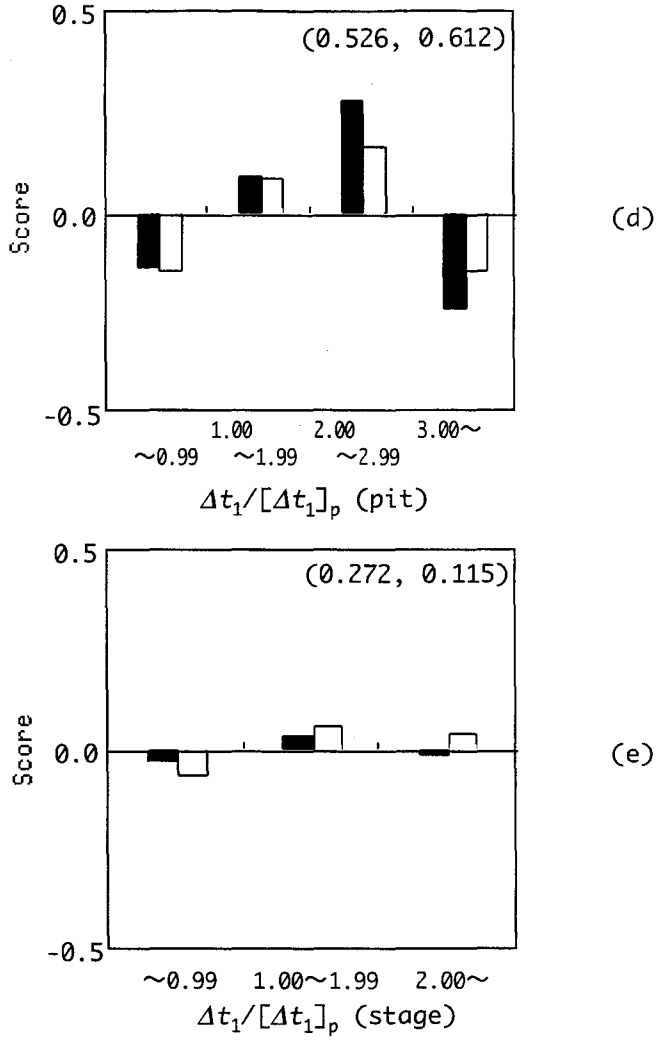

Figure 3.5(d-e) Scores for each category of physical factors obtained by factor analysis. The number signifies the partial correlation coefficient between the score and each factor. Filled bar: Group M; and Open bar: Group N. (d) Normalized Δt_1 (pit); and (e) Normalized Δt_1 (stage).

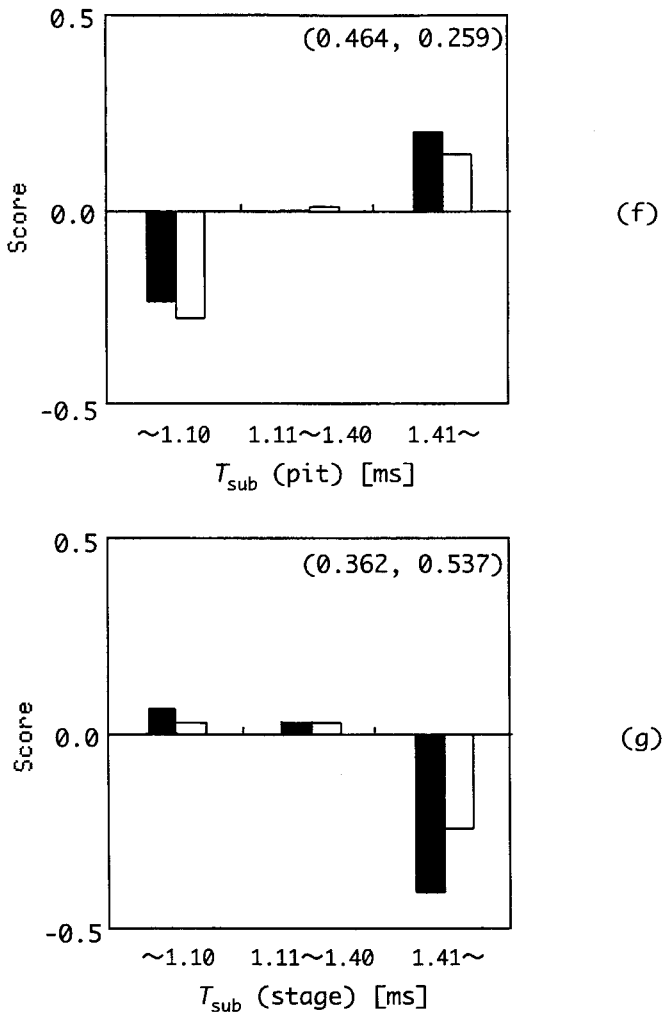

Figure 3.5(f-g) Scores for each category of physical factors obtained by factor analysis. The number signifies the partial correlation coefficient between the score and each factor. Filled bar: Group M; and Open bar: Group N. (f) T_{sub} (pit); and (g) T_{sub} (stage).

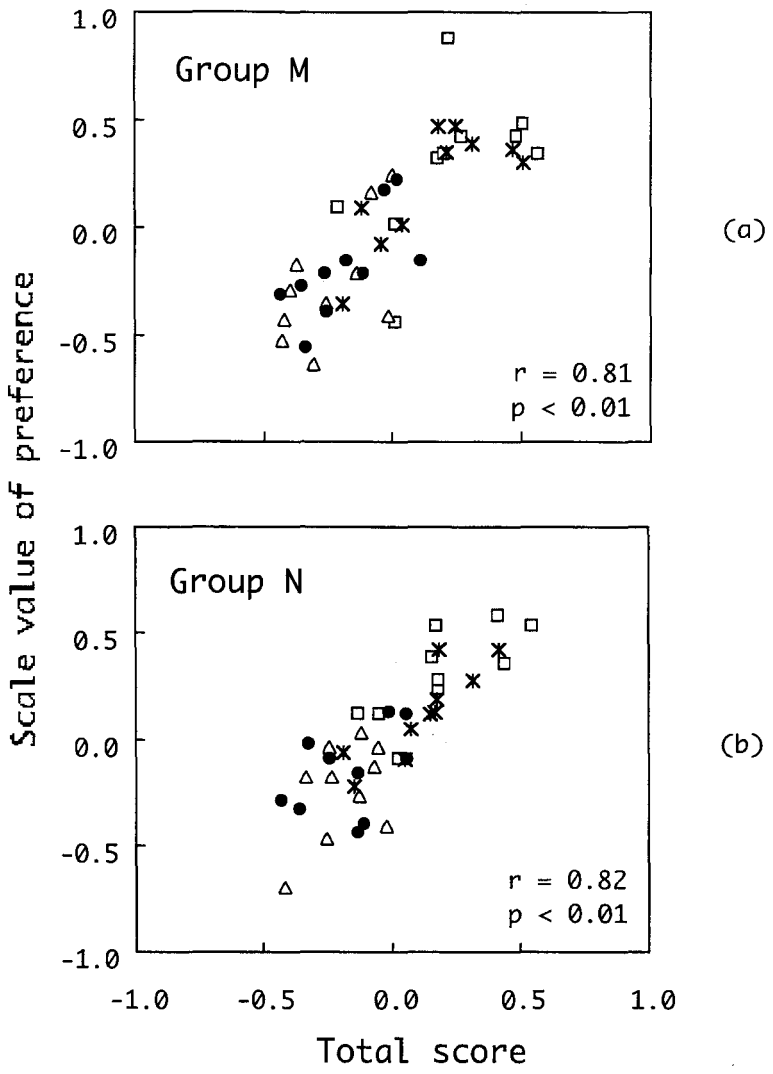

Figure 3.6 Relationship between scale values obtained by subjective judgments and total scores calculated by factor analysis using scores shown in Figure 3.5 (□: Condition 1; △: Condition 2; *: Condition 3; and ●: Condition 4); (a) Group M; and (b) Group N.

3.3 Conclusion of Chapter III

To confirm the subjective preference theory for an opera house, the relationship between the scale values of subjective preference and the orthogonal physical factors was examined by factor analysis. The scale values of preference for different source locations on the stage and in the orchestra pit in an opera house were obtained using a paired comparison method. The results showed that the scores obtained by factors analysis is similar to that of the concert hall investigated. The scale values of preference are well predicted using the total score obtained by factor analysis.

In this experiment, it was impossible to confirm individual preference in an existing theater because of a limited number of test series for each subject. However, difference between students with or without musical experience was well predicted.

CHAPTER IV. INDIVIDUAL SUBJECTIVE EVALUATION FOR SOUND FIELDS

4.1 Introduction of Chapter IV

Schroeder, Gottlob, and Siebrasse (1974) described subjective preference evaluations of European concert halls and attempted to correlate the subjective data with objective (geometric and acoustic) parameters of the halls. Although individual differences and intra-individual changes are extensively researched in psychology, subjective evaluation of sound fields has not been studied deeply. For sound fields such as concert halls and opera houses, environments, which satisfy each person, are desired. For example, in the present stage, seat-selection system, which can determine the preferred seat area in a concert hall, is realized (Sakurai et al. 1997).

Since 1970's, relationships between subjective preference and physical factors in a sound field have been investigated by psychological experiments as average characteristics among a number of persons. The paired-comparison method is selected for this purpose. Previous investigations for subjective evaluations in sound fields are described in Section 1.2. In this chapter, subjective differences and intra-individual changes of subjective preference in a sound field are described. Intra-individual change is defined the changes in relation to subjective responses for each person; for example, changes in a day (daytime and night), for seasons, or for ages. As a typical example, a person's hearing level may be affected by aging. In this study, intra-individual changes for changes of preference among test series in psychological experiments. Among the orthogonal factors, the individual differences and intra-individual changes of subjective preference for listening level (LL) and subsequent reverberation time T_{sub} are investigated.

In sound field simulation rooms, subjective preference tests are conducted in changing each orthogonal factor independently. A law of comparative judgments (Thurstone, 1927) is applied. The intra-individual changes are represented by the most preferred values for each factor and individual coefficient α.

4.2 Subjective Preference Tests in Laboratory

4.2.1 Listening level

This section offers an analysis of intra-individual changes in preference judgments of listening level (LL) with respect to a set of sound fields. A method based on paired-comparison tests was developed to obtain a linear scale value of preference in the probability range $0.05 < P < 0.95$ and its corresponding Z value of the normal distribution.

In this study, the individual scale value of subjective preference is formulated in terms of the most preferred conditions, using weighting coefficients of the preference evaluation scale in Eqn. (1.10). Here, normalized objective parameter x is represented as; $x = LL - [LL]_p$ (the suffix p signifying the most preferred condition).

The experimental design chosen for obtaining estimates of individual differences consists of presenting a pair of sound fields. Ando and Singh (1996) have described how the scale value of sound fields for each individual can be expressed as Eqn. (1.15).

Music motif B was used as sound source. Five sound fields with their LL from 66 dBA to 90 dBA were chosen. Subjects were required to state their preference one of two sound fields. Thirteen male students (21 $\pm$ 3 years of age) were used as subjects. They had no previous experiences in preference judgment.

The preference evaluation curves are interpolated by a non-linear fitting as expressed by Eqn. (1.10). Each individual is characterized by two values, the most preferred value $[LL]_p$ and individual coefficient α of the preference evaluation curve. The coefficient β was fixed at 3/2.

Figure 4.1 shows an example of the preference evaluation curve for subject G (series 2), and the method of estimating $[LL]_p$. The peak of this curve denotes the most preferred value of this subject, and it is 75.0 dBA for this figure. Estimations of α are evaluated by Quasi-Newton method.

Figure 4.2 shows individual differences for $[LL]_p$ for 10 test series. Clearly, the most preferred LL of each individual differs greatly. Since the degree of drop off of the preference evaluation curves is different above and below $[LL]_p$ (Figure 4.1), two values of the coefficient α, $\alpha(\leq [LL]_p)$ and $\alpha(\geq [LL]_p)$, from preference curves in every test series were obtained, as shown in Figure 4.3. Figure 4.4 indicates the relationship between the range of values of $[LL]_p$ obtained from the 10 test series and the average coefficient α. Note that the tendency that when the coefficient α is large, then the range of intra-individual changes of $[LL]_p$ is small.

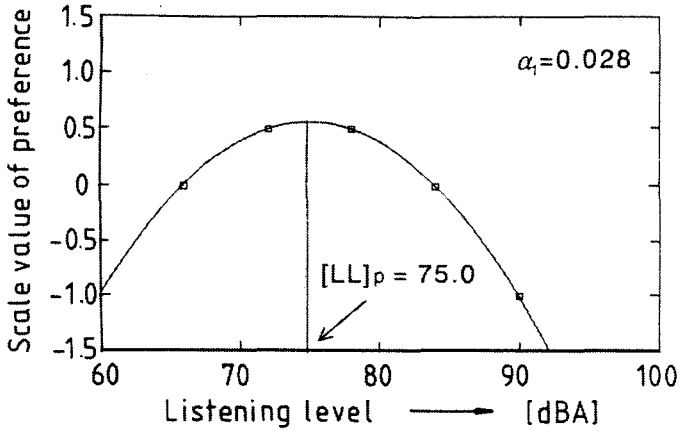

Figure 4.1 An example of the regression curve for scale values of subjective preference (subject G, series 2). $[LL]_p$ is found at 75.0 dBA.

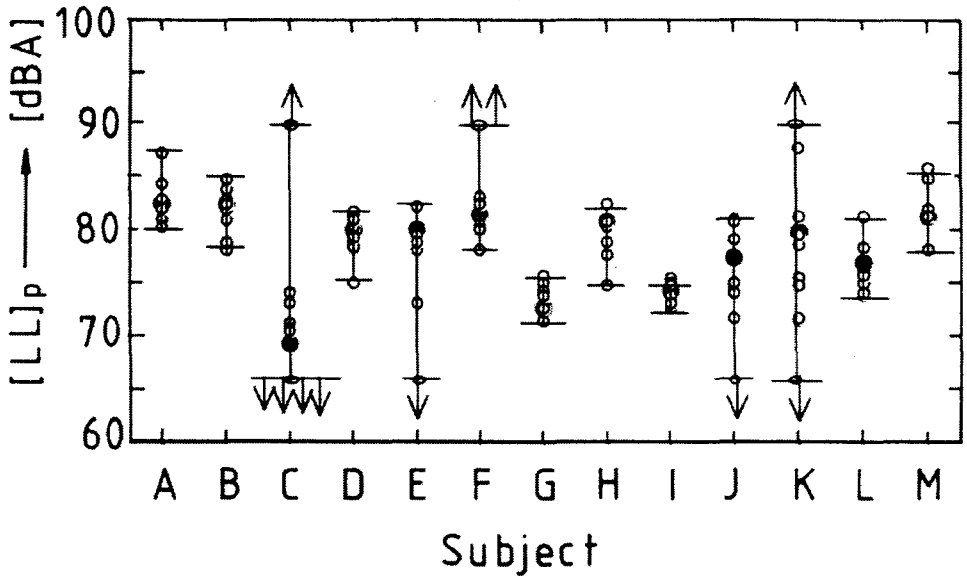

Figure 4.2 Results of intra-individual changes of $[LL]_p$ for each subject. Arrows indicate values of $[LL]_p$ that were out of the range 66 dBA to 90 dBA that was examined. ●: average value of $[LL]_p$.

As shown in Figure 4.5(a), For $[LL]_p$ for subject G, for example, 4.2 dB. This is the smallest range in all subjects and coefficient of α is greater than 0.022 in any series of this subject. On the contrary, in the case of subject K, the range of $[LL]_p$ is much greater than 19 dB and the average coefficient α is near zero, indicating no sharp preference for the listening level in the range of sound pressure levels, as shown in Figure 4.5(b).

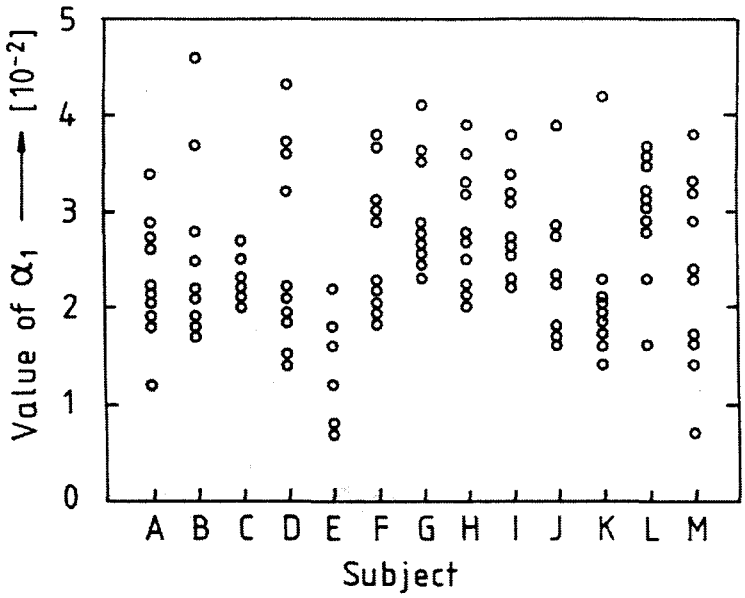

Figure 4.3 Values of weighting coefficient α_1 obtained from ten test series for each subject.

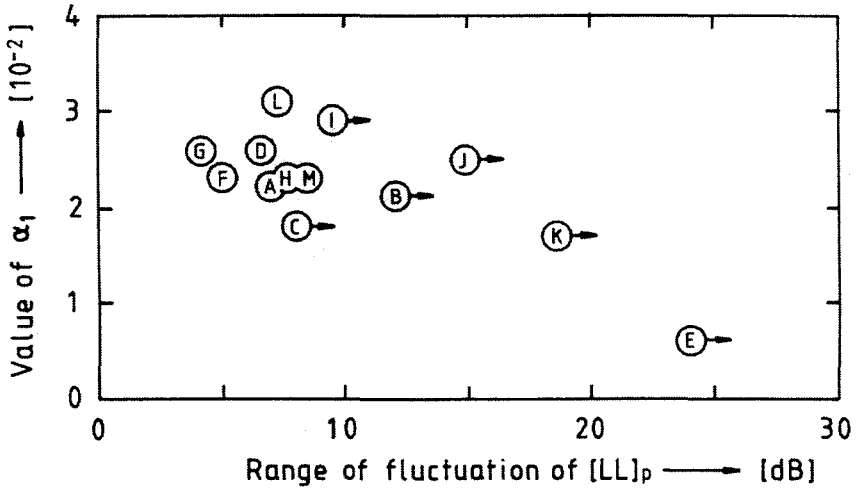

Figure 4.4 Relationship between the range of fluctuation of $[LL]_p$ and the weighting coefficient α_1.

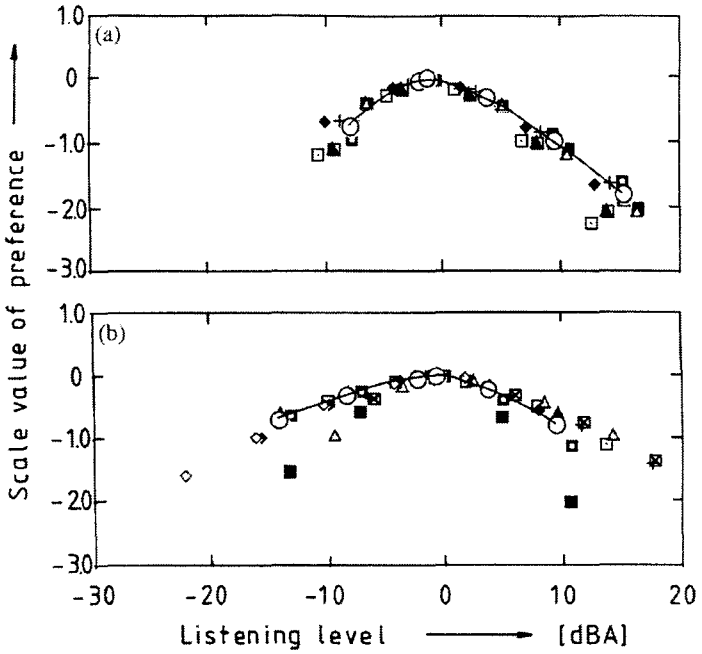

Figure 4.5 Examples of the scale values of preference obtained from ten test series. Different symbols correspond from the ten test series. (a) Subject G with a large value of α_1 (= 2.6 × 10^{-2}) and (b): subject K with a small value of al (= 1.7 × 10^{-2}).

4.2.2 Subsequent reverberation time

Using vocal music, which is one of the main components of performances in opera houses, this study evaluates listener's individual differences and intra-individual changes in subjective preference to various simulated sound fields. Subjective preference tests were conducted by changing subsequent reverberation time, T_{sub}. The sound source used was an initial 6.0-s piece of a solo performance of a soprano singer ("O mio babbino caro" from "Gianni Schicchi" composed by G. Puccini) recorded in an anechoic chamber. Values of τ_e of a short-time moving ACF or running ACF ($2T$ = 2.0 s with the interval of 100 ms) for the initial 6.0-s part of the source reproduced in the listening semi-anechoic chamber, were calculated. The waveform and values of running τ_e are indicated in Figures 4.7(a) and (b), respectively. The short-time moving ACF was calculated in order to obtain the minimum of its running τ_e, which represents the most rapid movement of music, activating the left cerebral hemisphere (Ando et al., 1989). The most preferred T_{sub} averaged for a number of listeners can be calculated by using the following equation (Ando, 1998):

$$[T_{sub}]_p \approx 23(\tau_e)_{\min}, \tag{4.1}$$

where $(\tau_e)_{min}$ is the minimum value of τ_e for the source music. The calculation of global preferable subsequent reverberation time $[T_{sub}]_p$ is about 0.53 s, which is shorter than usual

music sources but longer than that of speech signals.

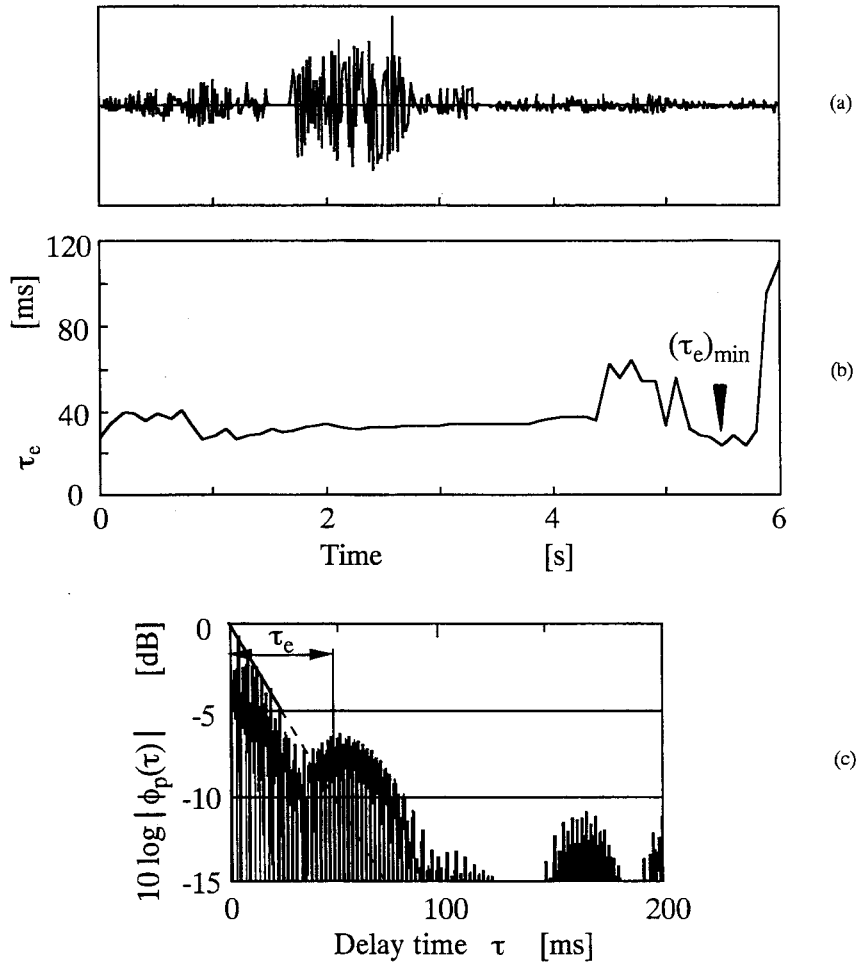

Figure 4.7 The effective duration τ_e of the running normalized autocorrelation function of the vocal source used in the tests. The integration interval, $2T$, is 2.0 s. (a): The waveform of the vocal source reproduced in the listening-semi-anechoic room; (b): The minimum value of τ_e, which is the most active part of the source containing important information and influencing subjective responses to the temporal criteria, is found to be about 23 ms; and (c): An example of determining the value of τ_e fitting 0 to -5 dB of the envelope.

Paired-comparison tests were conducted in a semi-anechoic room (Figure 4.8). Taking $[T_{sub}]_p$ to be about 0.53 s as mentioned above, subsequent reverberation time T_{sub} of the sound field was changed from 0.1 to 1.6 s (Table 4.1). The conditions of the other orthogonal parameters were fixed as indicated in Table 4.1. The Δt_1 was fixed at 14 ms near to the most preferred value $[\Delta t_1]_p \approx (1 - \log_{10}A)(\tau_e)_{min} \approx 16$ ms. The IACC is near to unity because the two loudspeakers were set in front of the subjects. The total amplitude of reflections A is kept constant at 2.0. The duration of each stimulus presented to subjects was 6.0 s. The time interval between the two stimuli in a pair was 1.0 s and between each

pair lasted 4.0 s. There are ten pairs in a series which are all the available pairs for five sound fields (N (N – 1) / 2 = 10, N = 5). A series of 20 paired-comparison tests were conducted on each subject. The number of subjects was eight (subject A–H: seven males and one female; 21–26 years old). The stimuli were produced by two loudspeakers placed in front of the subjects in the listening room. The distance between a subject and the loudspeakers was 0.8 ± 0.01 m. One speaker provides a direct sound and the first reflection, and the other provides reverberation including some initial reflections. Subjects were required to select the most preferred sound field of the two they listened to.

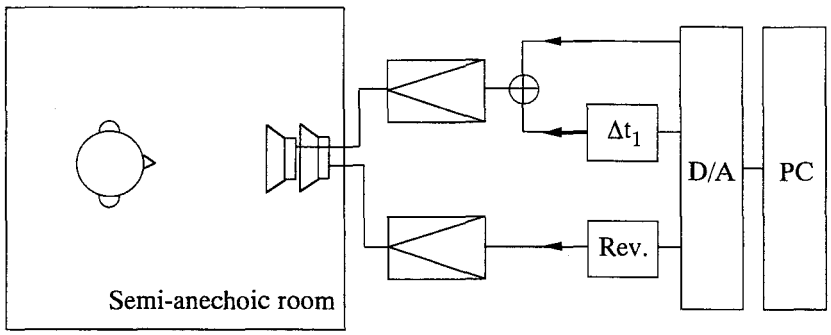

Figure 4.8 Experimental setup of subjective preference tests controlling both the initial time delay gap between the direct sound and the first reflection, Δt_1, and the subsequent reverberation time, T_{sub}.

Table 4.1 Subsequent reverberation time T_{sub} varied under fixed conditions of LL, Δt_1, IACC and the total amplitude of reflections A.

Factors varied or fixed	Value(s) of each factor				
T_{sub} [s]	0.1	0.2	0.4	0.8	1.6
LL [dBA]	75.0±0.2				
Δt_1 [ms]	14				
IACC	≈ 1.0				
A	≈ 2.0				

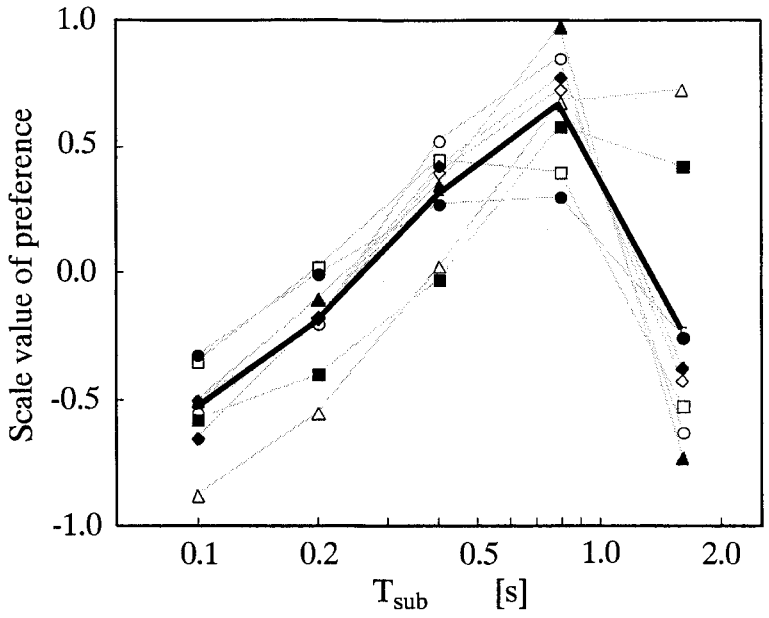

Figure 4.8 Scale values of preference for each subject as a function of T_{sub}. Different symbols indicate results from different subjects: ◇, ○, △, □, ◆, ●, ▲, and ■ for subject A through H, respectively. The bold line represents the averaged values.

The measured results of the scale values of preference as the function of the T_{sub} for each subject and its global case are indicated in Figure 4.9. In this figure, different symbols represent the results from each subject, and the bold line represents the averaged value as the global result. As the sharpness of the curves are found to be different for each side of the preference curves' peaks, two values of α for both sides of the peak are considered as α_s for $T_{sub} < [T_{sub}]_{p,m}$ and α_l for $T_{sub} > [T_{sub}]_{p,m}$ in Eqn. (4.1). The range of most preferred values of subsequent-reverberation time $[T_{sub}]_{p,m}$ obtained for all subjects in the tests was between 0.55 and 1.22 s. The largest value of α_s was 2.02 (subject B) and the smallest one was 0.97 (subject F). On the other hand, the largest value of α_l was 11.04 (subject G) and the smallest one was 1.69 (subject C). The values of α_l are always greater than those of α_s, for all subjects tested without exception. The experimental measurements of $[T_{sub}]_{p,m}$, α_s, and α_l for each subject as well as global results are listed in Table 4.3. The goodness of fit of this model for each subject, expressed using λ in Appendix representing the poorness of the model for each subject, gives zero except for 0.04 for subject B. The values of d in Appendix were also zero for all subjects except for 0.1 for subject B. These small values indicate that a consistent model is achieved for this test. Individual difference is found in $log([T_{sub}]_{p,m}/[T_{sub}]_p)$ ($p < 0.05$) and α_s ($p < 0.01$) by use of analysis of variance (ANOVA), as shown in Table 4.2. For example, subject B (α_s = 2.02 and α_l = 7.09) and subject G (α_s = 1.87 and α_l = 11.04) show a sharper preference curve than subject D (α_s = 1.38 and α_l, = 3.27) and subject F (α_s = 0.97 and α_l = 2.12). In the global results obtained in the tests,

$[T_{sub}]_{p,m}$ was 0.78 s, and values of α_s and α_l were 1.53 and 5.24, respectively. This means that for T_{sub} greater than the most preferred value, preference curves are sharper than those for T_{sub} less than the most preferred value.

The measured results of intra-individual changes of subjective preference for each subject (A-H) are indicated in Figure 4.10. In this figure, different symbols represent the results in every four series of tests performed over three or four days. Each peak value of the preference curves is shifted to the origin without losing any information, because a scale value is a relative and a linear scale. For example, curves of subjects B and G are almost the same, but those of subjects D and F are greatly changed over five sets of tests. There are only two curves of both subjects C and H, because the other three sets could not be obtained. The measured results of $log([T_{sub}]_{p,m}/[T_{sub}]_p)$, α_s, and α_l for each set are indicated in Figure 4.11. Subjects with large α values, like subjects B and G, have small intra-individual changes with respect to values of $log([T_{sub}]_{p,m}/[T_{sub}]_p)$. Standard deviations of these factors obtained from each set of tests are listed in Table 4.5. The values of subjects C and H, with only two sets, are not listed. Subject B (0.033) and subject G (0.035) have the two smallest standard deviations of all subjects, and subject D (0.163) and subject F (0.168) have larger standard deviations. In relation to those of α_s and α_l, subject B (α_s: 0.16; α_l: 1.84) and subject G (α_s: 0.26; α_l: 1.68) have smaller standard deviations as well as the values of $log([T_{sub}]_{p,m}/[T_{sub}]_p)$. On the other hand, subject D (α_s: 0.61; α_l: 3.21) and subject F (α_s: 0.55; α_l: 3.67) have larger standard deviations.

Table 4.2 Values of $[T_{sub}]_{p,m}$, α_s (for $T_{sub} < [T_{sub}]_{p,m}$) and α_l (for $T_{sub} > [T_{sub}]_{p,m}$) obtained for global and each subject.

		Subject							
	Global	A	B	C	D	E	F	G	H
$[T_{sub}]_{p,m}$ [s]	0.78	0.81	0.69	1.22	0.55	0.74	0.59	0.81	1.07
α_s	1.53	1.53	2.02	1.61	1.38	1.86	0.97	1.87	1.40
α_l	5.24	7.65	7.09	1.69	3.27	6.19	2.12	11.04	4.08

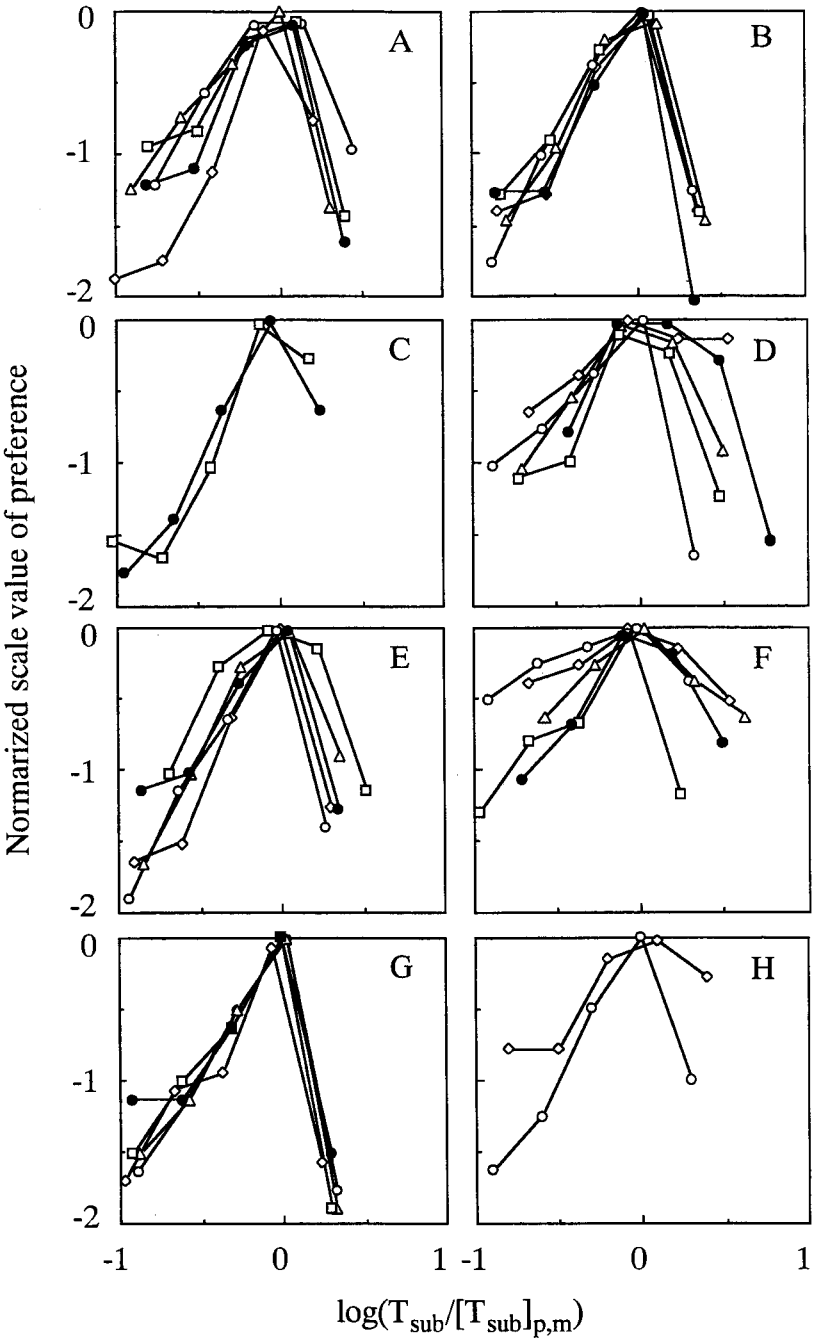

Figure 4.9 Individual scale values of preference obtained from every four series of each subject as a function of the normalized subsequent reverberation time. The peaks of the curves are shifted to the origin without any loss of information. Different symbols indicate values of a different series of tests: ◇, ○, △, □, and ●.

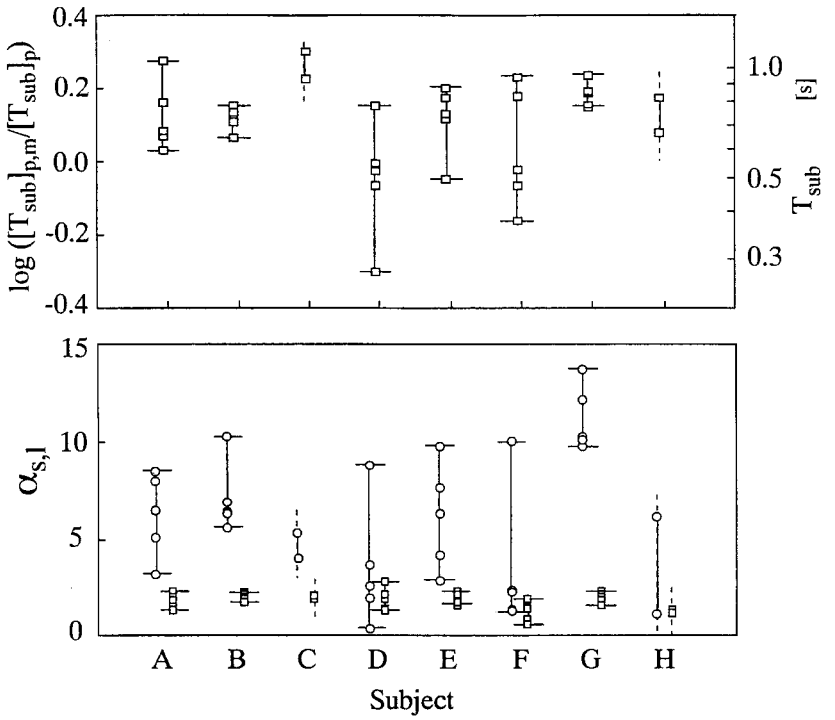

Figure 4.10 Intra-individual changes of $log([T_{sub}]_{p,m}/[T_{sub}]_p)$ (a); α_s (□) and α_l (○) for each subject (b). Broken lines show that preferred values are out of the range between 0.1 s and 1.6 s.

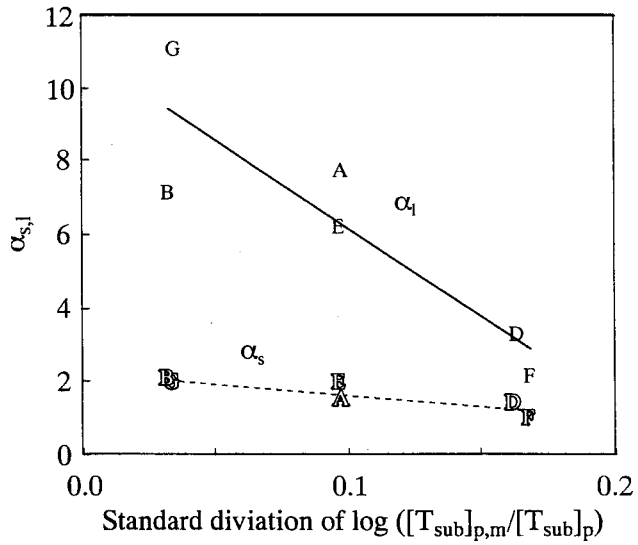

Figure 4.11 Relationship between α_s and α_l, and standard deviation of preferred reverberation time on a logarithmic scale, $log([T_{sub}]_{p,m}/[T_{sub}]_p)$, for each subject (except for subjects C and H). Solid line represents α_l (subjects A to H with R^2 = 0.76) and dotted line represents α_s (subjects A to H with R2 = 0.70).

Values of both α_s and α_l of subjects B and G were greater than those of the other subjects and have almost the constant values, and these values of subjects D and F are significantly different in each set. The results of $\log([T_{sub}]_{p,m}/[T_{sub}]_p)$, the values of α_s, and α_l in every four series for each subject are indicated in Figure 4.10. On both sides of the peaks, for subjects who have larger α, such as subjects B and G, the standard deviations of $log([T_{sub}]_{p,m}/[T_{sub}]_p)$ for each set are small. On the other hand, for subjects who have smaller α, such as subjects D and F, the preferable T_{sub} values are larger: 0.163 and 0.168, respectively.

Relationship between the standard deviations of $log([T_{sub}]_{p,m}/[T_{sub}]_p)$, α_s and α_l values for each subject (except subjects C and H) are plotted in Figure 4.11. Subjects with large α values, such as subject B or subject G, have smaller intra-individual changes, so that the standard deviations of preferable T_{sub} is small. On the other hand, subjects with small α values such as subjects D and F show minor preferences as T_{sub} changed. This result is similar to that of previous results for LL.

The value of $[T_{sub}]_p$ calculated by using Eqn. (4.1) with $(\tau_e)_{min}$ (= 23 ms) is 0.53 s. For the global subjects, the value of $[T_{sub}]_{p,m}$ obtained by the tests was 0.78 s, longer than the calculated value.

4.3 Conclusion of Chapter IV

The investigation in relation to LL shows that subjects with a large value of α have small intra-individual changes, so that the range of $[LL]_p$ was small. On the other hand, subjects with small α value have minor preference as the parameter changed.

The investigation in relation to T_{sub} shows that subjects with large α values indicate smaller intra-individual changes, so the standard deviation of $log([T_{sub}]_{p,m}/[T_{sub}]_p)$ is small as well as the investigation for LL. On the other hand, subjects with small α values without sharp curves show minor preference as T_{sub} changed. The averaged value of preferred T_{sub} for vocal sources was 0.78 s, which is greater than the value (0.53 s) calculated by Eqn. (4.1). Individual differences are observed in values of $log([T_{sub}]_{p,m}/[T_{sub}]_p)$ and α_s but not in values of α_l.

CHAPTER V. APPLICATIONS

5.1 Introduction of Chapter V

As applications for the investigations described as acoustical measurements and individual subjective evaluations, a concert hall with a number of columns and acoustical measurements for environmental noise are described. The concert hall is an application for the effect of multiple scattering from trees or bamboos described in Chapter 2. Also, acoustical measurement system for environmental noise based on the model of auditory-brain system is introduced.

5.2 Concert Hall with a Number of Columns

Through acoustical measurements in general forest and bamboo forest, it is clarified that the outdoor space with trees or bamboos is specific sound fields as performance space of music. Especially, they are effective for the factors T_{sub} and IACC. As an applications of this, a concert hall with a number of columns (Tsuyama Music Cultural Hall "Bell Folet Tsuyama") is introduced.

Suzumura et al. (2000) designed a number of columns in front of the walls in the hall to act as the scattering obstacles, and investigated the effects of the columns to evaluate of sound field that involve scattered reflections (see also ref. Ando et al., 1999b). For this purpose, MLS measurements were performed by use of a 1/10-scale model of the hall. The acoustic properties of the hall were measured both with and without the columns. Scattered sound fields are evaluated by the four physical factors (LL, Δt_1, T_{sub}, IACC) and additional factors τ_{IACC} and W_{IACC}. It is found that the Δt_1 and IACC of sound field in the hall are improved by use of the circular column array. The IACC at central seats near the stage and seating area near the columns were improved by the arrays of columns. It was impossible to use acoustical simulation system on a personal computer for the evaluation of sound field with columns, because it has too much calculation for the multiple reflections between columns. As a result, it was clarified that columns array on the stage and in the seat area improve IACC in frontal seat area along the lateral walls and lateral seat area, respectively.

Thus, the effects for the improvement of the sound field in a concert hall are

clarified by introducing the multiple scattering effects.

Considering some historical theaters and the ancient theater, columns or statues are distributed along them. Of course, they were originally built in terms of the purpose of decorations. However, such columns or statues are also considered to play also a role for the multiple scattering effect acoustically as well as visual effects. Their unknown effects can be materials of future works.

5.3 Measurement for Environmental Noise Field

A system for measurement, identification and evaluation of environmental noise are proposed as shown in Figure 5.1. It (1) measures the environmental noise and analyzes its physical factors, (2) identifies the noise source using the extracted physical factors, and (3) it evaluates subjectively. The key feature of the system is that the physical factors to be evaluated are extracted from the autocorrelation functions (ACF) and interaural crosscorrelation function (IACF) for signals arriving at a person's ears in accordance with the model of human auditory-brain system (Ando 1998) as shown in Figure 1.3. This auditory-brain model has been studied in the field of subjective evaluations of sound fields as concert hall acoustics. Thus, the receiver is actually a dummy head with binaural microphones as ears so as to reflect human psychology. The difference between previous procedure and the present method is to conduct binaural measurements considering actual human listening condition, and to evaluate environmental noises not in the frequency domain but in the time domain. Environmental noise is usually evaluated statistically as a sound pressure level (SPL) and its frequency characteristic by using a sound-level meter. Significant physical factors in a noise field are extracted from the ACF and the IACF of binaural signals every moment as temporal and spatial factors, which can be obtained by the procedure in Subsection 1.2.2 (Ando, 2001; in print). Identification and subjective evaluation are evaluated by use of these factors.

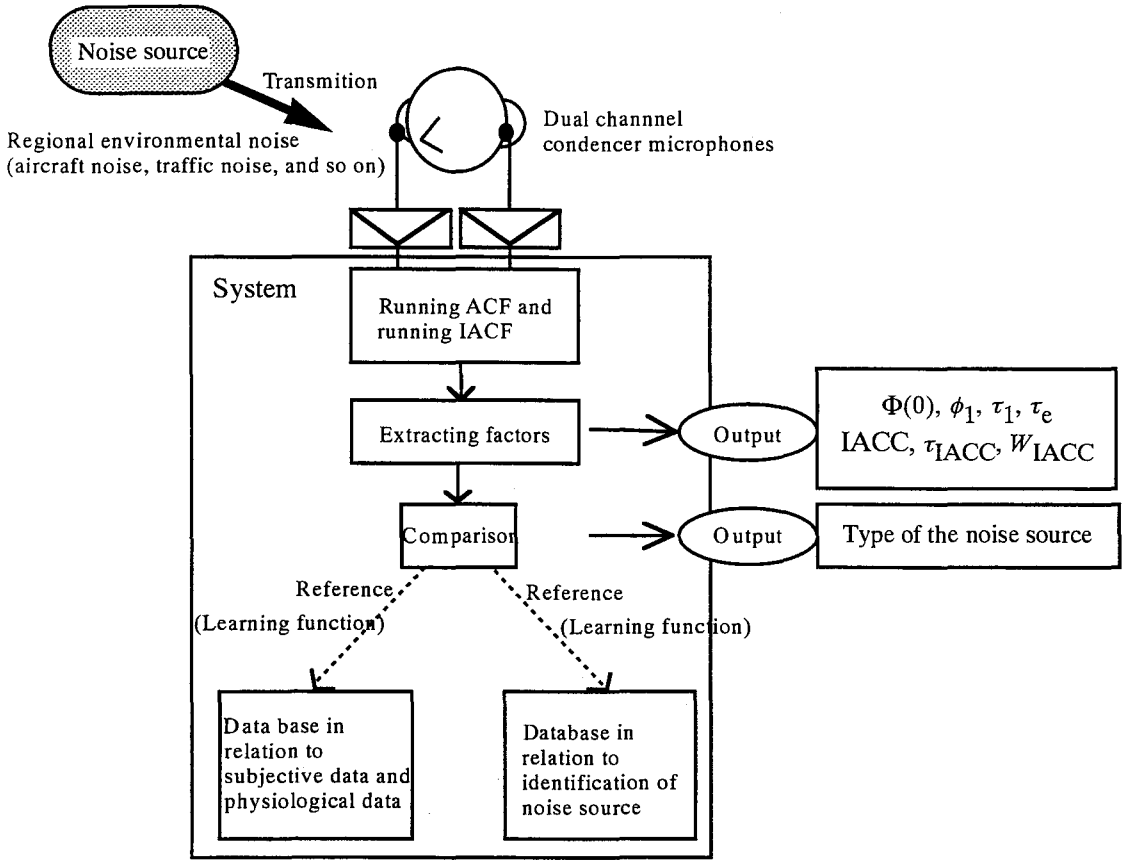

Figure 5.1 New system for measurement, identification and evaluation of regional environmental noise

The measurement system consists of binaural microphones and a laptop PC which analyzes correlation functions (Sakurai et al., 2000). Physical factors are extracted as fine structures of running ACF and running IACF of binaural noise signals in every constant interval (integration interval) in accordance with the auditory-brain model. Thus, monaural-temporal factors in relation to subjective evaluations are extracted as monaural temporal factors from ACF and binaural-spatial factors from IACF. From ACF, (1) energy, which is corresponding to the sound pressure level $\Phi(0)$, (2) effective duration τ_e, (3) amplitude of the first reflection ϕ_1, (4) its delay time τ_1, are extracted at each ear. From IACF, (5) IACC, (6) interaural time delay τ_{IACC}, (7) width of the maximum peak W_{IACC}, are extracted as well as (8) averaged energy for both ears as LL.

In September 1999, measurements of aircraft noise using the present system were conducted near an airport. Also, measurements of aircraft noise were conducted in Japan (Fujii et al., 2001; in print). By use of the factors obtained, characterizations of each noise source were conducted. Characterizations are conducted for each source of aircraft noise,

traffic noise, and railway noise. In this process, integration interval for the calculation become shorter value comparing to that of music, say 0.2-0.5 s for aircraft noise. This value is accordance with the time window of auditory psychology. Recommended interval has been found to be $(2T)_r \approx 30(\tau_e)_{min}$ (Mouri et al. 2001; in print).

Noise measurements were conducted in a residential area near the airport 'G.Marconi' in Bologna on October 5 and 6, 1999 (Figure 5.2). They were taken at two locations around the airport, marked A and B in Figure 5.2. The distances between the airstrip and the two locations were about 200 and 250 m. There is only one airstrip at the airport. At location A, some apartments or houses were situated behind the receiver. At location B, there were no buildings near the receiver, as measurement was conducted on the bank along the airport.

The target sound sources were aircraft landing and taking off. Information on the types of aircraft and their flight schedules were available for the measurement days. The sound sources were categorized in five different states: landing ("land"), taxing just after landing ("land_stop"), taking off ("takeoff"), taxing for takeoff ("takeoff_2"), and waiting for takeoff ("waiting") (Table 5.1). The category names are given in parentheses.

Noise radiated from aircraft is caused by (1) the sound of the engine (jet engine or propeller), (2) the resistance or friction between the aircraft body and the airstrip, and (3) the resistance or friction between the aircraft body and the atmosphere. Noise from fans or propellers has strong directivity in the direction of the shaft. Noise from a jet engine also has strong directivity diagonally behind the exhaust gas. The takeoff and landing speeds for each aircraft were not measured during the noise measurements. In general, the speed of a B747 is between 200 and 400 km/h, and aircraft land into the airstrip with about three-degree inclination.

The measurement system was controlled by a laptop computer (CPU speed: 366 MHz; Main memory: 143 MB) with the measurement software. Noise was recorded in the computer at a sampling frequency of 44.1 kHz. Half-inch dual-channel condenser microphones were attached to opposite sides of a sphere made of styrene foam and having a diameter of 200 mm. The sphere was uses as a dummy head during the measurements. The thickness of the styrene foam was 20 mm. The microphones were set 1.5 m above the ground, and electrical power was supplied by the batteries of the computer. The two microphones were fixed to be parallel to the airstrip.

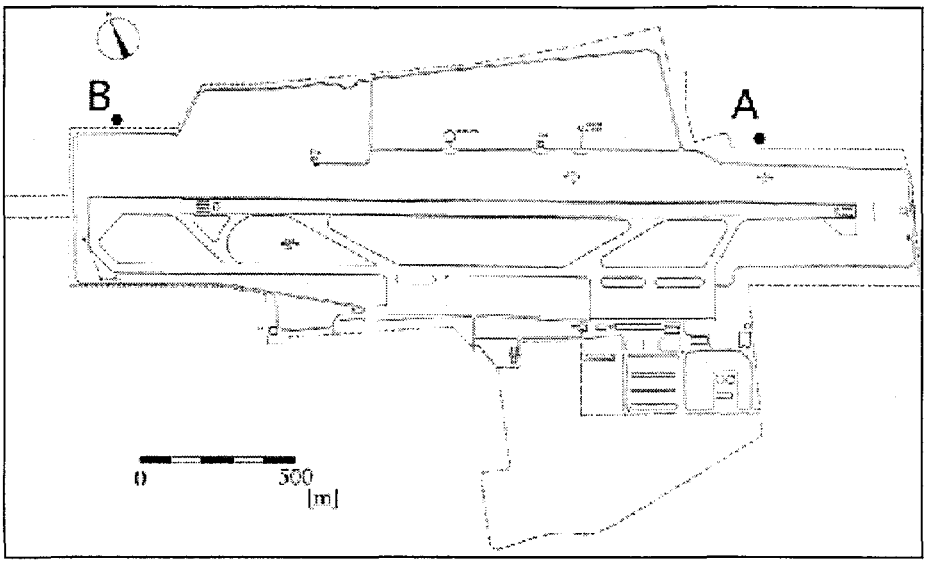

Figure 5.2 Map of the airport where the measurements were conducted. A and B represent the two locations for the measurements.

Table 5.1 Measurement data categories and number of sessions.

	Location A	Location B
Landing	2	12
Land_stop	0	5
Takeoff	7	14
Takeoff_2	1	2
Waiting	2	3
Total	12	36

Temperature, wind speed, and wind direction data were also available from the control tower were available for the measurement days. The average temperature was 13.8 degrees for both days. The average wind speed was 5.0 m from the north-northwest on the first day, and 4.2 m from the west-northwest on the second day.

Physical factors in noise fields, described in the following subsections, were obtained as fine structures of ACF and IACF for dual channel signals after passing through the A-weighting network, which approximates human ear sensitivity. As environmental noise varies continuously, these functions are calculated in at every certain interval (integration

intervals). The starting time of each integration interval is delayed for a short time (say, every 100 ms). The time is called the running step. In the case of sound source for music, the length of the integration interval may be decided within psychological present with its duration between 2 and 5 s, which a person feels the duration of time of what is considered to be "now" (Freisse, 1982). However, it is probably better to use a shorter integration interval, say 0.5 s, for aircraft noise. The measurement time for one session was 10.0 s with the mid point of this duration at the center of the maximum $\Phi(0)$, which is one of the ACF factors.

As an example, the results of all eight physical factors obtained from ACF and IACF are shown in Figure 5.3 (14 sessions). Each factor can be represented as a temporal function. As described above, values for each factor were obtained every 100 ms with an integration interval of 0.5 s.

As the measurements were conducted at two different locations, the results were divided between locations because of the following reasons. First, the distances between the airstrip and the receivers at the each location were different. As a result, for example, average values of $\Phi(0)$ at both locations greatly differed because of attenuation. Second, as shown in Figures 5.4(a) and (b), strong reflections from the surface of the buildings around location A reduced the IACC values, while location B had no reflective surface around the receiver. Third, the measurement results of the factors were closely related to the directivities of noise sources. The direction of takeoffs was not constant during the measurements, although all landing aircraft moved in a constant direction (from west to east in Figure 5.2). In practice, the direction of landings or takeoffs depends on atmospherical conditions according to indications from the control tower. Because of the direction of movement, the physical characteristics of noise radiating from specific parts of aircraft vary greatly. For example, for an aircraft landing from the west, the noise around the moment when the aircraft touches the ground gives the $\Phi(0)$ peak at location B, although this peak does not appear at location A until the aircraft is running on the airstrip after landing. Considering this fact, the landing condition at location A can be regarded as having characteristics similar to those of "land_stop". These are the reasons for dividing the measurement results according to the location.

Average values for the factors $\Phi(0)$, τ_e, τ_1, ϕ_1, and IACC are shown in Figure 5.5. The upper four categories indicate the results for location A, and the lower ones for location B. The open circles indicate the average values over 10 s for each session. The closed circles indicate the average values for all sessions for each category.

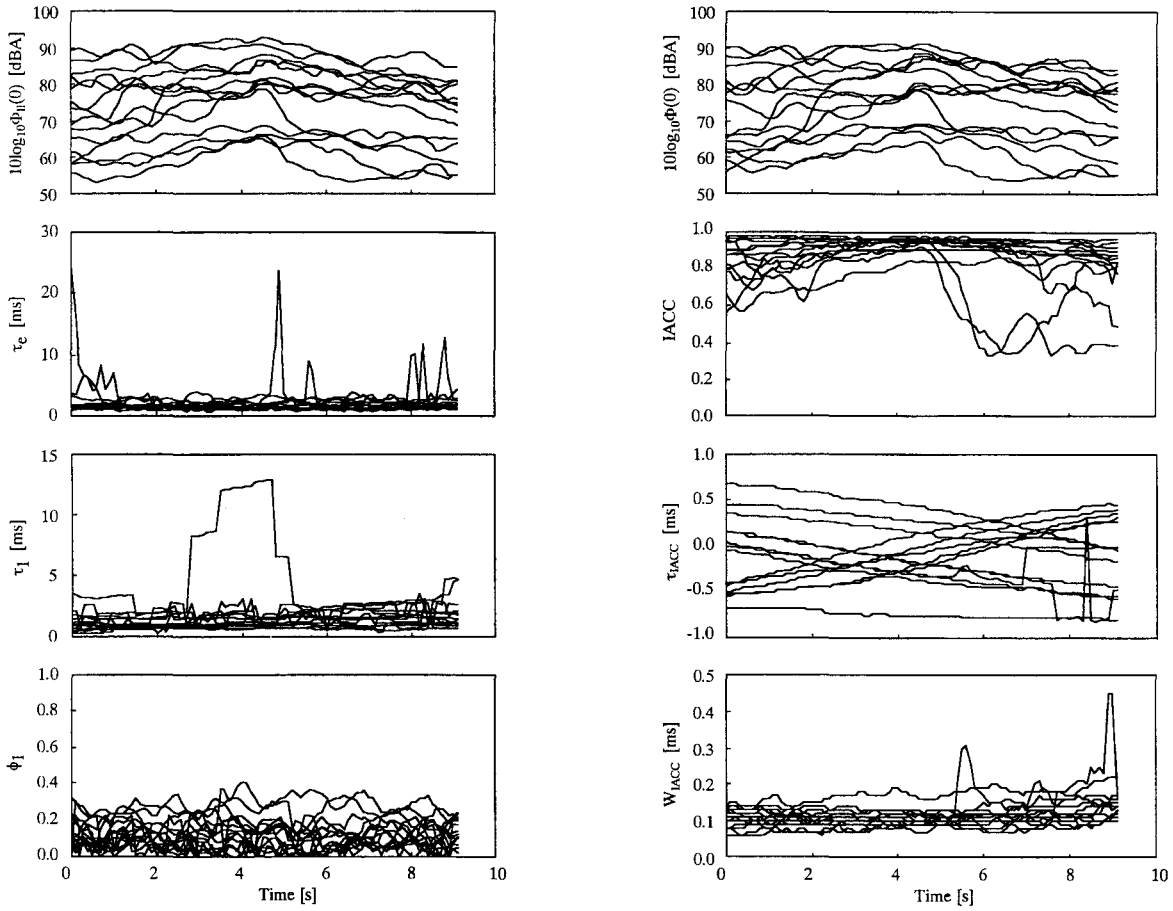

Figure 5.3 Examples of measurement results for all physical factors extracted from the autocorrelation function (ACF) and interaural crosscorrelation function (IACF).

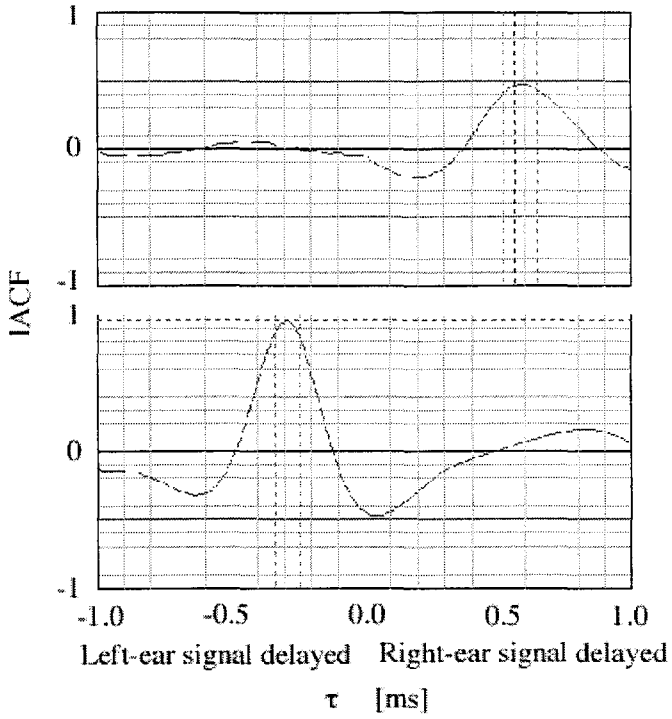

Figure 5.4 Examples for IACF. (a) IACF with IACC reduced by reflective surface of the buildings at location A (landing); (b) IACF with larger IACC at location B (landing).

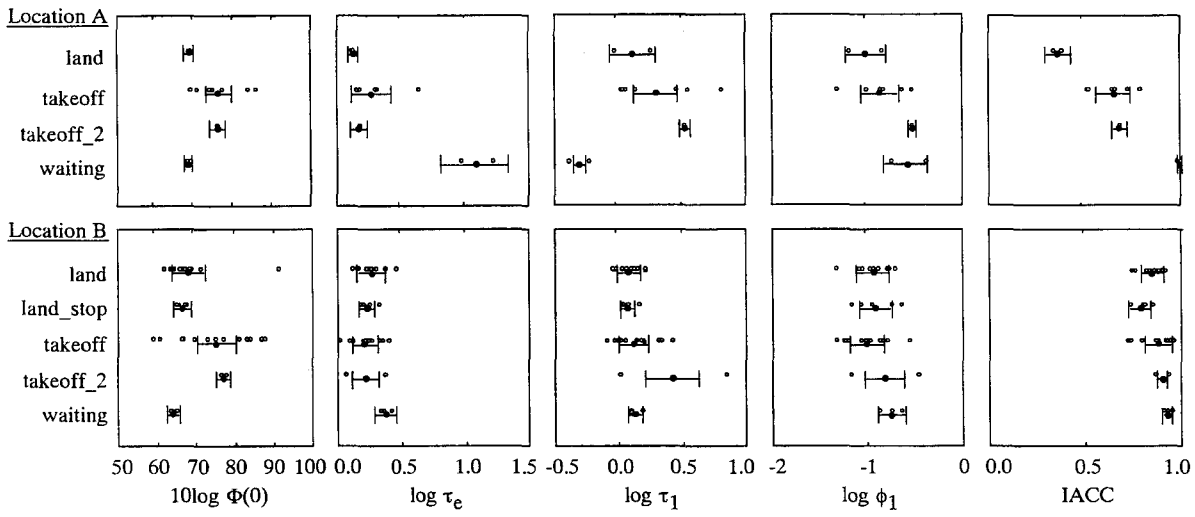

Figure 5.5 Average values for factors $\Phi(0)$, τ_e, τ_1, ϕ_1, and IACC. Upper four categories for each figure indicate results for the location A and lower five categories for location B. Open circles indicate the average values over 10 s for each session and closed circles indicate average values for all sessions for each category. Error bars represent the standard deviation from running data in all sessions.

As shown in Figure 5.6(a) and (b), the $\Phi(0)$ values for landing were distributed over a smaller range (standard deviation = 4.90 in dBA at location B when the one exception with the largest $\Phi(0)$ is eliminated) than those for takeoff (SD = 10.3 at location B).

As shown in Figure 5.6(c), for "land_stop" at location B, the factor $\Phi(0)$ rapidly increased before its peak, although the variation in $\Phi(0)$ was smaller after the peak. For just after landing at location B, values of $\Phi(0)$ remained near the $\Phi(0)$ peak because of the strong directionality of the noise of the jet engine.

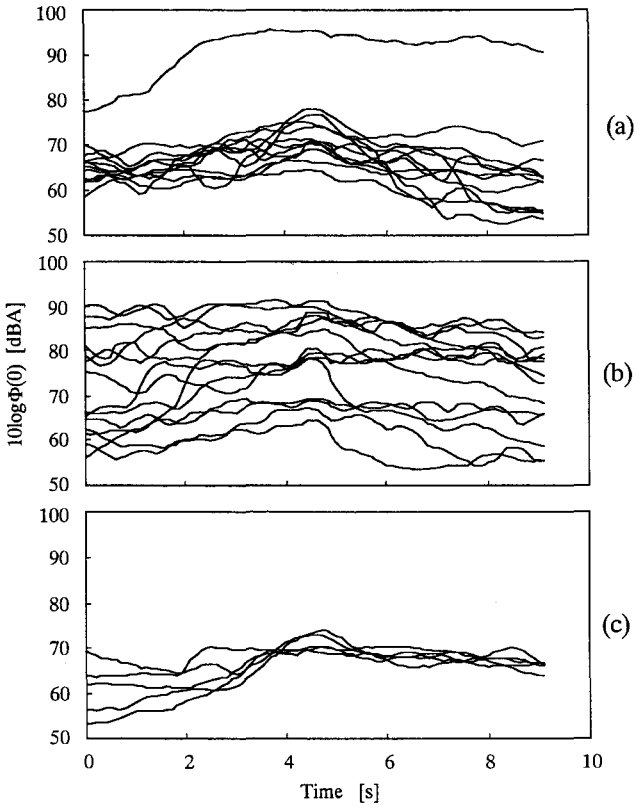

Figure 5.6 Measurement data of $\Phi(0)$. (a) Data from landing at location B (12 sessions); (b) data from takeoff at location B (14 sessions); (c) data from "land_stop" at location B (4 sessions).

For both locations, in some cases, the τ_e values temporarily became larger near the $\Phi(0)$ peak, especially in the case of takeoff (τ_e = 88.7 ms), as shown in Figure 5.7.

The τ_1 values were distributed between 1 and 2 ms for most sessions, indicating the dominance of the noise component for such cases. When the tonal components from an aircraft increased, the τ_1 value became larger, as shown in the example of the ACF waveform in Figure 5.8(a). The ϕ_1 values were usually distributed below 0.2, and increased to be above 0.5 in some cases. In such cases, the tonal components, including the noise, increased. Thus, the pitch became stronger at the dominant pitch corresponding to its τ_1 value. An example of the ACF waveform is shown in Figure 5.8(b). The corresponding τ_e values in the same category are shown in Figure 5.8(c). In only one case, the τ_e value increased according to the increase of the ϕ_1 value, although each physical factor was orthogonal. But considering that almost all τ_e values were distributed near 1 ms, the noise components of aircraft were dominant compared to the tonal components.

The IACC values at location A were smaller than those at location B. The average value of IACC for landing at location A was 0.34, while it was 0.85 at location B. The average values for takeoff were respectively 0.66 and 0.88. Relatively strong reflections from the surface of the building wall caused the lower IACC at location A.

The values for τ_{IACC}, which is the factor that gives the directional information of the source, clearly represent the directions of aircraft in landing or takeoff as shown in the example in Figure 5.9. When the τ_{IACC} is zero, the target source should be located in front of the receiver. If the distance between the airstrip and the receiver is already known, information on the source speed may be obtained from the τ_{IACC} activity.

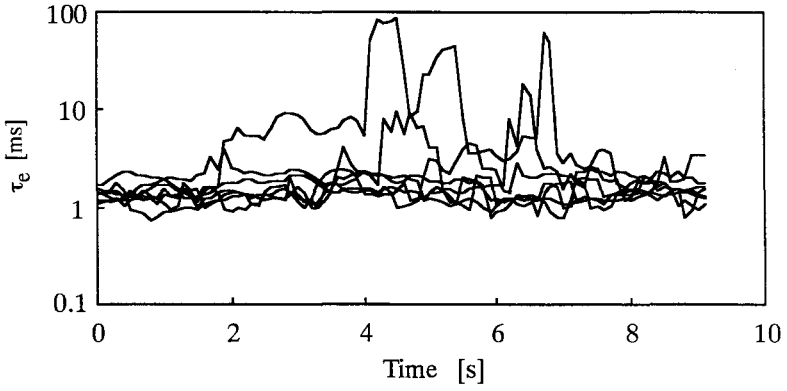

Figure 5.7 Measurement data of τ_e from takeoff data at location A (τ_e = 88.7 ms).

The variety of $\Phi(0)$ values for "land_stop" at location B is larger before the $\Phi(0)$ peak than after the peak. The corresponding τ_1 did not indicate the perceived pitch in this case, although lower frequency components from the jet engine increased in actual listening condition during the measurement. This fact indicates that the first ACF peak does not always correspond to the dominant pitch for such a complicated ACF waveform as aircraft noise. There are some cases in which clear ACF peaks with regular time intervals appear after the first ACF peak, as shown in Figure 5.8(c). Psychological experiments on pitch perception with different τ_1 and ϕ_1 values must be conducted in order to determine the dominant pitch.

Noise from fans, propellers, or jet engines has strong directivities, as already described. The τ_{IACC} values vary greatly in both landing and takeoff according to the motion of the source. In waiting for takeoff, the τ_{IACC} value should be almost constant. Thus, the directional information of landing and takeoff by use of the τ_{IACC} factor can be obtained to characterize the noise source, including the directivity of noise from the specific parts of aircraft.

These four ACF factors have been used to describe the speech intelligibility of Japanese single syllables by using a multi dimensional analysis (Ando et al., 1999). For sound fields which consist of the direct sound and a single reflection, the speech intelligibility can be well described in terms of the distance between the template source signal and a sound field signal by using ACF factors. If the method is applicable to regional environmental noises, the identification of a noise source may be achieved.

Thus, binaural measurements of aircraft noise in landing and takeoff conditions were conducted based on a model of the human auditory-brain system. The physical factors extracted from running ACF and IACF analyses of the noise sources well characterize the landing and takeoff activities of aircraft. Especially, the binaural effects, including IACC and τ_{IACC}, are effective for the characterization of noise sources. These results will become the basis for subjective evaluations including annoyance and spatial perception as well as primary sensations (loudness, pitch, and timbre), and identification of aircraft noises or other kinds of noise.

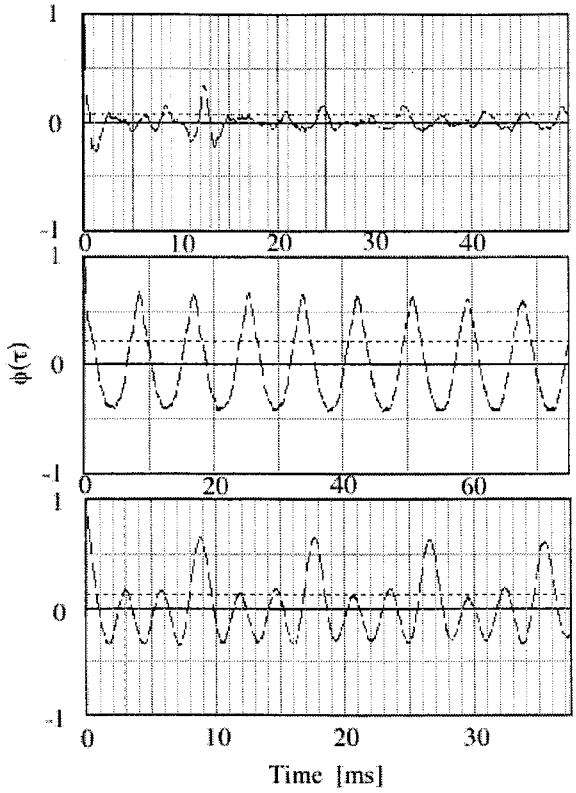

Figure 5.8 Examples for ACF. (a) ACF waveform with longer τ_1 value; (b) ACF waveform with longer ϕ_1 value; (c) τ_e values corresponding to longer ϕ_1 value.

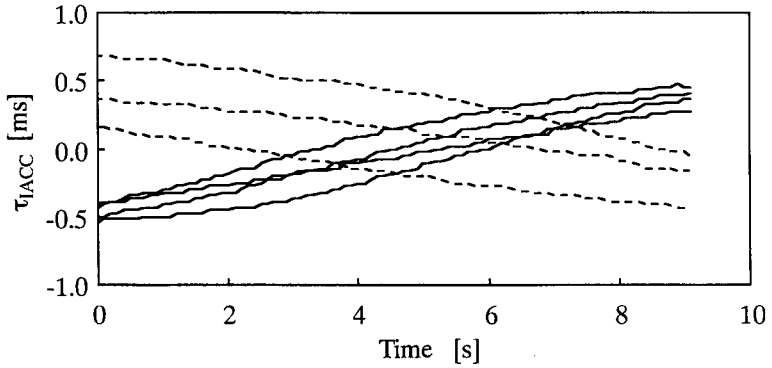

Figure 5.9 Examples for τ_{IACC}. The values of τ_{IACC} clearly represent the directions of aircraft in landing or takeoff.

CHAPTER VI. SUMMARY AND COUNCLUSIONS

6.1 Summary and Conclusions

In Chapter 2 in relating to acoustical measurements in a sound field of historical opera houses, it was made clear followings. Acoustical measurements were conducted for sound fields for (1) a singer on the stage, (2) musicians in the orchestra pit, (3) a conductor, and listeners in the box in terms of the temporal and spatial factors in relation to subjective preference. Through the measurements in these opera houses, sound fields under these conditions can be characterized. Especially, impulse responses, which the first reflection do not have maximum amplitude, are obtained at many receivers. These results suggest the necessity of the further psychological experiments in a laboratory regarding to the complicated initial reflections. Considering actual opera performances, as there are stage sets and some singers on the stage, more complicated sound fields may be constructed. Accumulation of such a measurement data in relation to sound fields on the stage and in the orchestra pit inside a historical opera houses, physical characteristics of their sound fields will be known, and they will give valuable and useful information in designing a stage and an orchestra pit inside opera houses.

In the outdoor sound field in an ordinary forest and a bamboo forest, it is found that the forest has excellent acoustic properties, especially for factors of subsequent reverberation time (T_{sub}) and IACC. The effective frequency range for these factors was found to be related to the diameter of the trunks of a tree or a bamboo.

Also it is clarified that the acoustical measurement procedures for a concert hall

can be applied for a sound fields in an opera house and outdoor sound fields in forests. Some specific sound fields, which are different from that in a concert hall, are obtained for both sound fields. Especially complicated initial reflections are obtained such sound fields.

In Chapter 3, to confirm the subjective preference theory for an opera house, the relationship between the scale values of subjective preference and the orthogonal physical factors was examined by factor analysis. The scale values of preference for different source locations on the stage and in the orchestra pit in an opera house were obtained using a paired comparison method. The results showed that the scores obtained by factors analysis is similar to that of the concert hall investigated. The scale values of preference are well predicted using the total score obtained by factor analysis.

In Chapter 4 in relating to subjective preference judgments in a sound field simulation room, it was made clear followings. The investigation in relation to LL shows that subjects with a large value of coefficient α have small intra-individual changes, so that the range of $[\mathrm{LL}]_p$ was small. On the other hand, subjects with small α value have minor preference as the parameter changed. The investigation in relation to T_{sub} shows that subjects with large α values indicate smaller intra-individual changes, so the standard deviation of $\log([T_{sub}]_{p,m}/[T_{sub}]_p)$ is small as well as the investigation for LL. On the other hand, subjects with small α values without sharp curves show minor preference as T_{sub} changed. The averaged value of preferred T_{sub} for vocal sources was 0.78 s, which is greater than the value (0.53 s) calculated by Eqn. (3.1). Individual differences are observed in values of $\log([T_{sub}]_{p,m}/[T_{sub}]_p)$ and α_s but not in values of α_l.

In Chapter 5, as an application, a concert hall with a number of columns and acoustical measurements for environmental noises are described. The concert hall is an application for the effect of multiple scattering from trees or bamboos described in Chapeter 2. Also, acoustical measurement system for environmental noises is based on the model of auditory-brain system.

6.2 Further Problems

Through the measurements in these opera houses, especially, impulse responses, which the first reflection do not have maximum amplitude, are obtained at many receivers. These results suggest the necessity of the psychological experiments in a laboratory regarding to the complicated initial reflections. Considering actual opera performances, as there are stage sets and some singers on the stage, more complicated sound fields may be constructed.

Subjective preference theory to calculate scale value cannot apply directly to the conductor's preference as same as listeners due to the short initial time delay gap. It should be clarified for conductor's preference more in detail by psychological tests, although such a test may be difficult to conduct because of multiple sources in front of the conductor in an actual condition in a theater.

Individual preference theory should be properly applied for listening conditions of listeners in concert halls, opera houses, and other sound fields including a forest. This is partially realized as a seat selection system in Kirishima International Concert Hall, Japan. Also conditions of musicians, a singer, a performer, a conductor should be improved by applying this theory.

APPENDIX A.
SIMPLE METHOD OF CALCULATING SCALE VALUE OF SUBJECTIVE PREFERENCE

The paired-comparison method usually needs a number of judgments for a single pair. However, from a single observation datum for a set of sound fields, an approximate method is described for obtaining the scale value of subjective preference. This method is applied to this study in Chapter 4. The method is based on the law of comparative judgment (Thurstone, 1927) using the linear range of cumulative normal distribution between the probability and the scale value (Z-value) as shown in Figure A.1.

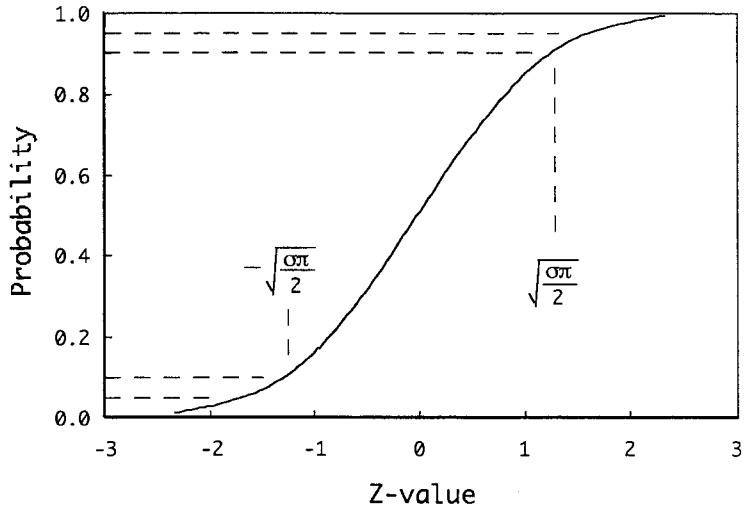

Figure A.1 Cumulative normal distribution (normal ogive) between the probability and the scale value (Z-value). σ: Standard deviation.

The probability that a sound field B is preferred to another sound field A is expressed by

$$P(B>A)=\frac{1}{\sigma_d\sqrt{2\pi}}\int_0^{\infty}\exp\left\{-\frac{\left(X_d-\langle X_d\rangle\right)^2}{2\sigma_d}\right\}dX_d$$

$$=\frac{1}{\sqrt{2\pi}}\int_{Z_{ab}}^{\infty}\exp\left(-\frac{y^2}{2}\right)dy \qquad \text{(A.1)}$$

where

$$Z_{ab}=-\frac{\langle X_d\rangle}{\sigma_d}. \qquad \text{(A.2)}$$

$\langle X_d\rangle$ is the average scale value between sound fields A and B, $X_d = X_b - X_a$, if σ_d is being used as the unit for the scale value: $\sigma_d = 1$. Thus,

$$P(B>A)=erfc\left[Z_{ab}\right] \qquad \text{(A.3)}$$

$$Z_{ab}=erfc^{-1}\left[P(B>A)\right] \qquad \text{(A.4)}$$

The first order approximation of the Taylor series of Eqn. (A.4) is given by

$$Z_{ab}=\sqrt{2\pi}\left(P(B>A)-\frac{1}{2}\right). \qquad \text{(A.5)}$$

The linear range can be obtained for $0.05 \le P(B>A) \le 0.95$.

Let us now consider a number of sound fields given by $F(i, j = 1, 2,..., F)$, and suppose a single response of each pair for simplicity. Then the probability $P(B>A)$ in Eqn. (A.5) is replaced by (Ando and Singh, 1996),

$$P(i>j)=\frac{1}{F}\sum_{i=1}^{P}Y_i \qquad \text{(A.6)}$$

where $Y_i = 1$ responds to a preference of i over j, $Y_i = Y_j = 0.5$ $(i = j)$, while $Y_i = 0$ corresponds a preference of j over i. In order to improve the precision of the probability $P(i > j)$, a certain number of sound fields within the linear range are needed to keep the

accuracy by use of Eqn. (A.6). This is performed by a preliminary investigation, avoiding an extreme sound field outside the linear range. In such a manner, the scale value $S_i = Z_{ij}$ (i = 1, 2, ..., F) may be obtained approximately, when Z_{ij} with $P(j > i)$ is obtained by Eqn. (A.5).

Next, let us consider an error in a single observation. The poorness of fit for the model is defined by

$$\lambda = \frac{\sum_{(i,j)} |S_i - S_j|_{poor}}{\sum_{(i,j)} |S_i - S_j|}, \quad 0 \le \lambda \le 1 \tag{A.7}$$

where

$$|S_i - S_j|_{poor} = S_j - S_i > 0 \quad \text{if} \quad Y_i = 0,$$
$$= 0 \quad \text{if} \quad Y_i = 1. \tag{A.8}$$

Thus, in spite of j is being preferred over i (Y_i = 0), it is possible that $S_j - S_i < 0$, and the amount $|S_i - S_j|_{poor}$ is added as in Eqn. (A.7). When i is preferred over j (Y_i = 1), it is natural that $S_i - S_j > 0$, and the amount is not added to the numerator. The value of λ corresponds to the average error of the scale value. This should be small enough, say, less than 10%.

Another observation is that, when the poorness number is K according to the condition expressed by Eqn. (A.8), then the percentage of violations d is defined by

$$d = \frac{2K}{N(N-1)} \times 100, \tag{A.9}$$

where N represents the number of sound fields. Table A.1 lists the value of λ, K, and d calculated for the preference test for LL. Values of λ or d may be used to evaluate the inconsistency of responses in a paired-comparison test. The value of K is the times of inconsistent model at preference score. The percentage violation of condition measured by d is less than 30% except subject E (60%), whose values of α are extremely low and show the wide range of preferred LL. If the value of λ is equal to zero, then the model is fitted consistently. We can consider values of K or d as the first test of goodness of fit. Value of

λ can be considered as the second test of goodness of fit of this method.

Table A.1. Results of the test of the goodness-of-fit test for the *LL*

Subject	*K*	*d*	λ
A	2	0.2	0.07
B	2	0.2	0.07
C	1	0.1	0.01
D	1	0.1	0.01
E	6	0.6	0.67
F	1	0.1	0.00
G	1	0.1	0.29
H	2	0.2	0.18
I	1	0.1	0.01
J	3	0.3	0.11
K	3	0.3	0.13
L	1	0.1	0.03
M	3	0.3	0.25

APPENDIX B.
THEORY OF INDIVIDUAL PREFERENCE

B.1 Introduction

A simple method (Ando and Singh, 1996) calculating scale value of subjective preference is developed to apply into evaluations for intra-individual changes of subjective responses. As the simple method evaluates scale values by using a single observation from a single pair, this method is quite useful to investigate intra-individual changes of subjective preference. This developed method may be applied not only to preference but also to other subjective responses. After that, scale values obtained from Case-V of Thurstone's law of comparative judgment (Thurstone, 1927) and the simple method are compared, and the difference between both method is discussed. The simple method is explained in Appendix A with its test of goodness of fit.

B.2 A Simple Method Calculating Subjective Preference

For calculating scale values of subjective preference, a simple method was used as an approximation for Case-V of Thurstone's law. This method was derived by two hypotheses as follows.

1) On the basis of Case-V of Thurstone's law of comparative judgment
2) Using linear range ($0.05 \leq P \leq 0.95$, P: probability) of normal ogive (see Figure A.1)

This method provides scale values that can be calculated from a single observation of a pair from psychological tests as shown in Table A.2. Scale value of preference S_i is obtained from a following equation;

$$S_i \approx \frac{\sqrt{2\pi}(2T_i - N)}{2N} \tag{A.10}$$

where T_i is total number of preference score for a sound field, N: number of sound field. If we put $p_i = T_i / N$, Eqn. (A.10) become

$$S_i = \sqrt{2\pi}\left(p_i - \frac{1}{2}\right) \tag{A.11}$$

where p_i is the probability of preference score for a sound field. Thus, this method converts the probability of preference score into scale value linearly.

Table A.2. Calculation of scale value of subjective preference changing *LL* (Subject G, series 1, simple method). T_i: total score of a stimulus; P_i: probability; S_i: scale value.

	Sound field					T_I	P_i	S_i
	1	2	3	4	5			
1	0.5	0	0	0	0	0.5	0.10	-1.00
2	1	0.5	0	0	1	2.5	0.50	0.00
3	1	1	0.5	0	1	3.5	0.70	0.50
4	1	1	1	0.5	1	4.5	0.90	1.00
5	1	0	0	0	0.5	1.5	0.30	-0.50

B.3 Application of a Simple Method to Intra-individual changes

As described previous section, the simple method was derived in order to calculate scale value from a single observation of a single pair. The main purpose is ordinarily to save time against psychological tests (paired-comparison tests) with a number of stimuli. However, in the case of a psychological test in changing only a single physical factor, it is rare that a subject become so tired during a test. It is so easy to evaluate scale value from a single observation, but a subject sometimes judge differently for a same pair of stimuli. Namely, such responses are due to intra-individual changes of subjective judgment. In this study, a simple method is applied not only to judgment for many sound fields but also to represent such intra-individual changes. As the simple method is an approximation of Case-V, Case-V is considered to be more useful for a test with many responses for a pair. However, as described in next section, there are some differences between scale values obtained from Case-V and the simple method. For this reason, it is better to apply the simple method for individual scale values as average from a many responses in the case, which intra-individual differences are obtained from the simple method.

Table A.3 shows the preference score obtained from subjective preference tests with 20 repetitive judgments for a single pair. Scores on the diagonal positions in the table are all 10 (= 0.5×20) as a "tie." In this case, Eqn. (A.12) is rewrote to

$$T_i = \sum_{r=1}^{R} \sum_{i=1}^{N} Y_{ij,r} \qquad \text{(A.12)}$$

where $Y_{ij,r}$ is a preference score ("+1" or "0") for a pair (i, j). R is a number of test series for a same pair. Substituting Eqn. (A.12) into Eqn. (A.10), scale value can be obtained from a number of test results.

Table A.3. Calculation of scale value of subjective preference changing *LL* (Subject G, series 1-20, simple method). T_i: total score of a stimulus; P_i: probability; S_i: scale value.

	Sound field					T_I	P_i	S_i
	1	2	3	4	5			
1	10	3	2	0	15	30.0	0.30	-0.501
2	17	10	1	0	18	46.0	0.46	-0.100
3	18	19	10	0	17	64.0	0.64	0.351
4	20	20	20	10	19	89.0	0.89	0.978
5	5	2	3	1	10	21.0	0.21	-0.727

B.4 Comparison between Case-V and a Simple Method

Scale values are calculated from a number of responses for a pair in Case-V of Thurstone's law. Also scale value can be obtained from a number of test results by the simple method as described in previous section. Thus, scale values between both methods can be compared.

Procedure to calculate scale value by Case-V is as follows:

1) Probability for each pair of stimuli are calculated as shown in Table A.4,
2) Scale value for each pair is obtained by Z conversion from probability as indicated in Table A.5, and
3) Scale value for each sound field can be obtained by averaging of scale values as indicated in the table.

A difference between the two methods is described. Scale values obtained from both methods have high correlation each other, but there is some difference for values. For the simple method, scale value is calculated as an average of all pairs for a sound field. And for Case-V, scale value is calculated as an average of scale values for each pair as shown in Table A.5. For Case-V, quite large scale value is obtained around probability, 0 or 1.

Around probability 0.5, there is little difference between them. Considering these facts, the difference between the two methods is different for a number of sound fields or individual. Namely, for Case-V, if a number of sound fields increase, possibility of pair with probability around 0 or 1 become large. In terms of each individual, the difference between two methods may be large for subjects with large α value, which have large dynamic range of scale values. In opposite, as probability is around 0.5 for subjects with small α value, the difference between them may be small.

In order to compare between scale values obtained from Case-V and those from a simple method, coefficient k is evaluated using a model: (scale value by Case-V) = k(scale value by simple method). Coefficient k is obtained by iterations of least mean square as shown in Figure A.2. Following three cases are calculated.

Case 1) Results from preference test changing T_{sub}

Results from preference test changing T_{sub} (Sound source: vocal; 8 subjects; 5 sound fields; 40 data in total), coefficient k is evaluated as: $k = 1.303$.

Case 2) Results from preference test changing Δt_1 (Sakai et al., unpublished)

Results from preference test changing Δt_1 (Sound source: music motif B; 10 subjects; 5 sound fields; 50 data in total), coefficient k is evaluated as: $k = 1.242$.

Case 3) Results from both Case 1 and Case 2

Results from preference test for Case 1 and 2 (90 data in total), coefficient k is evaluated as: $k = 1.258$.

Table A.4. Calculation of scale value of subjective preference changing *LL* (Subject G, series 1-20, Case-V). P_i: probability for a sound field i; n: number of stimuli.

	Sound field					$\Sigma P_i / n$
	1	2	3	4	5	
1	0.5	0.15	0.10	0.05	0.75	0.31
2	0.85	0.5	0.05	0.05	0.90	0.47
3	0.90	0.95	0.5	0.05	0.85	0.65
4	0.95	0.95	0.95	0.50	0.95	0.86
5	0.25	0.10	0.15	0.05	0.50	0.21

From these results, scale values obtained by using a simple method are less than those are by Case-V. Thus, scale values by Case-V is represented using coefficient k as:

$$S_{Case-V} \approx \frac{k\sqrt{2\pi}(2T_i - N)}{2N}. \tag{A.13}$$

In the present stage, k, obtained from two subjective tests above, is about 1.25. Note that an example with 11-12 sound fields in relation to a psychological test for ASW (Sato et al., 1999) shown k = 1.4. Thus, the coefficient k may be slightly changed also by the number of sound fields and individual differences.

Table A.5. Calculation of scale value of subjective preference changing *LL* (Subject G, series 1-20, case V). S_i: scale value for a sound field i; n: number of stimuli.

	Sound field					$\Sigma S_i / n$
	1	2	3	4	5	
1	0.00	-1.04	-1.28	-1.64	0.67	-0.658
2	1.04	0.00	-1.64	-1.64	1.28	-0.194
3	1.28	1.64	0.00	-1.64	1.04	0.464
4	1.64	1.64	1.64	0.00	1.64	1.316
5	-0.67	-1.28	-1.04	-1.64	0.00	-0.927

```
--------------------------------------------------
ITERATION      LOSS        PARAMETER VALUES
    0       0.1504D+02        0.100D+00
    1       0.1059D+00        0.134D+01
    2       0.9036D-01        0.130D+01
    3       0.9036D-01        0.130D+01
    4       0.9036D-01        0.130D+01

DEPENDENT VARIABLE IS     SV (VAR1)
MISSING DATA OR ESTIMATES REDUCED DEGREES OF FREEDOM

  SOURCE        SUM-OF-SQUARES    DF      MEAN-SQUARE
REGRESSION          17.538          1        17.538
RESIDUAL             0.090         39         0.002
TOTAL               17.629         40
CORRECTED           17.629         39

      RAW R-SQUARED (1-RESIDUAL/TOTAL)      =  0.995
CORRECTED R-SQUARED (1-RESIDUAL/CORRECTED) =  0.995

PARAMETER        ESTIMATE
    k              1.303
--------------------------------------------------
```

Figure A.2. An example of estimating coefficient k by least mean square method.

It must be noted that the estimated scale value obtained by this method is smaller than the result estimated by the case-V of Thurstone's law, though high correlation coefficient (r = 0.99) was found between the scale values obtained from both methods as shown in Figure A.3.

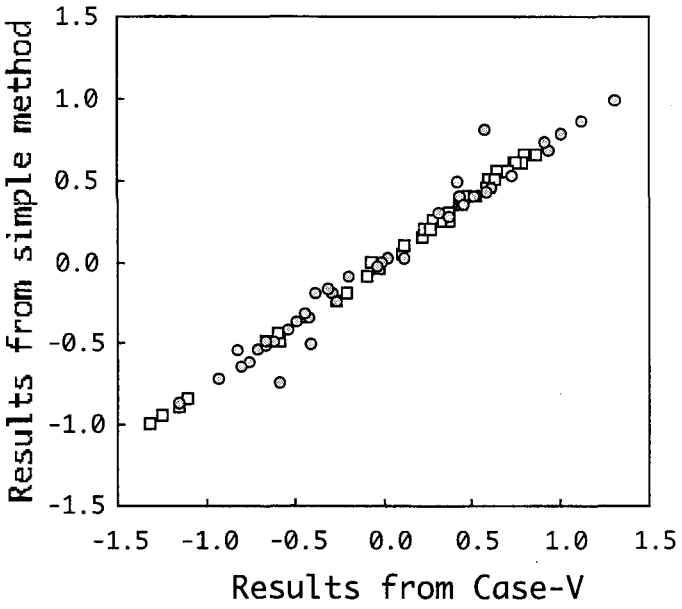

Figure A.3. Comparison of scale values between Case-V and a simple method. ●: Results from preference test changing T_{sub}; □: Results from preference test changing Δt_1 (Sakai et al., unpublished).

Thus, a simple method is developed to apply to evaluations of preference scale values for each individual and intra-individual changes of subjective responses.

Also, a difference of scale values between Case-V of Thurstone's law and a simple method is clarified. Although scale values obtained from both methods have high correlation each other, there is some difference for values. Scale values obtained from a simple method is smaller than those from Case-V are. Concerning to previous tests relating to T_{sub} and Δt_1, scale value from Case-V is approximately 1.25 times of that from a simple method.

REFERENCES

Ando, Y. and Gottlob, D. (1979). "Effects of early multiple reflections on subjective preference judgments of music sound fields," *J. Acoust. Soc. Am.* **65**(2), 524-527.

Alrutz, H. (1981). "Ein Neuer Algorithmus zur Auswertung von Messungen mit Pseudo-Rausch Signalen," *Fortschritte der Akustik DAGA 81* (Berlin), 525-528.

Ando, Y. (1983). "Calculation of subjective preference at each seat in a concert hall," *J. Acoust. Soc. Am.* **74**, 873-887.

Ando, Y. (1985). *Concert Hall Acoustics*, Springer-Verlag, New York .

Ando, Y., Okano, T., and Takezoe, Y. (1989). "The running autocorrelation function of different music signals relating to preferred temporal parameters of sound fields," *J. Acoust. Soc. Am.* **86**, 644-649.

Ando, Y. and Singh, P.K. (1996). "A simple method of calculating individual subjective responses by paired-comparison tests," *Mem. Grad. School of Sci. & Technol., Kobe University*. **14**-A, 57-66.

Ando, Y. (1998). *Architectural Acoustics -Blending Sound Sources, Sound Fields, and Listeners-*, AIP/Springer-Verlag, New York.

Ando, Y., Sakai, H., and Sato, S. (1999a). "Fundamental subjective attributes of sound fields based on the model of auditory-brain system," *In Computational Acoustics in Architecture*, WIT Press, Southampton, Ed. Sendra, J.J., Chap. 4, 63-99.

Ando, Y., Suzumura, Y., and Yamamoto, I. (1999b). "Acoustic design of Tsuyama-Music-Cultural Hall based on the preference theory," *Proc. 137th Meeting Acoust. Soc. Am., 2nd EAA, 25th DAGA* (Berlin). (see also *J. Acoust. Soc. Am.* **105**, 927).

Ando, Y. (2001). "A theory of primary sensations and spatial sensations measuring environmental noise," *J. Sound Vib.* **240**(4). (in print)

Barron, M. (1993). *Auditorium Acoustics and Architectural Design.* E & FN Spon, New York, 297-337.

Beranek, L.L. (1996). *Concert & Opera Halls -How They Sound,* Acoustical Society of America.

Blair, C.N. (1998). "Listening in the pit," *Proc. 16th International Congress on Acoustics and the 135th Meeting of the Acoustical Society of America* (Seattle), 339.

Borish, J. and Angell, J.B. (1983). "An efficient algorithm for measuring the impulse response using pseudorandom noise," *J. Audio Eng. Soc.* **31**, 478-488.

Cocchi, A., Farina, A., Garai, M., and Tronchin, L. (1997). "Computer assisted methods and acoustic quality: recent application cases," Conference Proceedings from MCHA 1995, Music & concert hall acoustics, Chapter 8, 67-84.

Cocci, A., Garai, M., and Tavernelli, C. (2000). "Boxes and sound quality in an Italian opera house," J. Sound and Vib. **232**(1) 171-191.

Davies, W.D.T. (1966). "Generation and properties of maximum-length sequences, part 1-3," *Control* **10**, 302-304, 364-365, and 431-433.

Embleton, T.F.W. (1963). "Sound propagation in homogeneous deciduous and evergreen woods," *J. Acoust. Soc. Am.* **35**, 1119-1125.

Embleton, T.F.W. (1996). "Tutorial on sound propagation outdoors," *J. Acoust. Soc. Am.* **100**, 31-48.

Eyring, C.F. (1946). "Jungle acoustics," *J. Acoust. Soc. Am.* **18**, 257-270.

Freisse, P. (1982) "Rhythm and tempo," *The Psychology of Music*, Academic Press, Orland, Fl, Chap. 6, Ed. Deutsch, D.

Fujii, K., Soeta, Y., and Ando, Y. (2001). "Acoustical properties of aircraft noise measured by temporal and

spatial factors," *J. Souond Vib.* **240**(4). (in print)

Gade, A.C. (1989a). "Investigation of musicians' room acoustic conditions in concert halls. Part I: Method and laboratory experiments," *Acustica* **69**, 193-203.

Gade, A.C. (1989b). "Investigation of musicians' room acoustic conditions in concert halls. Part II: Field experiments and synthesis of results," *Acustica* **69**, 249-262.

Glenn, W.A. and David, H.A. (1960). "Ties in paired-comparison experiments using a modified Thustone-Mosteller model," *Biometrics* **16**, 86-109

Hayashi, C. (1952). "On the prediction of phenomena from qualitative data and the quantification of qualitative data from the mathematico-statistical point of view," *Ann. Inst. Statist. Math.*, III, 69-98.

Hayashi, C. (1954). "Multidimensional quantification. I," *Proc. Japan Acad.* **30**, 61-65 and 165-169.

Hidaka, T. and Beranek, L.L. (2000). "Objective and subjective evaluations of twenty-three opera houses in Europe, Japan, and the Americas," *J. Acoust. Soc. Am.* **107**, 368-383.

Huisman, W.H.T. and Attenborough, K. (1991). "Reverberation and attenuation in a pine forest," *J. Acoust. Soc. Am.* **90**, 2664-2677.

Inoue, M., Ando, Y., and Taguti, T. (2001). "The frequency range applicable to pitch identification based upon the autocorrelation model," *J. Sound Vib.* **240**(4). (in print)

Jeon, J.Y. (2001). "Subjective evaluation of floor impact noise based on the model of ACF/ IACF," *J. Sound Vib.* **240**(4). (in print)

Katsuki, Y., Sumi, T., Uchiyama, H., and Watanabe, T. (1958). "Electric responses of auditory neurons in cat to sound stimulation," *J. Neurophysiol.* **21**, 569-588.

Kiang, N.Y.-S. (1965). *Discharge pattern of single fibers in the cat's auditory nerve*, MIT Press, Cambridge, MA.

Marshall, A.H., Gottlob, D., and Alrutz, H. (1978). "Acoustical conditions preferred for ensemble," *J. Acoust. Soc. Am.* **64**, 1437.

Marshall, A.H. and Meyer, J. (1984). "The directivity and auditory impressions of singers," *Acustica* **58**, 130-140.

Merthayasa, I Gde N. and Ando, Y. (1997). "The autocorrelation function of sound at each seat in a hall," *Music and Concert Hall Acoustics, Conference Proceedings of MCHA 1995*, Academic Press, London. Chap. 26. Eds. Ando, Y. and Noson, D.

Meyer, J. (1998). "Sound fields in orchestra pits," *Proc. 16th International Congress on Acoustics and the 135th Meeting of the Acoustical Society of America* (Seattle) 337.

Mosteller, F. (1951). "Remarks on the method of paired comparisons: III. A test of significance for paired comparisons when equal standard deviations and equal correlations are assumed," *Psychometorica* **16**, 207-218.

Mouri, K., Akiyama, K., and Ando, Y. (2001). "Preliminary study on recommended time duration of source signals to be analyzed, in relation to its effective duration of autocorrelation function," *J. Sound Vib.* **240**(4). (in print)

Nakayama, I. (1984). "Preferred time delay of a single reflection for performers," *Acustica* **54**, 217-221.

Nakayama, I. and Uehata, T. (1988). "Preferred direction of a single reflection for a performer," *Acustica* **65**, 205-208.

Noson, D., Sato, S., Sakai, H., and Ando Y. (2000). "Singer responses to sound fields with a simulated reflection," *J. Sound Vib.* **232**, 39-51.

O'Keefe, J. (1998). "Small scale modelling of stage to pit balance –a pilot study," Proceedings of 16th International Congress on Acoustics and the 135th Meeting of the Acoustical Society of America (Seattle) 341-342.

Okano, T., Beranek, L.L., and Hidaka, T. (1998). "Relations among interaural cross-correlation coefficient ($IACC_E$), lateral fraction (LF_E), and apparent source width (ASW) in concert halls," *J. Acoust. Soc. Am.* **104**, 255-265.

Osaki, S. and Ando, Y. (1983). "A fast method of analyzing the acoustical parameters for sound fields in existing auditoria," *Proc. 4th Comp. Environ. Eng. Build.* (Tokyo), 441-445.

Pompoli, R. and Prodi, N. (2000). "Guidelines for acoustical measurements inside historical opera houses: procedures and validation," *J. Sound Vib.* **232**, 281-301.

Price, M.A., Attenborough, K., and Heap, N.W. (1988). "Sound attenuation through trees: measurements and models," *J. Acoust. Soc. Am.* **84**, 1836-1844.

Sabine, W.C. (1900). *Reverberation.* The American Architect and the Engineering Record (Sabine, W.C. Prefaced by Beranek, L.L. (1992)). Collected Papers on Acoustics. Peninsula, Los Altos, CA, Chap. 1.

Saifuddin, K., Sakai, H., and Ando, Y. (2001). "Duration sensation of the simulated environmental noise in relation to its autocorrelation function," *J. Sound Vib.* **240**(4). (in print)

Sakai, H., Yamamoto, I., Kuroki, S., and Ando, Y. "Individual and intra-individual subjective preference of listeners to music in relation to a single reflection." (unpublished)

Sakurai, M., Korenaga, Y., and Ando, Y. (1997). "A sound simulation system for seat selection," *Music and Concert Hall Acoustics, Conference Proceedings of MCHA 1995*, Academic Press, London. Chap. 6. Eds. Ando, Y. and Noson, D.

Sakurai, M., Aizawa, S., Suzumura, Y., and Ando, Y. (2000). "A diagnostic system measuring orthogonal factors of sound fields in a scale model of auditorium," *J. Sound Vib.* **232**, 231-237.

Sato, S., Ando, Y., Nakajima, T., Merthayasa, I G.N., Chen, C.G., Sakai, H., Sumioka, T., Furuichi, H., Nishio, K., and Shoda T. (1994). "Architectural acoustical measurement of Kirishima International Concert Hall," *Report of the Meeting of the Acoustical Society of Japan*, 1003-1004. (in Japanese)

Sato, S., Mori, Y., and Ando, Y. (1997). "On the subjective evaluation of source locations on the stage by listeners," *Music and Concert Hall Acoustics, Conference Proceedings of MCHA 1995*, Academic Press, London. Chap. 12. Eds. Ando, Y. and Noson, D.

Sato, S. and Ando, Y. (1999). "On the apparent source width (ASW) for bandpass noises related to the IACC and the width of the interaural crosscorrelation function (W_{IACC})." *Proc. 137th Meeting Acoust. Soc. Am., 2nd EAA, 25th DAGA* (Berlin). (see also *J. Acoust. Soc. Am.* **105**, 1234).

Sato, S., Ando, Y., and Ota, S. (2000). "Subjective preference of cellists for the delay time of a single reflection in a performance," *J. Sound Vib.* **232**, 27-37.

Sato, S., Kitamura, T., Sakai, H., and Ando, Y. (2001). "The loudness of "complex noise" in relation to the factors extracted from the autocorrelation function," *J. Sound Vib.* **240**(4). (in print)

Schroeder, M.R. (1965). "New method of measuring reverberation time," *J. Acoust. Soc. Am.* **37**, 409-412.

Schroeder, M.R., Gottlob, D., and Siebrasse, K.F. (1974). "Comparative study of European concert halls; correlation of subjective preference with geometric and acoustic parameters," *J. Acoust. Soc. Am.* **56**, 1195.

Soeta, Y, Ohtori, K., Fujii, K., and Ando, Y. (2001). "Measurement of sound transmission by a hall doors," *J. Sound Vib.* **240**(4). (in print)

Suzumura, Y., Sakurai, M., Yamamoto, I., Iizuka, T., Oowaki, M., and Ando, Y. (2000). "An evaluation of the effects of scattered reflections in a sound field," *J. Sound Vib.* **232**(1), 303-308.

Sundberg, J. (1977). "The acoustics of the singing voice," *Scientific American* **236**, 82-91.

Thurstone, L.L. (1927). "A law of comparative judgment," *Psychological Review* **34**, 273-286.

LIST OF PUBLICATION

Full Papers

(1) Sakai, H., Singh, P.K., and Ando, Y. (1997). "Inter-individual differences in subjective preference judgments of sound fields," *Music and Concert Hall Acoustics, Conference Proceedings of MCHA 1995*, Eds. Ando, Y. and Noson, D., Academic Press, London, Chap. 13, 125-130.

(2) Sakai, H., Sato, S., and Ando, Y. (1998). "Orthogonal acoustical factors of sound fields in a forest compared with those in a concert hall," *J. Acoust. Soc. Am.* **104**(3), 1491-1497.

(3) Sakai, H., Ando, Y., and Setoguchi, H. (2000). "Individual subjective preference of listeners to vocal music sources in relation to the subsequent reverberation time of sound fields," *J. Sound Vibration* **232**(1), 157-169.

(4) Ando, Y., Sakai, H., and Sato, S. (2000). "Formulae describing subjective attributes for sound fields based on a model of the auditory-brain system," *J. Sound Vibration* **232**(1), 101-127.

(5) Noson, D, Sato, S., Sakai, H., and Ando, Y. (2000). "Singer responses to sound fields with a simulated reflection," *J. Sound Vibration* **232**(1), 39-51.

(6) Hase, S., Takatsu, A., Sato, S., Sakai, H., and Ando, Y. (2000). "Reverberance of an existing hall in relation to subsequent reverberation time and SPL," *J. Sound Vibration* **232**(1), 149-155.

(7) Takatsu, A., Hase, S., Sakai, H., Sato, S., and Ando, Y. (2000). "Acoustical design and measurement of a circular hall, improving a spatial factor at each seat," *J. Sound Vibration* **232**(1), 263-273.

(8) Takatsu, A., Sakai, H., and Ando, Y. (2000). "Acoustical design and measurement of a circular hall for improved spatial factors at each seat," *Journal of Building Acoustics* **7**(2), 113-125.

(9) Sakai, H., Sato, S., Prodi, N., and Pompoli, R. (2001). "Measurement of regional environmental noise by use of a PC-based system -an application to the noise near the airport 'G. Marconi' in Bologna-," *J. Sound Vibration* **240**(4). (in print)

(10) Sato, S., Kitamura, T., Sakai, H., and Ando, Y. (2001). "The loudness of "complex noise" in relation to the factors extracted from the autocorrelation function," *J. Sound Vibration* **240**(4). (in print)

(11) Saifuddin, K., Sakai, H., and Ando, Y. (2001). "Duration sensation of the simulated environmental noise in relation to its autocorrelation function," *J. Sound Vibration* **240**(4). (in print)

(12) Sakurai, M., Sakai, H., and Ando, Y. (2001). "A computational software for noise measurement and toward its identification," *J. Sound Vibration* **240**(4). (in print)

Under Review/ Under Preparation

(13) Sakai, H., Shibata, S., and Ando, Y. "Orthogonal acoustic factors of sound fields in a bamboo forest," *J. Acoust. Soc. Am.* (submitted)

(14) Sakai, H., Hotehama, T., Prodi, N., Pompoli, R., and Ando, Y. "A diagnostic system of measuring environmental noise based on the human auditory-brain system. An application to the railway noise." (under review for *J. Sound Vibration*)

(15) Sakai, H., Sato, S., Prodi, N., Pompoli, R., and Ando, Y. "Orthogonal factors for a singer on the stage in relation to the sound source in the orchestra pit in a historical opera house." (in preparation)

(16) Sakai, H., Sato, S., Prodi, N., Pompoli, R., and Ando, Y. "Orthogonal factors for performers in the orchestra pit in relation to the sound source on the stage in a historical opera house." (in preparation)

(17) Sakai, H., Sato, S., Prodi, N., Pompoli, R., and Ando, Y. "Orthogonal factors for a conductor in relation to the sound source in the orchestra pit and on the stage in a historical opera house." (in preparation)

(18) Sakai, H., Prodi, N., and Pompoli, R., and Ando, Y. "Orthogonal acoustical factors for listeners in boxes in an opera theatre." (in preparation)

(19) Sato, S., Sakai, H., Prodi, N., Pompoli, R., and Ando, Y. "Subjective evaluations of source locations for listeners on the stage in the orchestra pit in an opera house." (in preparation)

(20) Sakai, H. and Ando, Y. "Intra-individual differences of subjective preference judgements on simulated sound field with a single reflection." (in preparation)

Proceedings of International Congress/ Contributed Papers in English

(1) Sakai, H., Sato, S., Ando, Y., Prodi, N., and Pompoli, R. (2000). "A diagnostic system of measuring environmental noise based on the human auditory-brain system," 4th Japanese-Swedish Noise Symposium on Medical Effects (Stockholm).

(2) Sato, S., Sakai, H., Kitamura, T., and Ando, Y. (2000). "Loudness of complex tones in relation to the autocorrelation function of the source signals," 4th Japanese-Swedish Noise Symposium on Medical Effects (Stockholm).

(3) Sakai, H., Sato, S., Prodi, N., Pompoli, R., and Ando, Y. (2000). "An identification system for environmental noise," DAGA2000 Programmheft (Oldenburg), 72.

(4) Sakai, H., Sato, S., and Ando, Y. (1999). "A new system of environmental noise identification and subjective evaluation," *J. Acoust. Soc. Am.* **106**, 2210. (138th Meeting of the Acoustical Society of America, Columbus)

(5) Sato, S., Sakai, H., and Ando, Y. (1999). "On loudness and pitch of "complex noise" in relation to the factors extracted from the autocorrelation function," *J. Acoust. Soc. Am.* **106**, 2266. (138th Meeting of the Acoustical Society of America, Columbus)

(6) Sakai, H., Sato, S., and Ando, Y. (1999). "A new system of environmental-noise identification and subjective evaluation," Program of 1st International Workshop on New Systems for Identification and Evaluation of Regional Environmental Noise (Kobe), 4.

(7) Sato, S., Sakai, H., and Ando, Y. (1999). "On loudness and pitch of "complex noise" in relation to the factors extracted from the autocorrelation function." Program of 1st International Workshop on New Systems for Identification and Evaluation of Regional Environmental Noise (Kobe), 2.

(8) Saifuddin, K., Sakai, H., and Ando, Y. (1999). "Duration experience during listening to simulated environmental noise in relation to its effective duration of the autocorrelation function," Program of 1st International Workshop on New Systems for Identification and Evaluation of Regional Environmental Noise (Kobe), 5.

(9) Sakai, H., Shibata, S., and Ando, Y. (1999). "Orthogonal acoustical factors of sound fields in a bamboo forest," *J. Acoust. Soc. Am.* **105**, 1315. (Joint Meeting, 137th Meeting of the Acoustical Society of America (ASA), 2nd Convention of the European Acoustics Association: Forum Acusticum 99 (EAA), and integrating the 25th German Acoustics DAGA Conference (DEGA), Berlin).

(10) Sakai, H., Setoguchi, H., and Ando, Y. (1998). "Individual subjective preference of listeners for vocal music sources in relation to the subsequent reverberation time of sound field," Proc. 16th ICA/135th ASA (Seattle), 681-682.

(11) Ando, Y., Sakai, H., and Sato, S. (1998). "Fundamental subjective attributes for sound fields from a model of the auditory-brain system," Proc. 16th ICA/135th ASA (Seattle), 11-12.

(12) Kuroki, S., Yamamoto, I., Sakai, H., Setoguchi, H., and Ando, Y. (1998). "Individual differences of subjective preference for sound fields with different preferred delay time of reflection," Proc. 16th ICA/135th ASA (Seattle), 2155-2156.

(13) Takatsu, A., Hase, S., Sakai, H., Sato, S., and Ando, Y. (1998). "Acoustic design and measurement of a circular hall improving the subjective preference at each seat," Proc. 16th ICA/135th ASA (Seattle), 2469-2470.

(14) Hase, S., Takatsu, A., Sato, S., Sakai, H., and Ando, Y. (1998). "Reverberance of an existing hall in relation to subsequent reverberation time and SPL," Proc. 16th ICA/135th ASA (Seattle), 2769-2770.

(15) Sakai, H., Setoguchi, H., and Ando, Y. (1997). "Subjective preference judgements of simulated sound field by listeners for sound source in opera performance," *J. Acoust. Soc. Am.* **102**, 3187. (134th Meeting of the Acoustical Society of America (ASA), San Diego)

(16) Sakai, H., Sato, S., and Ando, Y. (1996). "Effects of multiple scattering by trees in a forest as a music performance space," *J. Acoust. Soc. Am.* **100**(A), 2819. (3rd Joint Meeting of the Acoustical Society of America (ASA) and the Acoustical Society of Japan (ASJ), Honolulu)

(17) Sakai, H., Singh, P.K., and Ando, Y. (1995). "Inter-individual differences in subjective preference judgments of sound fields," Proc. 1st International Symposium of Music and Concert Hall Acoustics (MCHA95) (Kirishima), 6 pages.

Books

(1) Ando, Y., Sakai, H., and Sato, S. (1995). Sound field in a forest. Hill-side Residence Plan, Architectural Institute of Japan, Chap. 4.5, Gihodo, 148-151. (in Japanese, joint writing)

(2) Ando, Y., Sato, S., and Sakai, H. (1999). Fundamental Subjective Attributes of Sound Fields Based on the Model of Auditory-Brain System. *Computational Acoustics in Architecture*, Ed. Sendra, J.J., WIT Press, Southampton, Chap 4, 63-99. (joint writing)

Translation

(1) Ando Y. (2000). Architectural Acoustics -Blending sound sources, sound fields, and listeners-, Trans. Sato, S. and Sakai, H., Springer-Verlag, Tokyo. (in Japanese)

Contributed Papers (Domestic)

(1) Hamada, M., Kuroki, S., Yamamoto, I, Sakai, H., and Ando, Y. (2000). "Individual difference of subjective preference in a sound field –effects of sex, sleeping, and physical condition to optimum initial time delay gap-," Summaries of Technical papers of Annual Meeting Architectural Institute of Japan **D**-1, 857-858. (in Japanese)

(2) Yamamoto, I, Sakai, H., Kuroki, S., Ando, Y., and Kawano, M. (2000). "Individual difference of subjective preference in a sound field –relationship between effective duration and optimum initial time delay gap," Summaries of Technology papers of Annual Meeting Architectural Institute of Japan, Kyusyu Chapter. (in Japanese)

(3) Sakai, H., Takatsu, A., Sato, S., and Ando Y. (1999). Effects of illuminance and listening level on subjective preference judgments for a sound field. Summaries of Technology papers of Annual Meeting Architectural Institute of Japan, Kinki Chapter, 39, 241-244. (in Japanese)

(4) Yamamoto, I., Sakai, H., Kuroki, S., Ando, Y., and Kawano M. (1999). "Individual differences in subjective preference for sound fields. Examination of change of relationship between preferred initial time delay gap and effective duration with reflections," Summaries of Technical papers of Annual Meeting Architectural Institute of Japan, **D**-1, 863-864. (in Japanese)

(5) Yamamoto, I., Sakai, H., Kuroki, S., and Ando, Y. (1998). "Individual differences in subjective preference for sound fields. Effective factors to preferred initial time delay gap," Summaries of Technology papers of Annual Meeting Architectural Institute of Japan, Kyusyu Chapter, **37**, 37-40. (in Japanese)

(6) Sakai, H., Doge, K., and Ando, Y. (1998). "Orthogonal acoustical factors of sound fields in forests (cedar forests and bamboo forests)," Summaries of Technology papers of Annual Meeting Architectural Institute of Japan, Kinki Chapter, 141-144. (in Japanese)

(7) Yamamoto, I., Sakai, H., Kuroki, S., and Ando, Y. (1998). "Individual differences in subjective preference for sound fields. Effective factors to preferred initial time delay gap," Summaries of Technical papers of Annual Meeting Architectural Institute of Japan, **D**-1, 709-710. (in Japanese)

(8) Sakai, H., Shibata, S., and Ando, Y. (1997). "Sound field in a general forest and a bamboo forest," Program of Symposium "Global Environment, Human Rhythm, and Aging" (Nagoya), WG of Psychology and Physiology in Environment, Architectural Institute of Japan. 57-62. (in Japanese)

(9) Sakai, H., Yamamoto, I., Kuroki, S., and Ando Y. (1997). "Inter-individual differences in subjective preference judgments of sound field with a single reflection," Summaries of Technology papers of Annual Meeting Architectural Institute of Japan. (in Japanese)

(10) Yamamoto, I., Sakai, H., Kuroki, S., and Ando Y. (1997). "Individual differences in subjective preference judgments of sound fields with single reflections," Summaries of Technical papers of Annual Meeting Architectural Institute of Japan. (in Japanese)

(11) Sakai, H., Kurakazu, M., Yamaoka, T., and Kitamura, T. (1996). "Studies on wind noise of louvers on the roof of a high-rise building. Part 1; an example of studies on wind noise on a building," Summaries of Technical papers of Annual Meeting Architectural Institute of Japan, **D**, 7-8. (in Japanese)

(12) Sato, S., Ando, Y., and Sakai, H. (1995). "Acoustic measurement of a clump of trees in Kirishima Shrine for music performance," Summaries of Technical papers of Annual Meeting Architectural Institute of Japan, **D**, 39-40. (in Japanese)

(13) Sakai, H., Kobayashi, Y., Owaki, M., Tokuhiro, H., and Ando, Y. (1995). "Acoustical estimation of IACC in rectangular rooms," Reports of the Meeting of the Acoustical Society of Japan, 797-798. (in Japanese)

(14) Kobayashi, Y., Sakai, H., Tokuhiro, H., Owaki, M., and Ando, Y. (1995). Acoustical design and characteristics of the atrium for music performance in a hotel, Reports of the Meeting of the Acoustical Society of Japan, 919-920. (in Japanese)

(15) Sakai, H. and Ando, Y. (1994), "Individual's difference in subjective preference for listening level of sound field," Summaries of Technology papers of Annual Meeting Architectural Institute of Japan, **D**, 137-140. (in Japanese)

(16) Sakai, H. and Ando, Y. (1994). "Inter-individual changes and individual difference in subjective preference for listening level of sound field," Summaries of Technical papers of Annual Meeting Architectural Institute of Japan, **D**,

1681-1682. (in Japanese)
(17) Sakai, H., Ando, Y., Nakajima, T., Merthayasa, I.G.N., Chen, C.G., Satoh, S., Sumioka, T., Furuichi, H., Nishio, K., and Shoda, T. (1994). Acoustic measurement of Kirishima Zinguu, Reports of the Meeting of the Acoustical Society of Japan, 1005-1006. (in Japanese)
(18) Satoh, S., Ando, Y., Nakajima, T., Merthayasa, I.G.N., Chen, C.G., Sakai, H., Sumioka, T., Furuichi, H., Nishio, K., and Shoda, T. (1994). Architectural acoustic measurement of Kirishima International Concert Hall, Reports of the Meeting of the Acoustical Society of Japan, 1003-1004. (in Japanese)